Mirror Neurons are Modulated by Reward Expectation and Grip Force in the Sensorimotor Cortices (S1, M1, PMd, PMv)

by
MD Moin Uddin Atique

A dissertation submitted to the Department of Biomedical Engineering,
Cullen College of Engineering
in partial fulfillment of the requirements for the degree of
Doctor of Philosophy

Chair of Committee: Dr. Joseph T. Francis

Committee Member: Dr. Nuri F. Ince

Committee Member: Dr. Yingchun Zhang

Committee Member: Dr. David J. Francis

Committee Member: Dr. Rose T. Faghih

University of Houston
May 2021

I dedicate this dissertation to my mother for her constant love and support.

ACKNOWLEDGMENTS

I want to thank my supervisor Dr. Joseph T. Francis who was always there throughout my Ph.D. life. He was a great mentor and teacher. I am really lucky to have a person like him as my guide. I want to thank my current and former lab members Taruna, Matt, Oman, Nivas, Adittya, and Jack for their constant support and help. I am grateful to Dr. Junmo An who was a post-doc in our lab and from whom I got a lot of resources about programming and paper writing. I am thankful to Dr. David J. Francis for his suggestions which improved my knowledge about statistics.

ABSTRACT

Mirror Neurons (MN) respond similarly when primates make, or observe, grasping movements. Recent work indicates that reward expectation influences M1 during manual, observational, and Brain Machine Interface (BMI) reaching movements. Previous work showed MN are modulated by subjective value. Here we expand on the above work utilizing two non-human primates (NHPs), one male *Macaca* Radiata (NHP S) and one female *Macaca* Mulatta (NHP P), that were trained to perform a cued reward level isometric grip force task, where the NHPs had to apply visually cued grip force to move and transport a virtual object. We found a population of (S1, M1, PMd, PMv) units that significantly represented grip force during manual and observational trials. We found the neural representation of visually cued force was similar during observational trials and manual trials for the same units, however, the representation was weaker during observational trials. Comparing changes in neural time lags between manual and observational tasks indicated that a subpopulation fit the standard MN definition of observational neural activity lagging the visual information. Neural activity in (S1, M1, PMd, PMv) significantly represented force and reward expectation. In summary, we present results indicating that sensorimotor cortices have MN for visually cued force and value.

TABLE OF CONTENT

LIST OF TABLES

LIST OF FIGURES

List of Abbreviations

- NHP – Non-Human Primate
- MN – Mirror Neuron
- S1 – Primary Somatosensory Cortex
- M1 – Primary Motor Cortex
- PMd – Dorsal Premotor Cortex
- PMv – Ventral Premotor Cortex
- BMI – Brain-Machine Interface
- BCI – Brain Computer Interface
- CS – Conditional Stimulus
- MC – Manual Cued Data Block
- MU – Manual Uncued Data Block
- OC – Observational Cued Data Block
- OU – Observational Uncued Data Block
- FDR – False Discovery Rate
- BH – Benjamini-Hochberg method
- R0 – Non-Rewarding Trials
- R1 – Rewarding trials
- ROS – Robot Operating System

CHAPTER 1

INTRODUCTION

The planning, controlling, and executing any voluntary movements is performed by motor cortex area of the brain. The major three parts of motor cortices are premotor cortex, primary motor cortex (M1) and supplementary motor area (SMA). An abstract figure of the Monkey brain indicating the motor cortex area is shown in Figure 1.

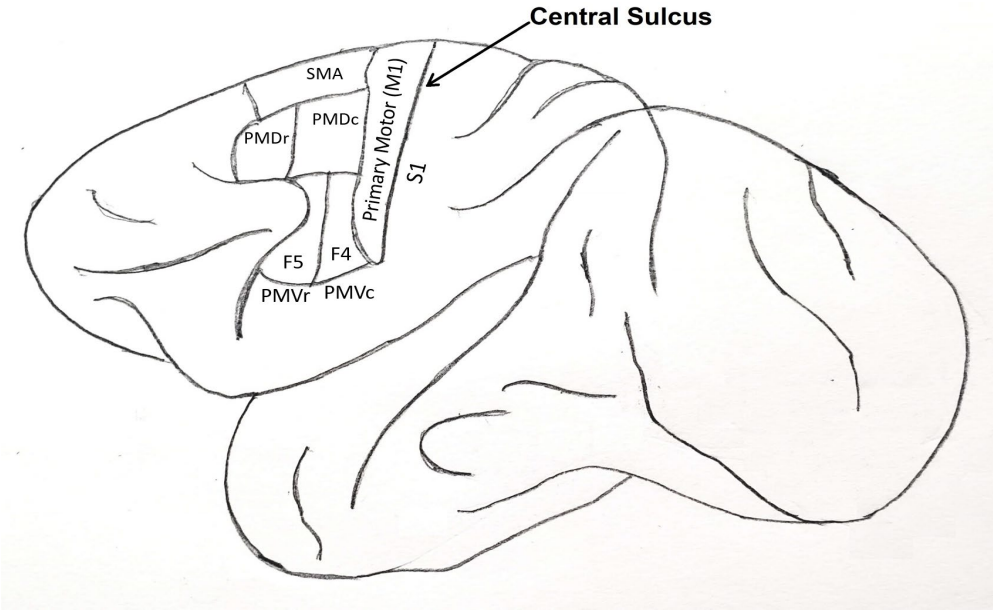

Figure 1: Motor cortex of Non-Human Primates (Monkey).

The Central Sulcus separates the parietal lobe from the frontal lobe and on the frontal lobe side (left on Figure 1) the area is known as Primary motor cortex (M1) which controls the execution of movement with association of other motor areas. The pre-motor area consists of Ventral Premotor cortex (PMv) and Dorsal Premotor ortex (PMd) is responsible for motor planning and sensory guidance of movement. The area on the opposite side of M1 with respect to central sulcus is primary Somatosensory cortex (S1).

Main task of the S1 cortex involves sensory activity like detecting touch and proprioception. Reward plays a major role in the motor activity. Expectation of a reward influences the motor learning as well as performance of the motor action (Klein et al., 2012).

Mirror neurons (MN) are a type of neuron that shows activity during an action performance and during the observation of the same action by any other agent (Figure 2). This activation of mirror neurons during observation and action makes them a crucial part during the development of Brain Machine Interfacing (BMI). They were first described in the ventral premotor cortex (F5) area of the Monkey (G. Rizzolatti et al., 1988; Giacomo Rizzolatti, 2005; Giacomo Rizzolatti et al., 2001). Mirror neuron (MN) activity has been observed while studying kinematic behaviors, (Cisek & Kalaska, 2004; Dushanova & Donoghue, 2010; Gallese et al., 1996; G. Vigneswaran et al., 2013), and through indirect measure in human motor cortex (Alaerts et al., 2012). In order to ask questions about force information at the single unit level, an isometric grip force paradigm with visual grip-force feedback needs to be utilized. As MN activity is modulated by variables such as subjective value (Caggiano et al., 2012), and cued reward level (An et al., 2019; Brandi T. Marsh et al., 2015), modulation of both force and reward level is necessary to study, while removing any production of kinematics by the subjects.

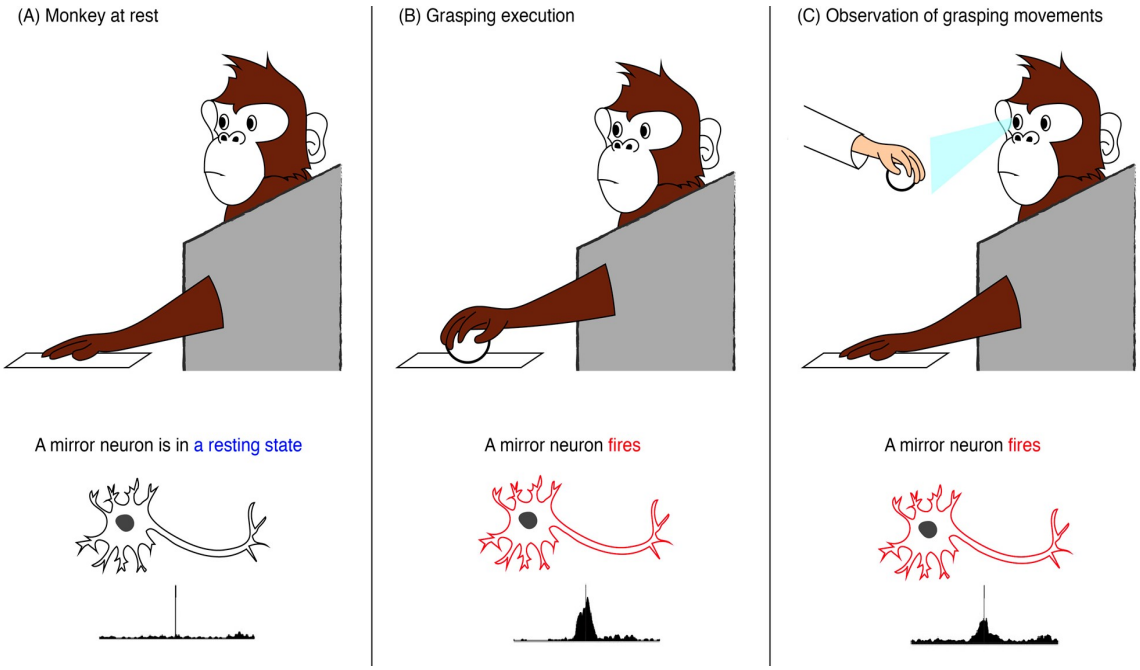

Figure 2: Mirror neuron illustration; Source: JohnMark Taylor, Harvard university.

A better understanding of how reward expectation influences the primary- and pre-sensorimotor cortices has practical implications towards the production of stable and autonomously updating brain machine interfaces (BMIs) (An et al., 2019, 2018; B. T. Marsh et al., 2015; Pohlmeyer et al., 2014, 2012; Sanchez et al., 2011). Neural modulation related to reward has been well characterized within many brain structures (Glimcher et al., 2008; Rolls, 2014; Schultz et al., 1997), and is known to occur at many levels, such as single units and local field potentials (LFP) within M1 (An et al., 2019). The neural response to both reward and conditioned stimuli (CS) that predict reward have been demonstrated in a multitude of brain regions (Cohen et al., 2012; B. T. Marsh et al., 2015; Murray et al., 2008; Ramkumar et al., 2016; Matthew R. Roesch & Olson, 2003; Sato & Hikosaka, 2002; Tremblay & Schultz, 1999; Zaghloul et al., 2009). It has recently been shown that reward expectation changes directional and force related tuning functions

within the primary sensorimotor cortices during reaching movements and BCI reaching movements (Ramakrishnan et al., 2017; Zhao et al., 2018).

The above studies indicate the need to conduct more research on the influence reward on these brain regions, and how such variables may modulate MNs. The influence of reward on the primary somatosensory cortex (S1) was reported in preliminary studies (Atique & Francis, 2019; D. McNiel et al., 2016; D. B. McNiel et al., 2016). While these experiments demonstrated our ability to classify reward expectation from S1 they did not provide insight on its influence on grip-force during action and action observation. Although a similar reward signal has been demonstrated in primary somatosensory cortex utilizing fMRI, where a stronger BOLD response was recorded for higher reward delivery (Pleger et al., 2008), the investigation of reward-correlated signals within S1 at the single unit level has not been fully developed. The main goal of the research presented here was to investigate the neural response to reward expectation and reward delivery within S1, M1, PMd and PMv in the presence of a conditioned stimulus (CS, cued) and absence (uncued) of explicit reward-level knowledge to be received for successfully completed trials, during both manual and observational trials. We focused on "grasping" movements with cued isometric grip-force control, to expand beyond reaching movements (An et al., 2019; Brandi T. Marsh et al., 2015). Below we show our ability to decode actual and observed grip-force neural responses during manual and observational trials, as well as reward's influence on the neural population during reward cued and uncued trials. Others have described activity of MNs in M1 during observation of movement (Dushanova & Donoghue, 2010; Brandi T. Marsh et al., 2015; Mazurek et al., 2018; Tkach et al., 2007; Ganesh Vigneswaran et al., 2013). A good example of mirror neuron activity is given on

Figure 3, which is taken from S1 cortex of NHP P. They categorized two types of mirror neuron as, Facilitation type for which during observation the unit's activity increases and Suppression type where the unit's activity reduces during observation of action.

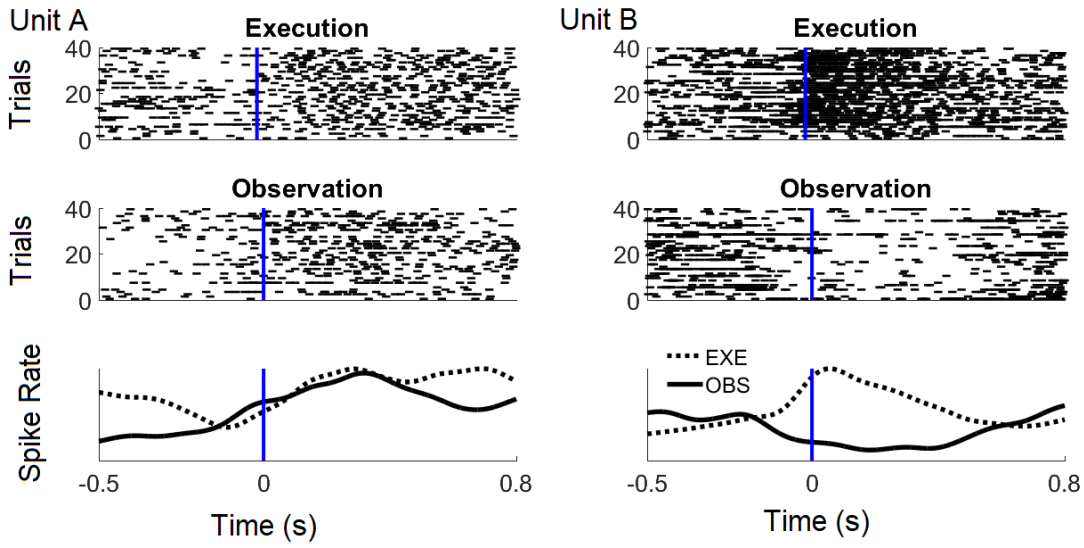

Figure 3: Facilition (Unit A) and Suppression (Unit B) type mirror neuron in S1 (NHP P).

So far, not as much has been reported on the activity in S1 single units, during observational tasks, or any of the 4 regions as it pertains to isometric grip-force control while modulating reward level as we do here. There are some studies on human and NHP that showed evidence of MN activation (Gazzola & Keysers, 2009; Keysers et al., 2010; Giacomo Rizzolatti & Craighero, 2004) and grip force related modulation (Keisker et al., 2009; Rossi et al., 2002) is present in somatosensory areas which implies the possibility of MN related activity due to grip force in cS1 cortex.

Generally, our paper presents findings of MN responses related to varying levels of grip force and reward in M1, S1, PMd and PMv during both manual and observational trials, with stronger responses during manual trials.

CHAPTER 2

SPECIFIC AIMS

The objective of this study is to understand the neural dynamics of single units from the sensorimotor cortices (S1, M1, PMd and PMv) and their role during action (Grip force) or action observation under the influence of different reward level. To comprehend the above stated dynamics, the following aims and hypotheses were established.

- **Aim1:** Detect the influence of reward and reward cue in S1, M1, PMd and PMv single units. It is known that reward influences the sensorimotor cortices, but a side by side comparison of that influence in all four cortices listed above would be crucial to understand the effect of reward expectation on action like grip force activity (section 4.2)
  - **Hypothesis:** Reward level effects single units' activity in Sensory motor cortices.
- **Aim2:** Decode the applied or observed grip force from sensorimotor cortices (S1, M1, PMd and PMv) and detect single units that represent the force during action and action observation. Record units that significantly represent grip force during action and action observation (section 4.3-4.5).
  - **Hypothesis:** Mirror Neurons encode the amount of grip force on S1, M1, PMd and PMv single units.
- **Aim3:** Measure the grip force tuning for different levels of reward and examine the difference between the tuning for reward vs. non-reward. A difference between the tuning will suggest that the grip force representation is modulated due to the expectation of reward (section 4.8).
  - **Hypothesis:** Reward expectation effects the grip force tuning in S1 and PMd units.

CHAPTER 3

METHODS

3.1 Introduction

All NHP manipulations described in this work were approved by the Institutional Animal Care and Use Committee of the State University of New York at Downstate Medical Center and conformed to National Institutes of Health (NIH) and United States Department of Agriculture (USDA) animal care and use guidelines. In addition, this work complies with the ARRIVE guidelines. Two non-human primates (NHPs), one 9.0kg male *Macaca Radiata* (NHP S) and one 5.0kg female *Macaca Mulatta* (NHP P), were trained to perform a behavioral grip force task using their right hand/arm and subsequently implanted with 96-channel electrode arrays in S1, M1, PMd and PMv.

3.2 Behavioral Task

Two NHPs were trained to perform psychophysical task for experiment. The study involves two types of task, Manual task and Observational task. During manual task the NHP used their arm to apply appropriate amount of grip force on a force transducer and for Observational task the computer performed the task automatically and NHPs only observed without any hand movement. The basic setup (Figure 4) of the task involves the NHP sitting on a restraint chair where they were only allowed to move their arm when they needed (manual task). A cover was placed to restrain their arm during observational task type, and they were trained to observe the task without any action. A vertical display in front of the NHP showed a simulated environment where a robot grabbed and transported a cylindrical object from a location to another cued location. A force transducer was placed

within their reach for the NHP to apply grip force during the manual task type. During observational the restraining cover prohibited the NHP from reaching the transducer.

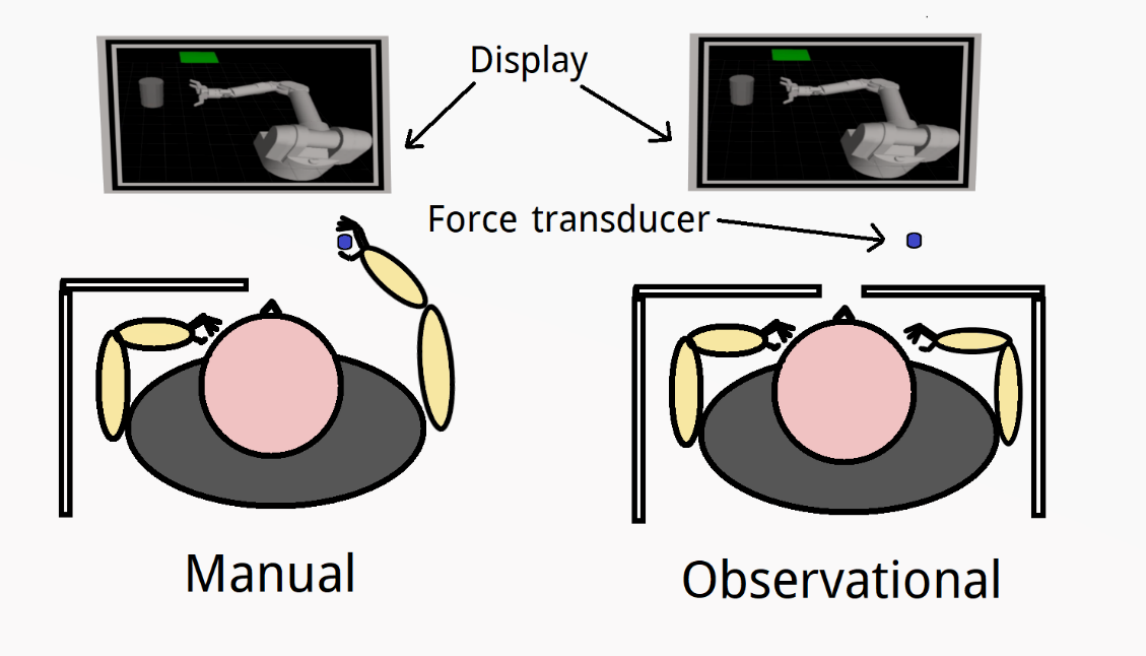

Figure 4: Task setup for the psychophysical task.

Both NHPs were trained to perform a grip force task that only required their input during object grasp and transport scenes during manual trials (see Figure 5). Additionally, in manual trials the NHPs had to produce and maintain adequate isometric force while they observed visual grip-force feedback in real-time (Figure 5 red rectangle's width). If NHPs applied the appropriate grip force (indicated by blue rectangular force cues) during object grasp and transport, then released when the object was touching the virtual ground at the target location, the trial was successful. If they did not apply proper force during initial grasp after the go cue, failed to maintain an acceptable force range at any time during the grasp or transport scenes, or released their grip early or late, the trial was considered a failure. The time limit to complete a successful trial was 10s. The NHPs had to repeat failed

trials under the same reward conditions until successful, thus giving incentive to perform non-rewarding trials. Depending on the trial, rewarding (**R1**) or non-rewarding (**R0**), successful execution of the task resulted in delivery of a fluid reward (R1) or lack of reward (R0). Juice rewards were delivered via a system-controlled solenoid driven by task logic (Crist instruments). All elements of the grip force task were developed in Linux using robot operating system (ROS) (Quigley et al., 2009). ROS and Python controlled the task logic, outputs to the reward delivery system, and provided timestamp synchronization with external systems to simultaneously and accurately record task state, reward delivery, and neural data.

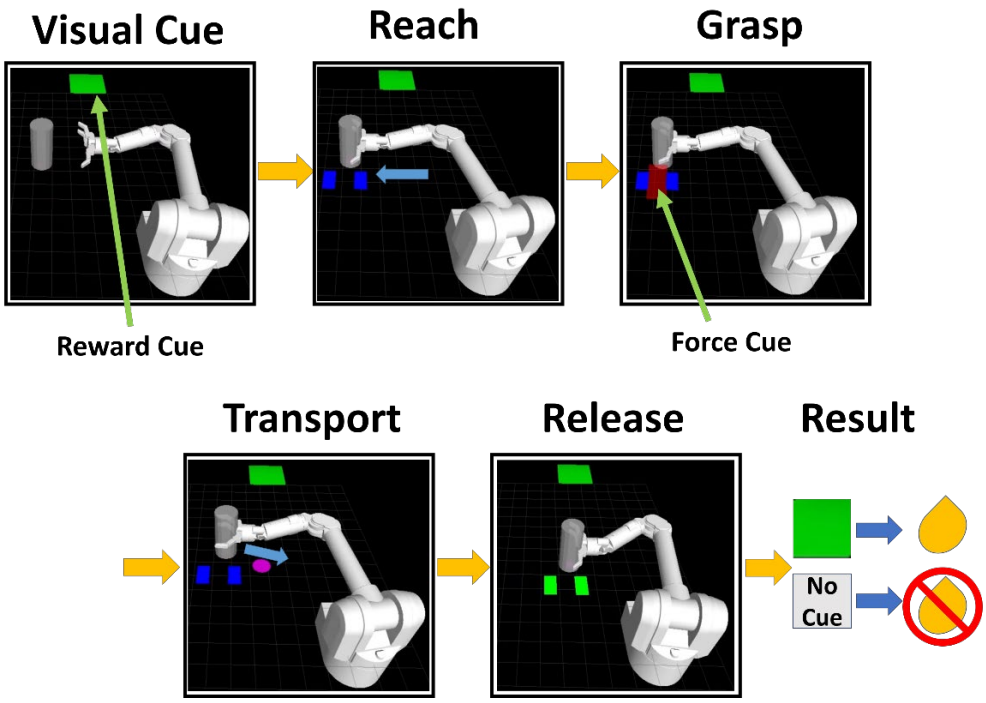

Figure 5: Flow diagram illustrating one reward cued (green square, R1) trial for the grip force task. Absence of the green square indicated a non-rewarding (R0) trial.

We analyzed single unit activity from four types of task blocks for each NHP. The four types of task blocks consisted of the following, and in this order for each NHP: first, manually performed tasks with the presence of a reward level conditioned stimulus cue (CS) (manual cued); second, manually performed tasks without a reward level CS (manual uncued); third, observational task with the presence of a reward level CS (observational cued); forth, observational task without a CS (observational uncued). The manually recorded block that was cued for reward level is mentioned as MC in the short form for the rest of the paper especially for plots. The acronyms for other blocks are, MU is manually performed uncued block, OC is observational cued block and OU is observational uncued block. Each of the blocks contained two types of trials, R1 for rewarding trial and R0 for non-rewarding trial. The structure of the experiment is represented diagrammatically in Figure 6.

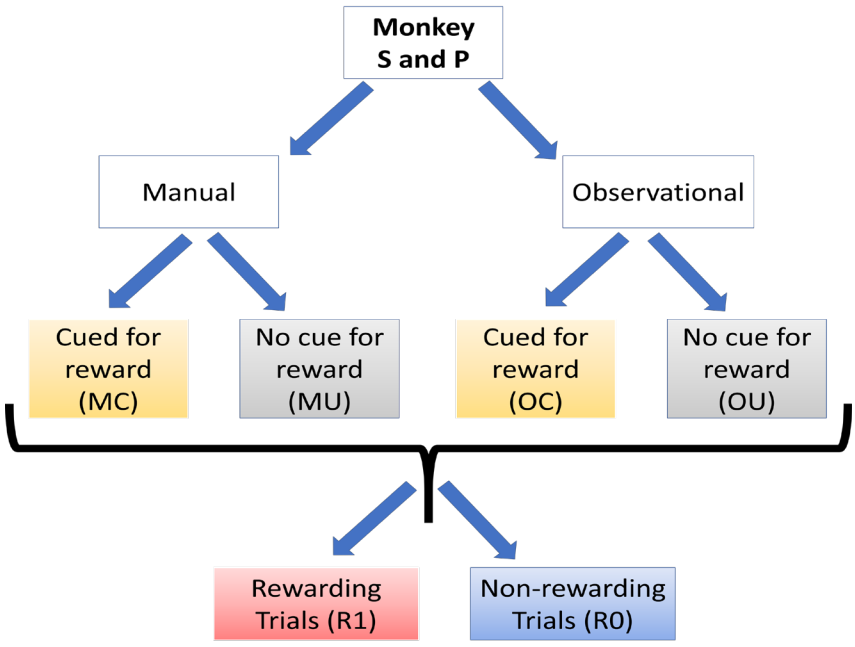

Figure 6: Diagram of the recorded data block type.

NHPs were well trained for the grip-force task prior to data collection. NHP S achieved success rates of 89 and 85 percent during the two manual-task blocks, while NHP P achieved rates of 84 and 90 percent. We considered only successfully completed trials for all analyses and results presented in this paper. Successful completion of each R1 trial led to a 0.5s solenoid-controlled fluid delivery. However, successful completion of R0 trials led to no reward, a reset time of 250ms, and progression to the next trial. Some of the recorded blocks contained a visual cue (CS, cued blocks) that indicated whether each trial was rewarding or not, while other blocks were uncued. The start of each trial was marked by the robotic arm traveling to a rest position. During cued blocks, when the robotic arm was at rest, a reward cue "flew" in from the top left side of the screen to indicate a rewarding trial (R1). The visual cue flew across the screen for 0.5s before coming to rest at the top center of the screen, while such a cue was absent during the R0 trials. Also, the absence of a reward during cued blocks further indicated to the NHP that the trial was non-rewarding (R0). All trials (R0 and R1) during uncued blocks lacked a visual reward cue so the NHP had no indication of trial type until the post result period, and thus, no known expectation for reward outcome as the trial sequence was randomized with no clear autocorrelation (see Figure 7). For trials that contained a visual reward cue, the post-cue period began immediately after the green visual cue came to rest. In uncued trials, the "post-cue" period began when the robotic arm returned to its rest position from the previous trial. In the following Figure 7, plot a, c, e, and g are for NHP S and b, d, f, and h is for NHP P. The block type is given on the right side of each row. The x-axis represents lag and y axis represents corresponding autocorrelation R0 and R1 trial type as they appeared during the block.

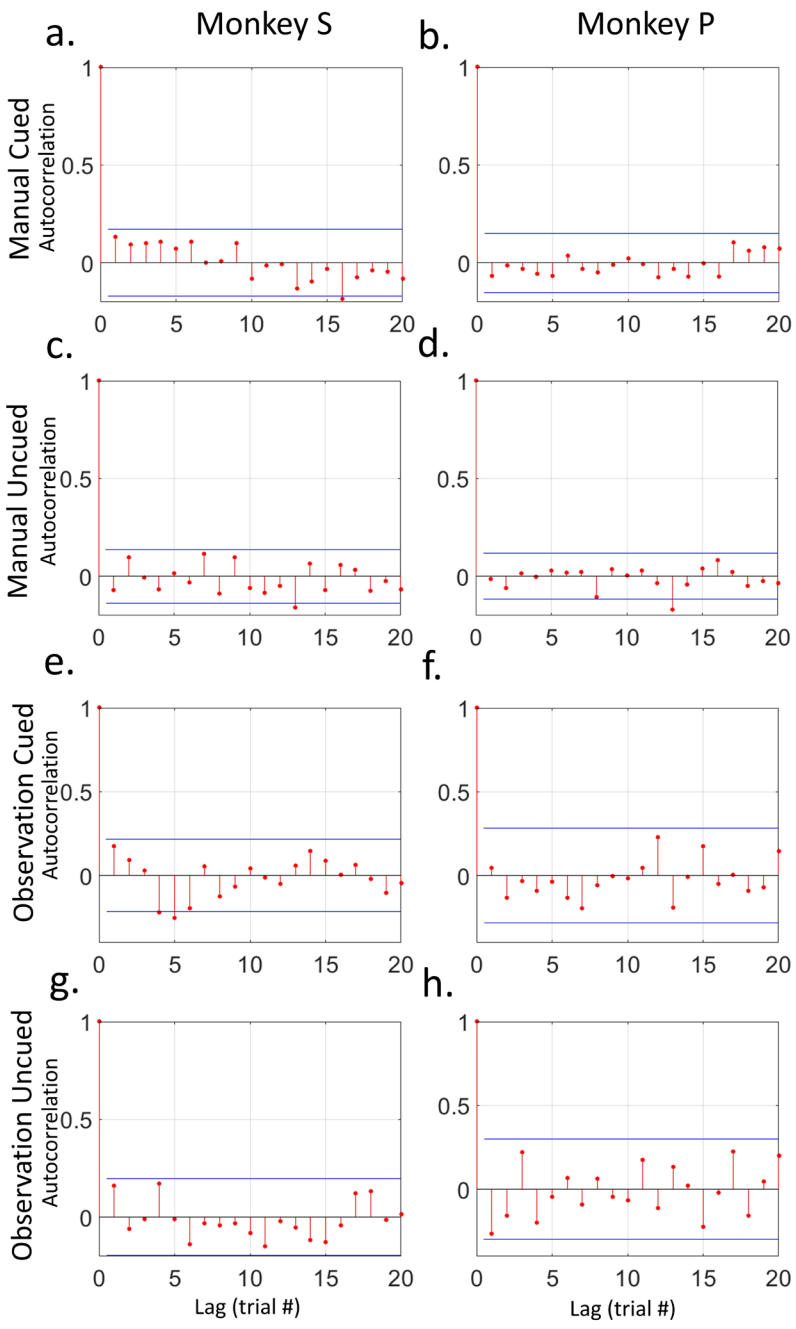

Figure 7: Autocorrelation on the reward level target sequence (R0 and R1) of trials for all the blocks.

We defined the post-result period as the time when the cylindrical object was successfully placed at the target location. Feedback was provided to NHPs for successful placement when the blue force squares turned green and the robotic arm released the

cylinder during the release scene. Some blocks were performed manually by the NHPs while others required the NHPs to remain attentive and observe the simulated robot arm perform the same type of reach-grasp-transport-release movements performed by the NHPs in the manual trials. NHPs were visually monitored by researchers in real-time via cameras during all sessions to make sure NHPs remained attentive and focused on the projection screen, especially during observational trials. During observational trials NHPs did not have access to the force transducer handle, and their arms were blocked behind a plexiglass box meant to keep the NHPs hands away from the trainers (BKIN's Arms-Free restraint chair, Figure 8Figure 8: Primate restraint chair). Additionally, NHPs were trained, and performed all experiments in a dark, quiet, and distraction-free isolation chamber to encourage their attention remained on the large projection screen. Each NHPs' rear-mounted cranial head post was affixed to the BKIN primate chair to restrict head movement for neural recordings. The virtual environment was projected onto a vertical screen in the animal's visual field. Recording sessions were broken into blocks of trials that averaged ten minutes of randomized R1 and R0 trials.

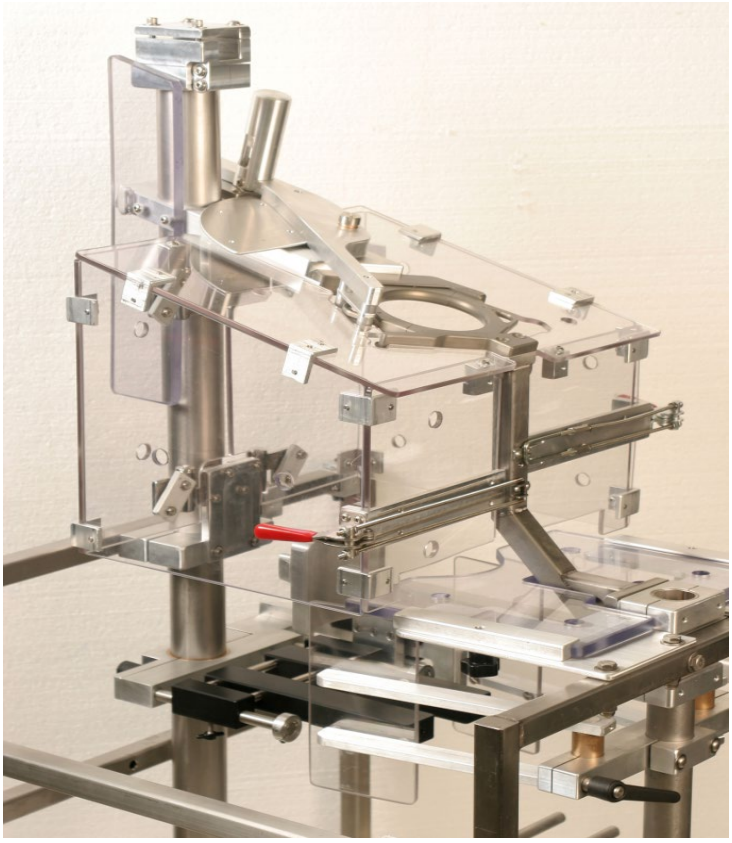

Figure 8: Primate restraint chair.

Here, we describe the sequence for one complete trial of a manually performed reward cued task. We have also provided an illustration of the task phases in Figure 5. First, a green square flew in from the left boundary to indicate a R1 trial. Absence of the green square indicated a R0 trial. Next, the robot autonomously moved its arm toward the cylindrical object in the reach scene. At the grasp scene, during manual trials, the NHPs had to apply grip force using a handle that contained a force transducer. The amount of force required was indicated by two blue rectangles (where the inner vertical edge of each blue rectangle indicated minimum force and the outer edges indicated maximum force). As NHPs applied force, visual force feedback was provided via the width of a single red rectangle located directly between the blue force cue rectangles. When the NHPs applied

force within the acceptable tolerance range (when the red force rectangle's edges were within the blue rectangles) the robot hand would grasp the object. During transport, the robot arm autonomously moved the object to a predetermined location, indicated by a pink circle. NHPs had to maintain an acceptable level of grip force during the transport phase, otherwise the trial was failed and repeated at the same reward level. After the object was transported to the specified location, NHPs had to release their grip. If all actions were completed successfully the blue rectangles turned green and the NHP was rewarded for R1 trials, but not for R0 trials. The motivation for NHPs to successfully complete R0 trials was the fact that they would have to repeat any unsuccessful trial until they were successful. Figure 5 depicts a "cued" block trial where reward information was fully provided to the NHPs.

3.3 Chronic Implantation

We performed implantation procedures as described in-depth in a previous methods paper (Chhatbar et al., 2010), but give a summary here. Following training, when both NHPs achieved greater than 80% success rate on all trials in a block, the animals were implanted with chronic electrode arrays (Utah array, Blackrock Microsystems) in primary somatosensory (S1, areas 1 and 2), primary motor (M1, rostral) dorsal premotor (PMd) and ventral premotor (PMv) cortices (Figure 9). All surgical procedures were conducted using aseptic technique. NHPs were initially anesthetized with Ketamine, followed by isoflurane and a continuous infusion of fentanyl. The NHP was then placed into a stereotactic frame before the surgical site was shaved and cleaned. An incision was made along the skull to expose the desired implant locations. The craniotomy window was large enough to accommodate implant locations while leaving enough margin between the dural flap and

skull. The dural flap was kept under tension using stay sutures until electrode arrays were implanted and the site was ready to close. We performed intraoperative probing of S1 to ensure implantation within the hand region, by using a four shank, 32-channel silicon microelectrode array (Kipke et al., 2003) within the post-central gyrus as determined by stereotactic coordinates. The NHP's contralateral hand was continuously stimulated by touch to assess S1 hand region boundaries. Neural responses were amplified and sent to an audio speaker to verify stimulation areas. Utah arrays were then chronically implanted in S1's hand region, in M1 directly reflected across the central sulcus rostral from S1, when possible as large blood vessels can interfere, and in PMd and PMv. The craniotomy was replaced according to previously described methods (Chhatbar et al., 2010).

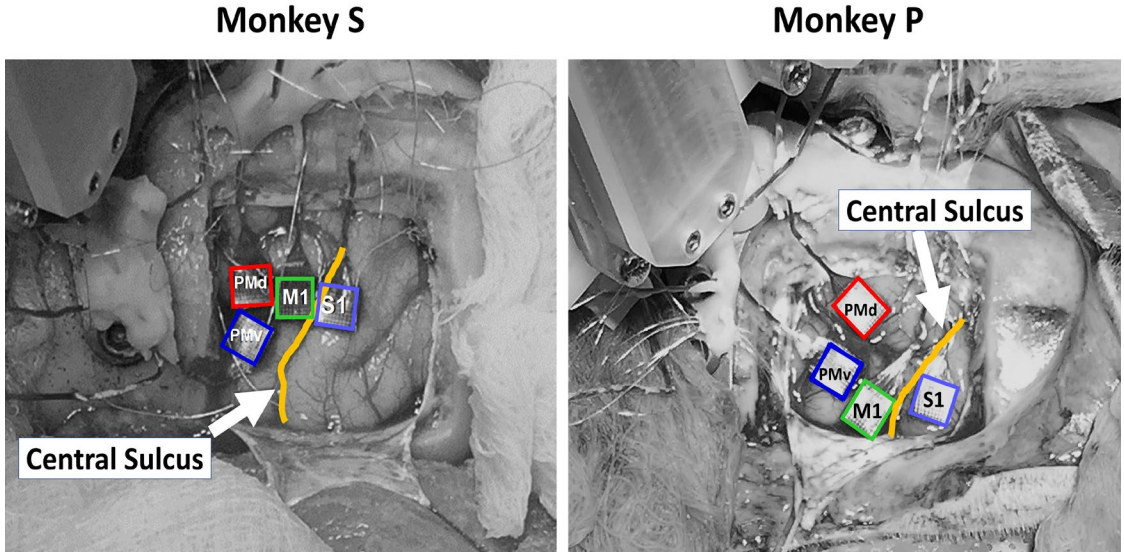

Figure 9: Position of four Utah arrays in relation to the central sulcus for NHP S (left) and P (right). The four arrays were implanted in S1 (light-blue), M1 (green), PMd (red) and PMv (blue) cortices. The green line indicates the Central Sulcus.

3.4 Neural Recording

Neural recordings were performed using three synchronized multi-channel acquisition processors (Plexon, Dallas, TX), each having 128-spike waveform recording channels and 32 analogue channels used for simultaneous recording of local field potentials (An et al., 2019, 2018). Single unit recordings were amplified and retained using waveform voltage thresholds. Thresholds were set using an auto-scale (Plexon recording software) feature, followed by manual adjustments that eliminated noise on channels prior to recording. Robot operating system (Quigley et al., 2009) and Python programs controlled task logic and embedded timestamps into neural recordings using a common clock. The common clock was maintained by a microprocessor that delivered a 2kHz pulse to keep task logic and neural data synchronized. Initially, unit waveforms were automatically clustered using a k-means algorithm in principal component space (Kretzberg et al., 2009; Yuan et al., 2012). Afterward, we used Plexon's offline sorter software to adjust clusters to remove noise and artifacts.

3.5 Spike Sorting

The Spike Sorting was done using Plexon Offline Sorter. For each NHP four blocks of data (two manual and two observational) were recorded on the same day and to track a single unit's activity through all the blocks we needed to sort the data blocks at the same time. The data from the Plexon MAP system was recorded on '*.plx' format and to sort multiple blocks together on the sorter software we had to convert the "plx" files to "pl2" format using PlexUtil software. After the conversion for each NHP the data blocks for each cortex was loaded at the same time and was sorted.

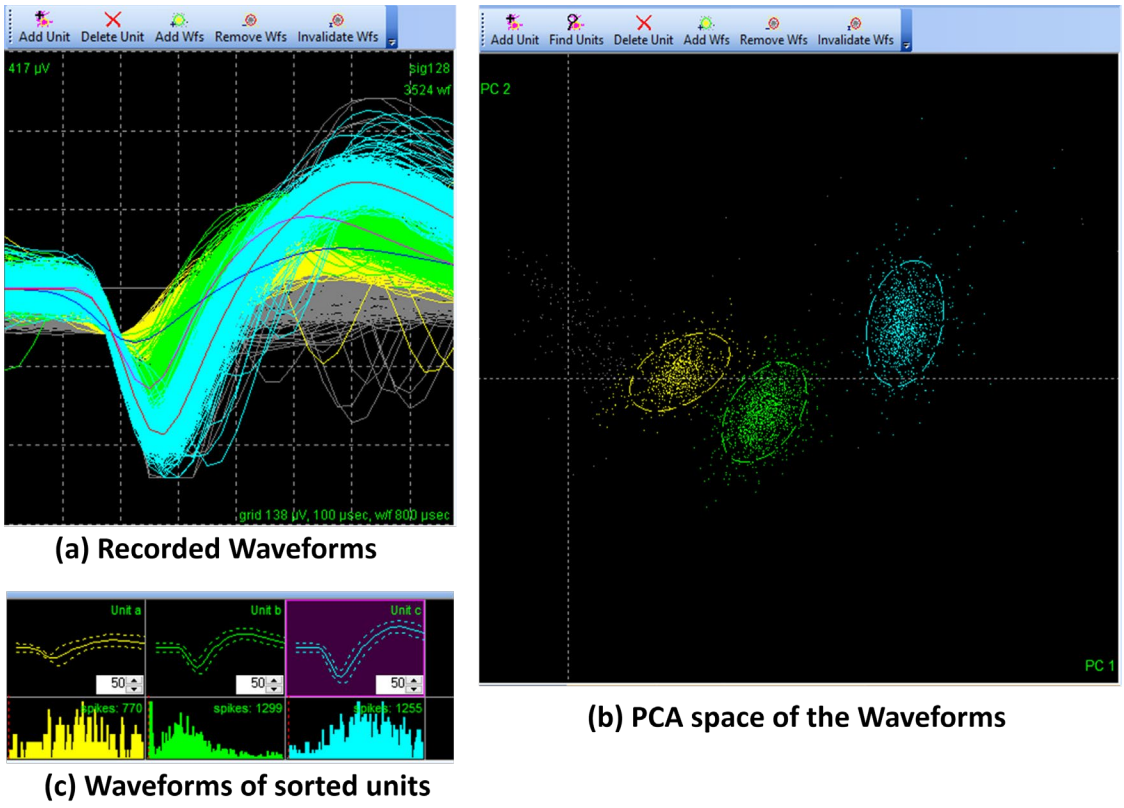

Figure 10: Sorted units from an example channel (Plexon Offline Sorter).

For sorting, we used K-mean clustering method where the value for "Range of units for K-means and Standard" (a default option from the software) was1 to 4, so that, it will search at most 4 clusters. Subsequently, we applied standard template sorting to keep the waveforms that have similar shapes (Figure 10 (a,c)). The above two method applied are automatic method from the Plexon Offline Sorter software. To ensure the quality of sorting a manual inspection was done on all the units from all the channel and units that might be noise was removed. The first two PCA (principal component Analysis) space (Figure 10, (b)) from all wave shape is observed carefully to detect activity from different units recorded on a single channel.

3.6 Recorded data and Pre-Preprocessing

The Number of units recorded from each cortex:

Figure 11 shows the total number of units recorded in all the cortices used (S1, M1, PMd, and PMv) and for each of the block types (MC, MU, OU, and OC). The block types are color cued and given as legend on the right subplot. The upper subplot shows the number of units from NHP S and the bottom subplot shows the same information from NHP P. The x-axis indicates which cortex is shown and the y-axis is the number of units for corresponding case.

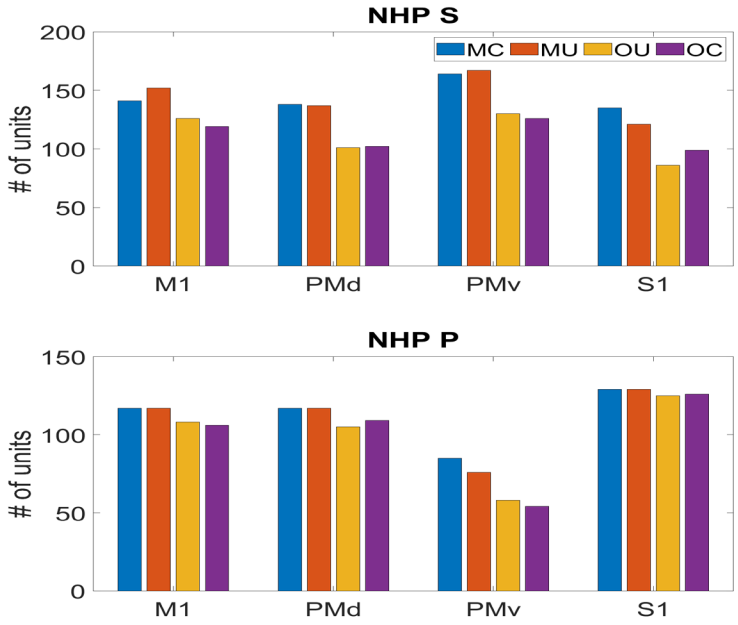

Figure 11: Number of units recorded from each cortex.

For each cortex there are four columns corresponding to the four data block types (MC, MU, OU, and OC) that are color cued as in the legend on the right subplot. The y-axis represents the number of units.

Force profile analysis:

For studying the Grip force activity recorded it is important that the force profiles of the trials used for analyses is homogeneous in terms of their shape due and that shape is expected to have a gaussian distribution type shape for ideal case because of the nature of the task. In our task structure the NHP had to apply grip force and maintain the grip force value in specified range and then release the sensor when the cylinder reached the target location and this mostly generated gaussian shaped force profiles. For some trials this shape was deformed when the NHP took more time to apply grip force above the threshold at the start of the trial or they released the sensor late. To use trials with homogeneous grip force profile a gaussian shaped force template was used to prune trials that had abnormal grip force profile shape like double peak or unusual lengths. For this whole procedure all collected force profiles were transformed into same length using linear interpolation.

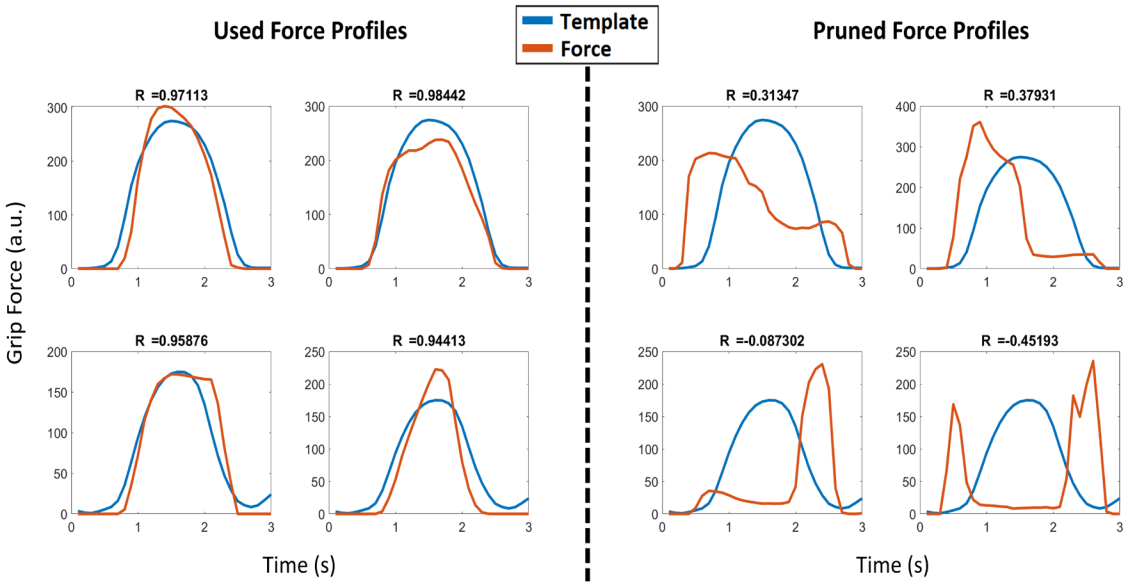

Figure 12: Used (left) and pruned (right) force profiles.

The mean of all the force profiles was computed to use as a temple for comparison. The correlation coefficient (R) between the grip force profiles for all trials and the template

was collected. The trials with correlation coefficient less than 0.8 was pruned for all the data analysis. Some example grip force profile shape used (left) and pruned (right) is shown on Figure 12. On each subplot the blue line shows the template force profile and the red line shows the profile for a particular trial. The corresponding correlation coefficient, R is given on the top of each subplot.

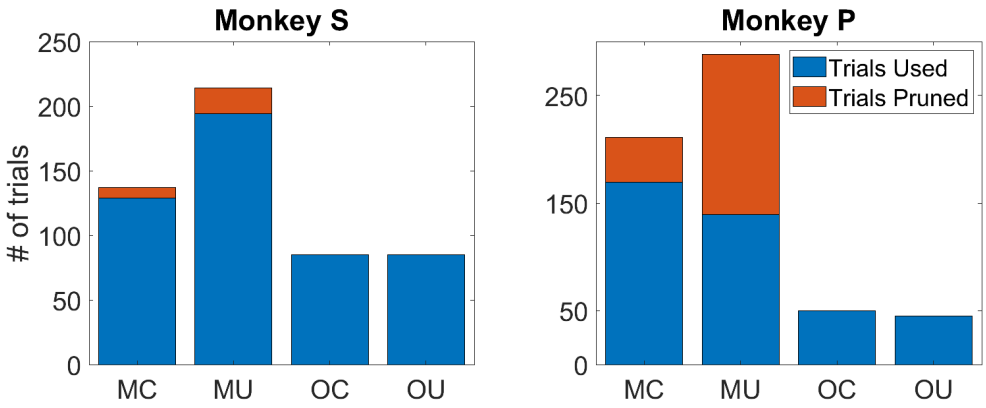

Figure 13: Number of trials used and pruned during preprocessing.

The total number of trials used in each of the block types for both NHPs is given in Figure 13, where for each case the column height represents the total number (y-axis) of trials performed by the NHP for that block (x-axis). The blue part of the bar is the number of trials used for the rest of the analysis and the red part shows the number of trials pruned. Between the two, NHP P was less consistent in maintaining a gaussian shaped grip force profile.

The number of trials in each data block:

Each data block contained two types of trials, the rewarding trials (R1) and the non-rewarding trials (R0). Figure 14 shows the number of R0 (blue) and R1 (red) trials in each of the data blocks. The manual blocks consisted of 129 (cued block, 40% R0 trials) and 194 (uncued block, 55% R0 trials) trials for NHP S and for NHP P the numbers were 127

(cued block, 50% R0 trials) and 139 (uncued block, 55% R0 trials). For observational blocks NHP S observed 85 (cued block, 44% R0 trials) and 104 (uncued block, 52% R0 trials), and NHP P observed 50 (uncued block, 56% R0 trials) and 45 (uncued block, 49% R0 trials) trials. These are the trials used for all the analysis for the rest of this thesis.

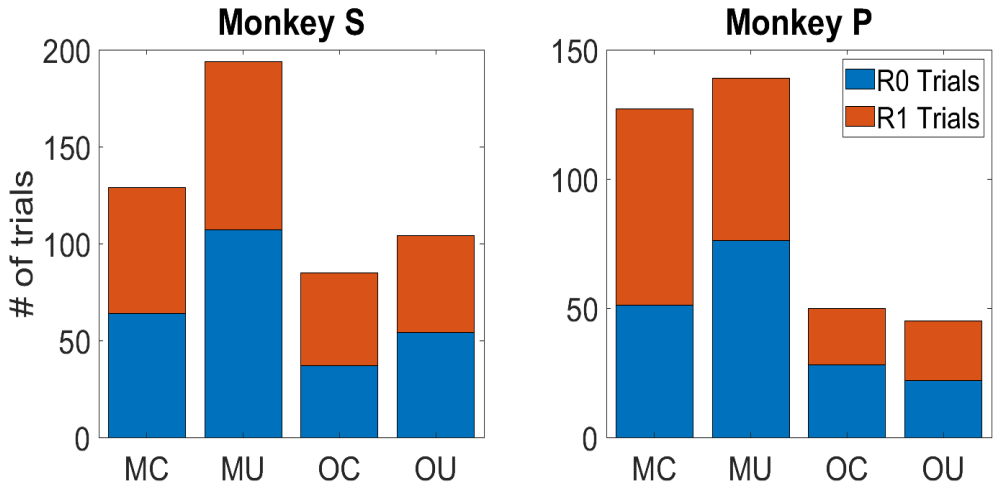

Figure 14: Number of rewarding (R1) and non-rewarding (R0) trials used for all data blocks.

The number of trials used for the data analysis is shown on the figure above for monkey S (left) and monkey P (right). Each bar represents the total number of trials and the blue part of the bar shows R0 trials where the red part is for R1 trials. The x-axis represents the block types (MC, MU, OC and OU) and the y-axis shows the number of trials.

The Grip Force duration for each data block:

The durations of applied grip force in R0 (blue) and R1 (red) trials are given on the box plots of Figure 15, for each of the block types (MC= Manual Cued, MU= Manual Uncued, OC= Observation Cued and OU=Observation Uncued). The box plots show the highest (upper line), 75th percentile, median, 25th percentile and the lowest values for force

duration of all the trials. A paired t-test (p-value <0.05) was performed to check if the R0 peak force was significantly different from R1 trials. The R0 and R1 force durations are significantly different only for the case of MC block of Monkey S. The grip force durations shown for the observational blocks are the duration grip force was applied by the automatic system.

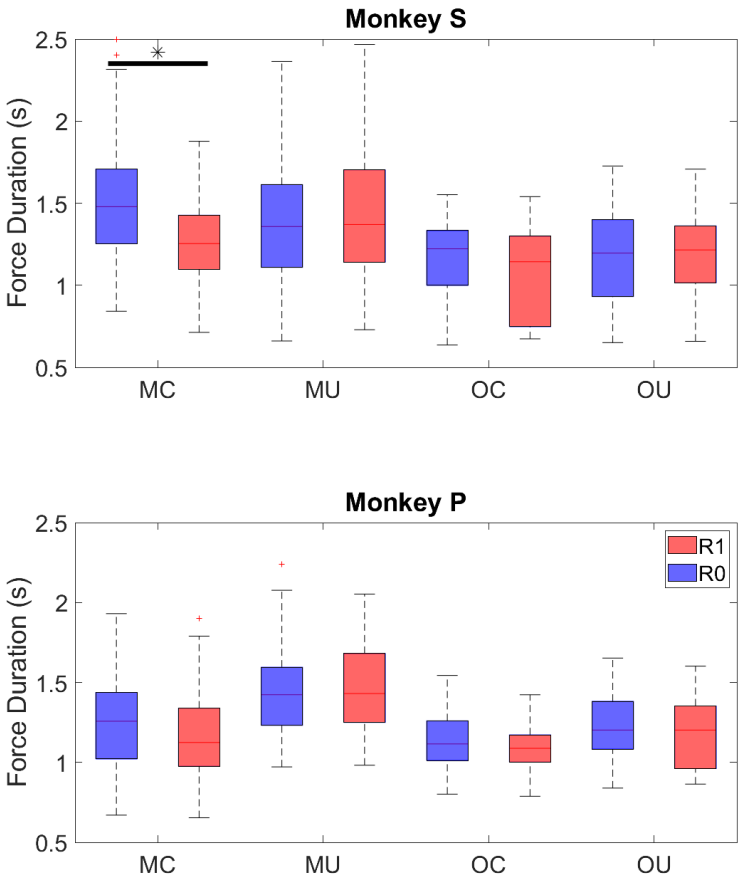

Figure 15: Force durations for used data blocks.

The mean duration that NHP S applied grip-force was 1.4 ± 0.4s (cued), 1.42 ±0.42s (uncued) during manual blocks. During observational blocks the "force" times were 1.12 ±0.26s (cued), 1.16 ±0.27s (uncued). For NHP P, the mean force duration was 1.2 ±0.28s

(cued), 1.45 ±0.29s (uncued) during manual blocks, and 1.12 ±0.18s (cued), 1.21 ±0.23s (uncued) during observational blocks. The box plot shows the median, maximum and minimum values with 75^{th} and 25^{th} percentile of the grip force duration of all the trials on each block individually. The x-axis shows the data block type (also shown on the legend which represents same information). The y-axis represents the force duration in seconds. The black line and asterisk (*) on the top shows the significant difference between R0 (blue) and R1 (red) trials.

Applied Grip Force for each data block:

The applied/observed peak grip force on each manual/observational block is plotted on the following Figure 16. The Red represents the R1 trials and blue is R0 trials. The block type (MC, MU, OC, OU) is mentioned in the x-axis. A paired t-test (p-value <0.05) was performed to check if the R0 peak force was significantly different from R1 trials. The significance test showed no p-value less than 0.05 and hence no asterisk (*) sign was plotted in any of the pairs. The minimum threshold of force for monkey S was 150 and P was 100 for the trial that had lowest force peak threshold. If the value goes below that value, the trial will be failed. The value mentioned is the minimum value for different trails a random value was added with the to increase the minimum threshold from 100 (monkey P) and 150 (monkey S).

The peak force from each block type is plotted on the following box plot and for each block type the R0 (blue) and R1 (red) trials are plotted separately for NHP S (left) and NHP P (right). The x-axis shows the block type (MC, MU, OC and OU). The y-axis represents the value of the grip force applied with arbitrary units. The grip force values from R0 and R1 trials were significantly different for any of the case and hence no asterisk

(*) is present. The grip force amount for the observational blocks are the amount applied by the automatic system where the system used a random grip force amount value within the boundary conditions given for each trial.

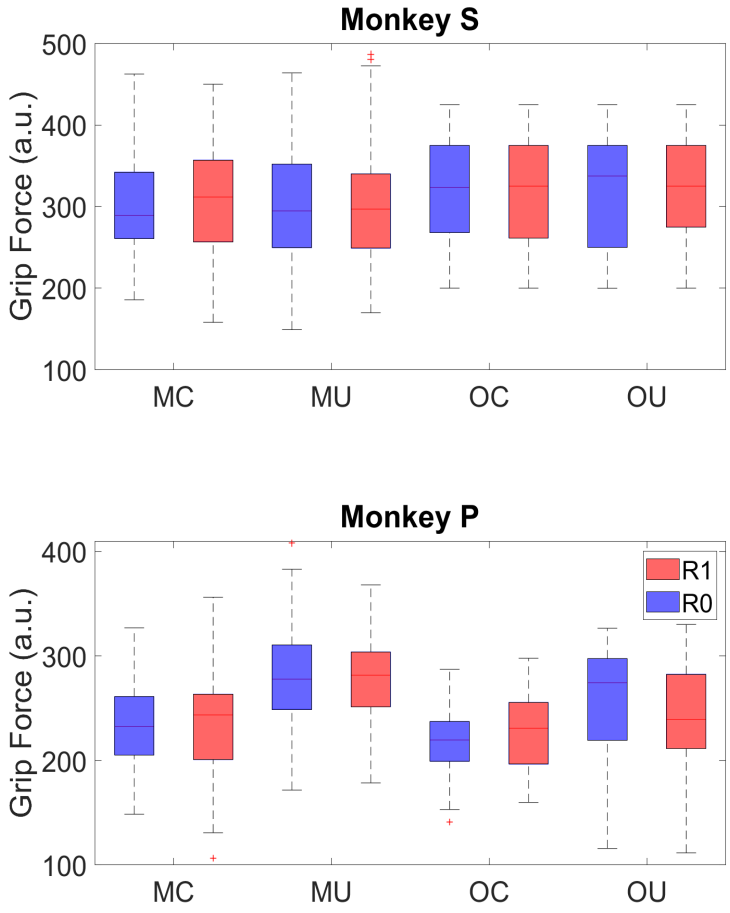

Figure 16: Peak force applied during each block for monkey S (top) and monkey P (bottom).

Reaction time to apply grip force:

The reaction time to apply grip force for R0 and R1 trials is plotted on the following Figure 17. The manual blocks for Monkey S (left) and Monkey P (right) were plotted. The blue and red color represents R0 (blue) and R1 (red) trials from the same data block (MC, MU).

The asterisk (*) on the top of the black line indicates the reaction time is significantly different between R0 and R1 trials (paired t-test, p-value <0.05). The reaction time in this case is the difference between the times, NHP was allowed to apply grip force (start of the grip force scene) to the time when they applied 10% of the peak grip force. From the following plot the reaction time is significantly different only for the manual cued block for Monkey S.

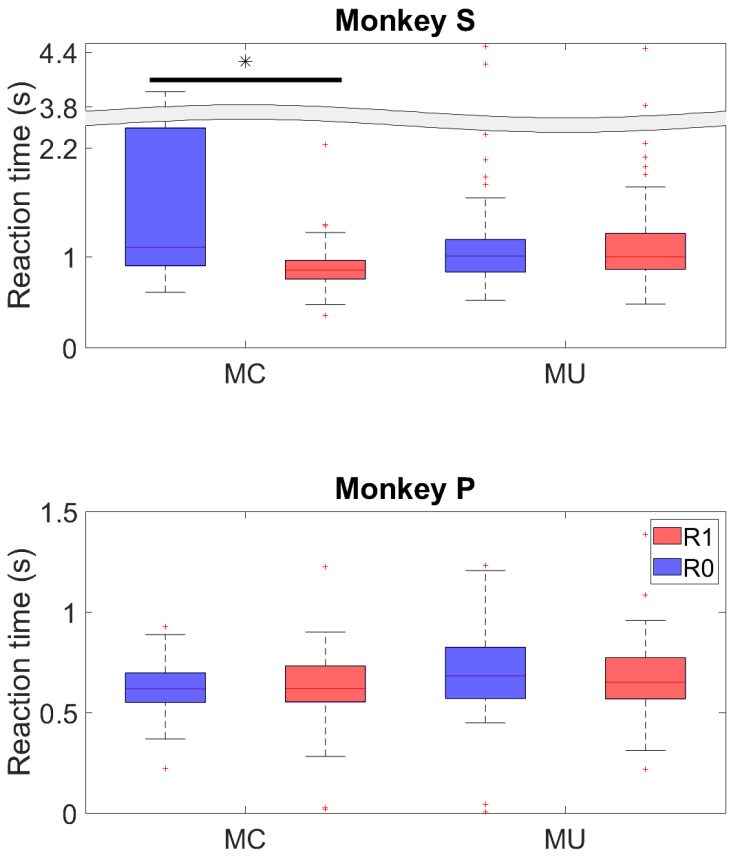

Figure 17: Reaction time to apply grip force for all data blocks.

The reaction time for R0 (blue) and R1 (red) trials for all the block type is given on the following plots. The x-axis shows the block types MC, MU for the case of manual blocks. The y-axis shows the reaction time in seconds. The asterix (*) on the top of each

pair represents they reaction time is significantly different between R0 and R1 trials. The left subplot is for Monkey S and right subplot is for Monkey P.

3.7 Significance Related to Reward

We only considered successfully completed trials for all analyses and results presented in this work. We analyzed single unit activity from four types of task blocks for each NHP, cued or uncued, and these were either manual or observational. For trials that contained a visual reward cue, the post-cue analysis window began immediately after the green visual cue came to rest. In uncued trials, the "post-cue" period (0-500ms) began when the robotic arm returned to its rest position from the previous trial. We defined the "post-result" period (0-500ms) as the time after the cylindrical object was successfully placed at the target location. We analyzed spike activity in the post-cue and post-result periods separately for cued and uncued blocks to identify units significant for reward modulation. We binned the spike activity and for that we utilized non-overlapping bins of 100ms covering 500ms for both the post-cue and post-result periods. We collected the p-values from t-test for Spearman Rank correlation and the test was done between the binned spike rate and corresponding reward levels (1 for R0 and 2 for R1). For reward level 1 is used for R0 and 2 is for R1 and 0 value was avoided for leveling to avoid any bias toward zero value. We then extracted units that were significant (t-test, $p < 0.05$) for reward expectation (post-cue activity, R1 vs. R0 trials) and reward result (post-result activity, R1 (after reward delivery) vs. R0 (after successful trial with no reward)). The p-values from the test are adjusted for multiple comparisons using the false discovery rate (FDR) procedure by Benjamini and Hochberg (FDR method) (Benjamini et al. 1995) for number of times t-test was applied which is equal to the number of units for each case. Finally, we compared

spike rate activity between cued and uncued blocks to gain better insight as to how reward feedback information was affected by the presence or absence of a reward cue that is reward expectation based on explicit environmental cues.

3.8 Force Trajectory Prediction

We applied linear regression in two steps to identify units that showed significant prediction of grip force from S1, M1, PMd and PMv. In these two steps, the first step identified all units that were significantly related to grip force, which was used below in the sections labeled "*Grip Force Tuning Curve Analysis"* and "*Identifying Observation Modulated Neurons*". The second step was applied to sort out a selective number of the units (from the units collected on the first step) for force prediction to reduce predictor numbers and avoid computational complexity. Unit activity from these cortices were analyzed along with force profiles for both NHPs during manual and observation task blocks (see supplementary material). During some trials, initially the NHP's applied more grip force than necessary and in an effort to meet the target value, reduced their grip force drastically. This resulted in an overcorrection where the NHP had to apply more force to meet the requirement and resulted in force profiles with multiple peaks. We manually inspected and pruned all force profiles that contained multiple peaks due to highly variable or corrective grip forces applied by NHPs. We defined force onset as the point where force values increased from zero to positive value and force offset when values returned to zero from positive applied force, because the NHPs only grasped the force transducer after the robotic arm reached the virtual object, and a trial was considered successful when they zeroed their output force, let go of the handle, to release the virtual object at the target position. Force data was collected from 0.5s prior to force onset through 0.5s after force

offset for all trials. The collected force data was smoothed using a Gaussian kernel (100ms wide). During observational trials the visually cued "force" output profiles were trapezoidal, therefore smoothening gave the force profile a gaussian shape like the force data on manual blocks. From the force data collected in each trial, we evaluated neural spike activity 0.5s prior to, and following each force sample value. This neural activity was further placed into ten non-overlapping time bins centered on each force value (100ms bins, covering 0.5s pre- and 0.5s post-force sample value) to determine a unit's significance to grip force, so for each unit there were 10-time bins used as predictors. We performed this separately on each unit from all four cortices. We smoothed the raw data using a Gaussian kernel (100ms wide). We wanted a generalized kernel width that would be used for both cued and uncued data blocks of the same kind, manual vs. observational. The force prediction accuracy for different kernel bin widths from 10ms to 250ms was determined for all data. We manually selected the above value of kernel width so that the predictions were close to the peak prediction values for all blocks.

Data recorded from each NHP was split into a fit (90%) and test (10%) set to check goodness of fit and verify predictive performance of the final linear regression model (equation 2). However, before testing the final linear regression model, we extracted significant units related to force in a two-step process. To do this, we subdivided the 90% fit set into 80% (fit) and 10% (validate) data subsets, see the supplementary section for a cartoon of this procedure. The equation used for linear regression model when each single unit was tested for force fit was,

$$\boldsymbol{y_f} = \boldsymbol{a}\mathbf{X}_{fr}^{n_i} + b. \qquad (1)$$

The model predicts the applied grip force value with time taken from all the trials. Equation 1 shows the linear model used, where $\boldsymbol{y}_f$ is the vector of force values, $\boldsymbol{X}_{fr}^{n_i}$ is the binned spike rate for neuron n_i, while $\boldsymbol{a}$ and b are coefficients fit to the data. In the first step, we tested each unit in the 80% subset for the fit related to force using equation 1 and F-test of the model parameters. Units were sorted according to their p-value from the force-fit test and only those with a significant fit ($p < 0.05$) were considered in the second step of the process. For the second step, we took significant force units, starting with the most significant (lowest p-value), and used it to test prediction of force values in the remaining 10% validation subset. We calculated the R-squared value after each unit was added to the model and if the R-squared value increased (improved prediction results), the unit was kept. Remaining units that did not improve the model's force prediction were pruned. After the two-step process, the subset of significant force units was utilized in the final linear regression model (eq. 2). This subset was used with updated coefficients fit to the original 90% dataset. Finally, we used the held out 10% test set to determine prediction and validate accuracy of the linear regression model (eq. 2) by comparing them against actual recorded force values. The model we used is,

$$\boldsymbol{y}_f = \boldsymbol{\alpha}\mathbf{X}_{fr} + \boldsymbol{\beta}. \qquad (2)$$

The regression model used for final grip force prediction from neural activity is shown in equation 2. Here $\boldsymbol{y}_f$ denotes grip force and $\mathbf{X}_{fr}$ represents binned firing rates for the population of units being used, $\boldsymbol{\alpha}$ and $\boldsymbol{\beta}$ are model coefficients fit to the data. The algorithm for the above procedure is summarized in the following figure.

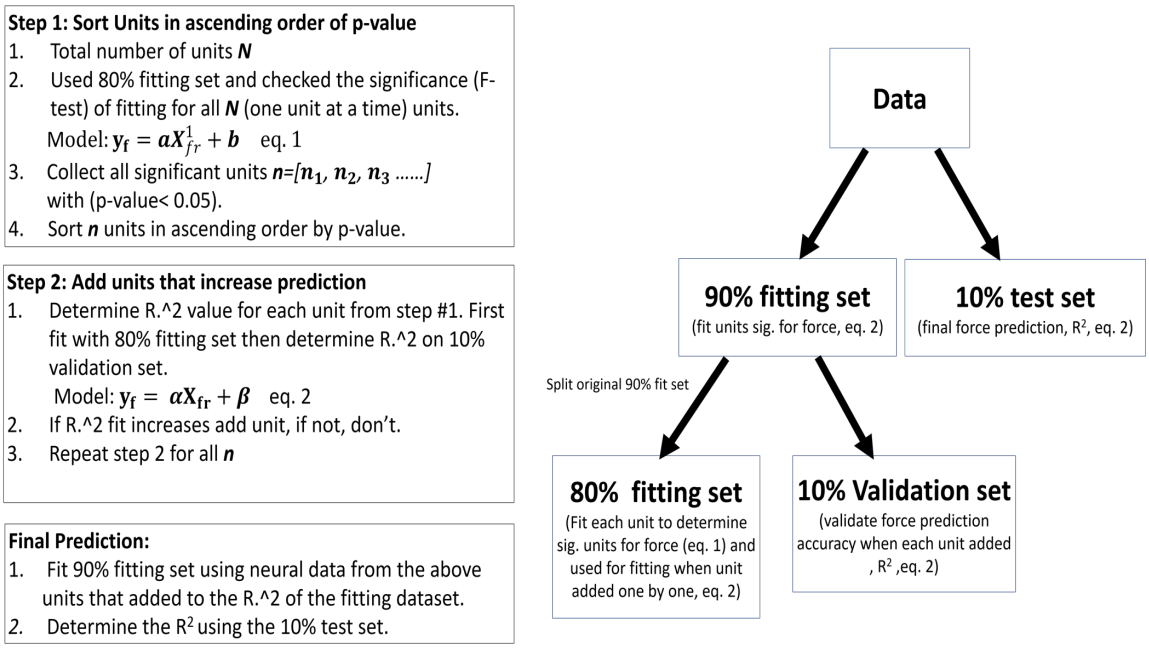

Figure 18: Algorithm for force decoding process using linear regression.

The algorithm on the above figures shows the two-step process of collecting a subset of units significant for force to achieve a comparatively better prediction of force using linear regression.

3.9 Grip Force Peak significance

As force profiles were stereotypical smooth Gaussian-like profiles, we wanted to make sure our regression model fits and predictions were meaningful, and not solely due to a unit having a phasic response that could be used to fit the stereotypical waveform. Therefore, we determined how neural activity correlated with the peak values of the Gaussian-shaped force profiles during each trial. We considered force values around the peak force applied on each trial (three values around the peak including the peak value) and we placed neural data, centered around each of them, into ten 100ms non-overlapping bins from 500ms pre peak force to 500ms post peak force neural activity. Each unit was

tested for peak force significance (F-test, FDR corrected for number of populations that is the number of corresponding units) by fitting a linear regression model with peak force values and spike rate for each of the ten bins.

3.10 Identifying Observation Modulated Neurons

Our previous work focused on identifying significant units related to reward and/or force within single blocks of data (Zhao et al., 2018) to expand on these findings, we thought it was important to investigate the cause behind each unit's modulated activity across multiple blocks, during both manual (Zhao et al., 2018), and observational tasks. We hypothesized modulation responses during observation might be explained by the presence of mirror neural activity when NHPs observed the task, received reward, or possibly both. To this end, our goal was to detect units that encoded the following: 1) Motor actions that is the physical application of force; 2) Cued "force" during visual observation; 3) units that encoded both 1, and 2. 4) Determine which of these (1-3) were further modulated by reward level, cued or uncued. We started by identifying and tracking single unit activity across multiple blocks of recorded data. We compared single unit activity between reward-cued manual and observational blocks, and again between reward-uncued manual and observational blocks for each NHP and cortices (S1, M1, PMd and PMv). We tracked single unit activity from the two manual and two observation blocks performed in a single day for each NHP. If a unit on a channel retained the same waveform over all 4 recorded blocks, we considered it the same unit. In addition, we verified this single unit activity by checking the correlation coefficient between the waveform shapes across all blocks, where a high correlation (> 0.98) indicated the same unit.

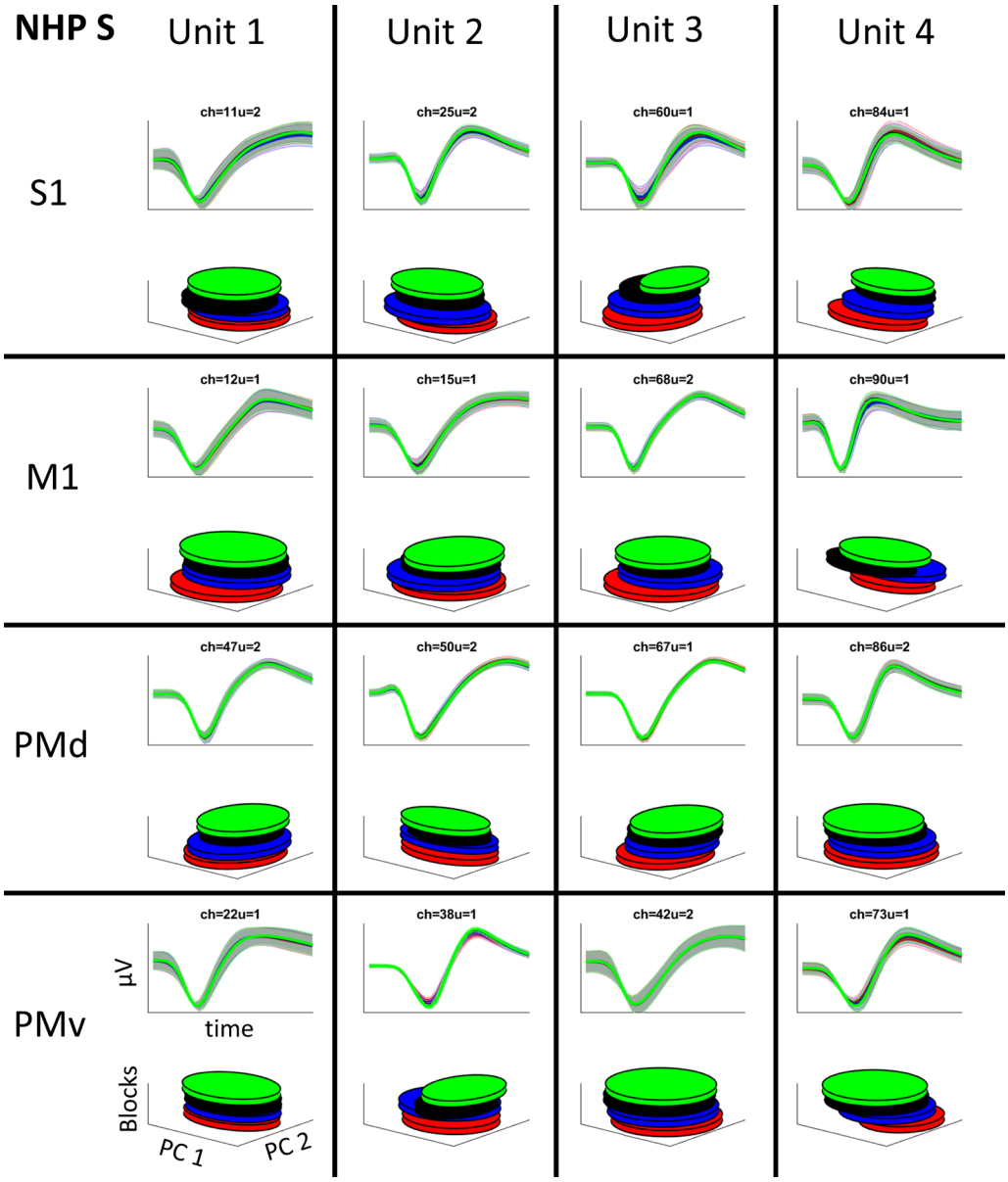

Figure 19: Waveform and PCA plot for example units that are tracked (NHP S).

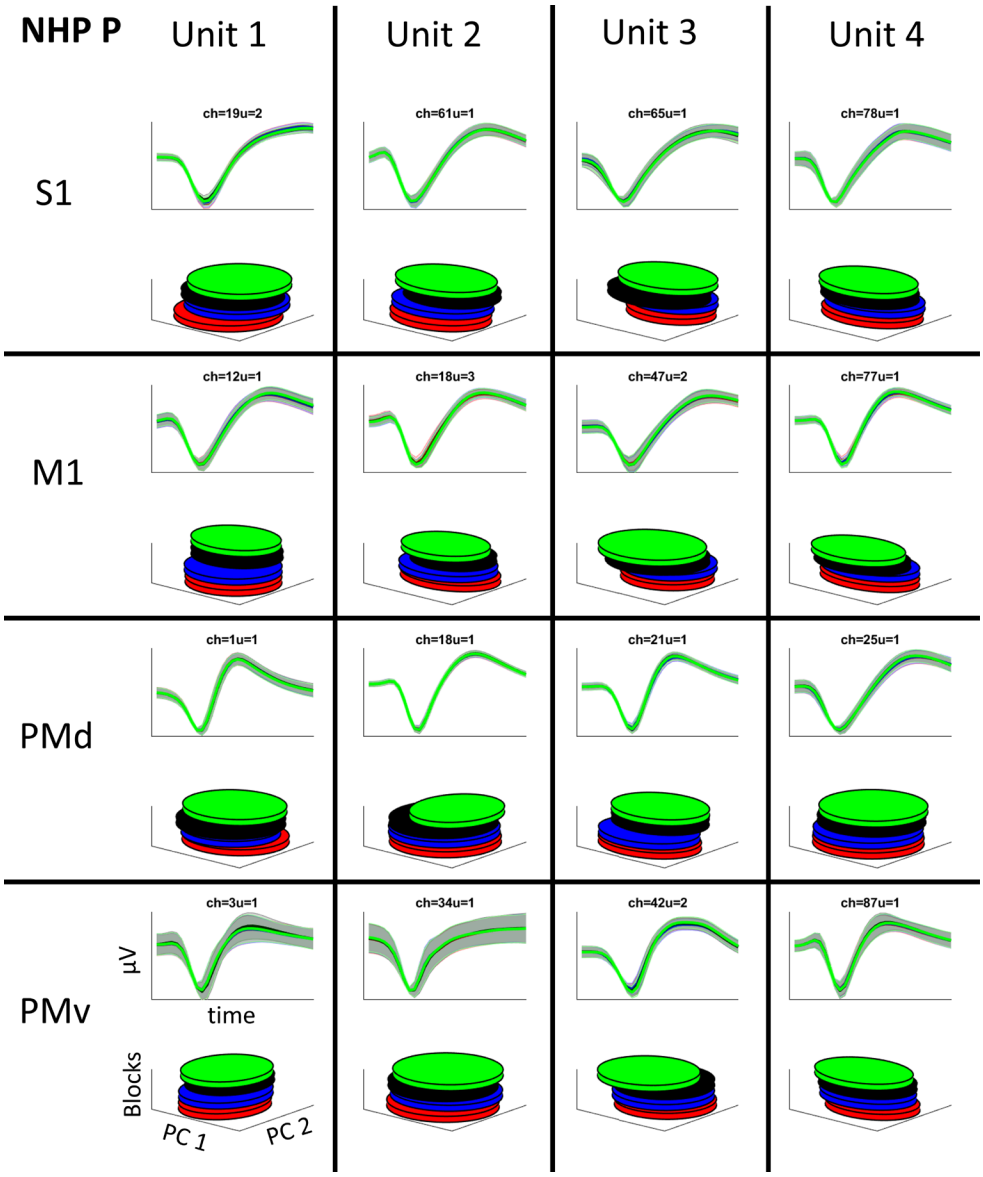

Figure 20: Waveform and PCA plot for example units that are tracked (NHP S).

We also confirmed the consistency of single unit activity across blocks by checking the first two principal components using principal component analysis (PCA). Figure 19 (NHP S) and Figure 20 (NHP P) shows four example units from all four cortices (S1, M1, PMd, and PMv). Performing these checks allowed us to track single unit activity with significant correlation to reward, force, or both during manual and observation task during cued and uncued blocks towards identifying putative mirror neural activity responding to

force and reward modulation. Performing these checks allowed us to track single unit activity with significant correlation to reward, force, or both during manual and observation task blocks towards identifying putative mirror neural activity responding to force and reward modulation.

3.11 Grip Force Tuning Curve Analysis

Our previous research concerning force tuning curves in M1 showed a significant difference between R1 and R0 trials (Zhao et al., 2018). We applied the same analysis to our M1, S1, PMd and PMv data to determine if neural activity led to different force tuning curves when taken from R1 vs. R0 trials. As in Zhao et al. 2018 we utilized analysis of covariance (ANCOVA). We analyzed each unit previously identified as significant for force to measure whether the slopes of the tuning curves between R1 and R0 were significantly different (F-test, $p < 0.05$). The p-values from the ANCOVA test are adjusted for multiple comparisons using the false discovery rate (FDR) procedure by Benjamini and Hochberg (FDR method) (Benjamini et al. 1995) for number of population. Significant units identified by ANCOVA were considered to have a force representation that was modulated by reward expectation, and units that also passed the FDR correction are stated explicitly.

3.12 NHP Behavioral Summary:

We used two NHP for our experiment, one male *Macaca* Radiata (NHP S) and one female *Macaca* Mulatta (NHP P). Both NHP performed manual and observational task. During the observational version of the task a plexiglass box restrained their hand from reaching the grip force sensor. For the manual version of the task they were able to reach

the force sensor. During manual trials when they were cued to apply grip force, they reached to the grip force sensor and at the end of a trial they usually rested their arm on the base of the grip force sensor. NHP S achieved success rates of 77% (cued manual) and 82% (uncued manual) during the two manual-task blocks, while NHP P achieved rates of 58% (cued manual) and 72% (uncued manual). This comparatively low success rate for the manual block when they were cued for reward at the beginning shows that both NHP had an idea about the reward information. Between the two monkeys, performance of S during the trial was affected more by reward cue information compared to P. Figure 15 shows the force duration is significantly different between R0 and R1 trials for NHP S which is not same for NHP P. Also, from Figure 17, we can see the reaction time is significantly longer when NHP S completes R0 trials compared to R1 trials. Both results are indication that NHP S task performance was more dependent on reward compared to NHP P. One thing that should be mentioned that, for NHP S, although reaction time and grip force duration was significantly different the peak force applied on each trial was not significantly different (Figure 16) since the applied grip force was supposed to be within a boundary value cued during task.

CHAPTER 4

RESULTS

The results section is structured as follows: we start by presenting raw data from manual and observational versions of our task showing peri-event-time-histograms (PETHs) and rasters of sample units, indicating the modulation of single units by both grip-force and reward during manual and observational trials in M1, S1, PMd and PMv, for NHP P and S, Figure 21 andFigure 22 respectively. Next, we present population results from linear regression focusing on grip force, showing that subpopulations of these regions can encode the grip force trajectories (Figure 33 and Figure 35) even during observational trials. In Figure 38, we test for temporal shifts between the neural representation of force between the manual and observational versions of the tasks, to determine if the same units are acting in response to the visual input, classical MNs or predicting such input as expected by mental simulation of the predicted visual stimulus, which could be either mental simulation of the expected movement (Cisek & Kalaska, 2004), or MNs responding in an anticipatory way due to the familiarity of the task (Maranesi et al., 2014). Subsequently, we give information on units that are modulated by both force and reward during the force output period of the manual and observational tasks for the same single units that is putative MNs for force and reward.

4.1 Neural Data

In Figure 21-Figure 22,b1-e1 we present raster plots for example units with all trials aligned to the onset or offset of the grip force. The mean force profile (indicated with green lines on the raster plots) shows force onset and offset, plotted with arbitrary units for R0

(blue raster) and R1 (red raster) trials. The mean duration that NHP S applied grip force was 1.4 ± 0.4s (cued), 1.42 ±0.42s (uncued) during manual blocks. During observational blocks the "force" times where 1.12 ±0.26s (cued), 1.16 ±0.27s (uncued). For NHP P, the mean force duration was 1.2 ±0.28s (cued), 1.45 ±0.29s (uncued) during manual blocks, and 1.12 ±0.18s (cued), 1.21 ±0.23s (uncued) during observational blocks, see Fig.S11 – S13 for more on force level, duration and reaction times. NHP S achieved success rates of 89% and 85% during the two manual-task blocks, while NHP P achieved rates of 84% and 90%. The R0 and R1 mean force profiles are plotted with the same scale for comparison. All four units shown in both Figure 21 and Figure 22, were significant (F-test, $p < 0.05$) for grip force. Plots ax (x=1, 2, 3 and, 4) show the mean spike waveform with standard error (shaded) for a single unit (top) and its PCA space (bottom) for all 4 blocks, manual cued (MC), manual uncued (MU), observational uncued (OU) and observational cued (OC), which were all recorded on the same day and in the aforementioned order for each NHP. Each raster subplot (b-e) shows activity for force onset (left) and force offset (right) periods.

Units in Figure 21 were chosen as they represented the variety of responses we saw in the population. We binned (100ms) the post force onset spike activity from the point when force sensor value crossed above 50 (a.u.) and pre force offset activity until the reading went below 50 (a.u.). This value of 50 was chosen because the simulation environment considered a trial successful when force sensor value went below 50 after a successful transport state (fig. 1). The binned spike rate was then fit using a Generalized linear regression model (GLM) with spike rate and corresponding reward level (0 for R0 and 1 for R1 trials). We plotted the significant p-values for the coefficient of predictor

variable (firing rate) with asterisk (*) on each corresponding plot subplot. For example, in Figure 21.b1-c1 we see an S1 unit that decreases its activity at or just after the onset of "force" and is suppressed around the force offset period. In addition, it shows some modulation by reward. Similarly, in Figure 21.b2-c2, we see an M1 unit within essence the similar response to the S1 unit, where the M1 unit is suppressed at force onset and activated at force offset with some reward modulation as well. In Figure 21.b3-c3 a PMd unit is shown that is suppressed before force onset and has its peak activation pre-offset. Monkey P data was not as responsive to reward activity as Monkey S. For the given units, there are two cases (Figure 22.c1-b4) for NHP P where the units were significant for the offset non-cued variable. However, after we adjusted the p-values using the FDR (for p=0.05) method for number of populations they did not remain significant.

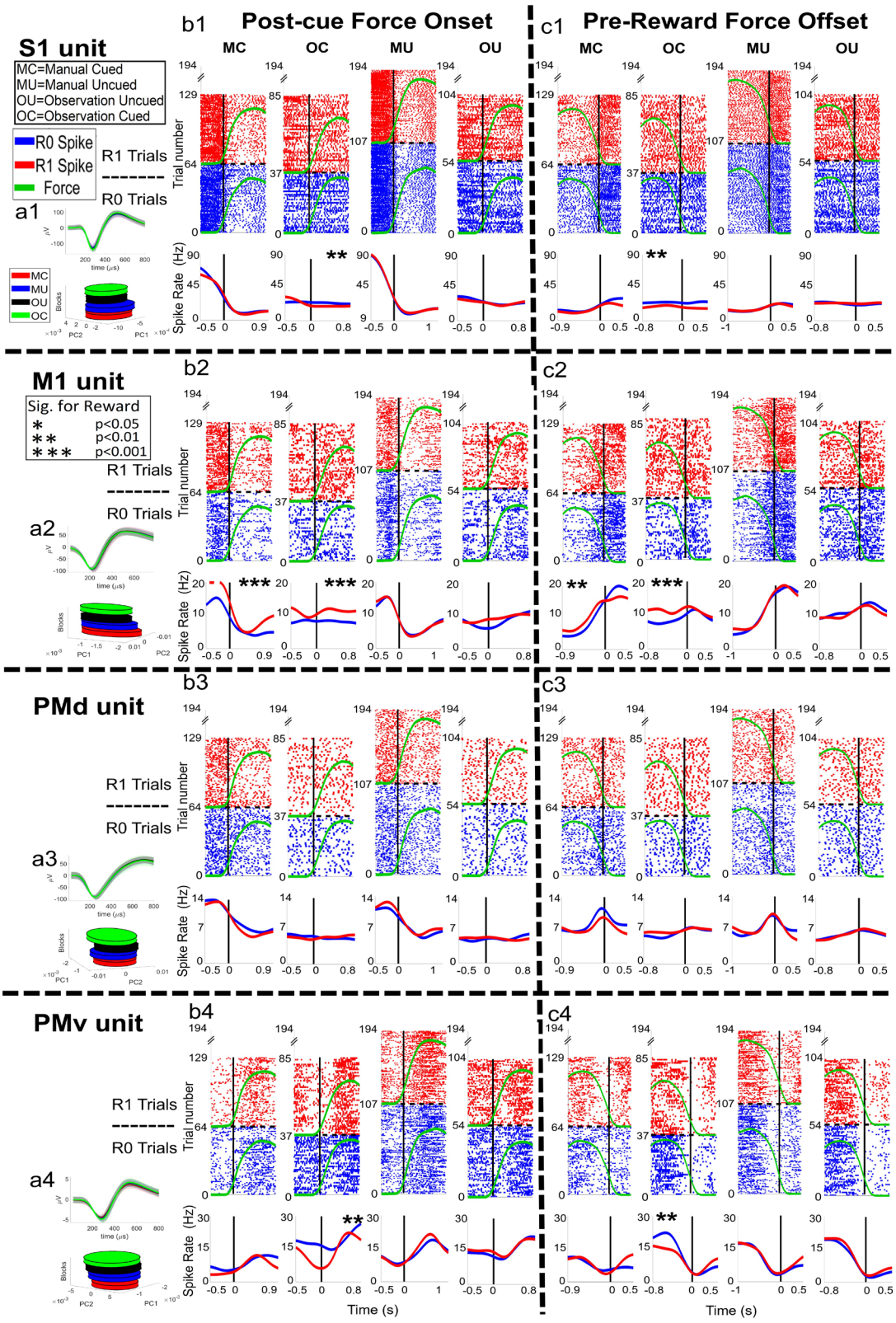

Figure 21: Mirror neuron activity in S1, M1, PMd and PMv (NHP S).

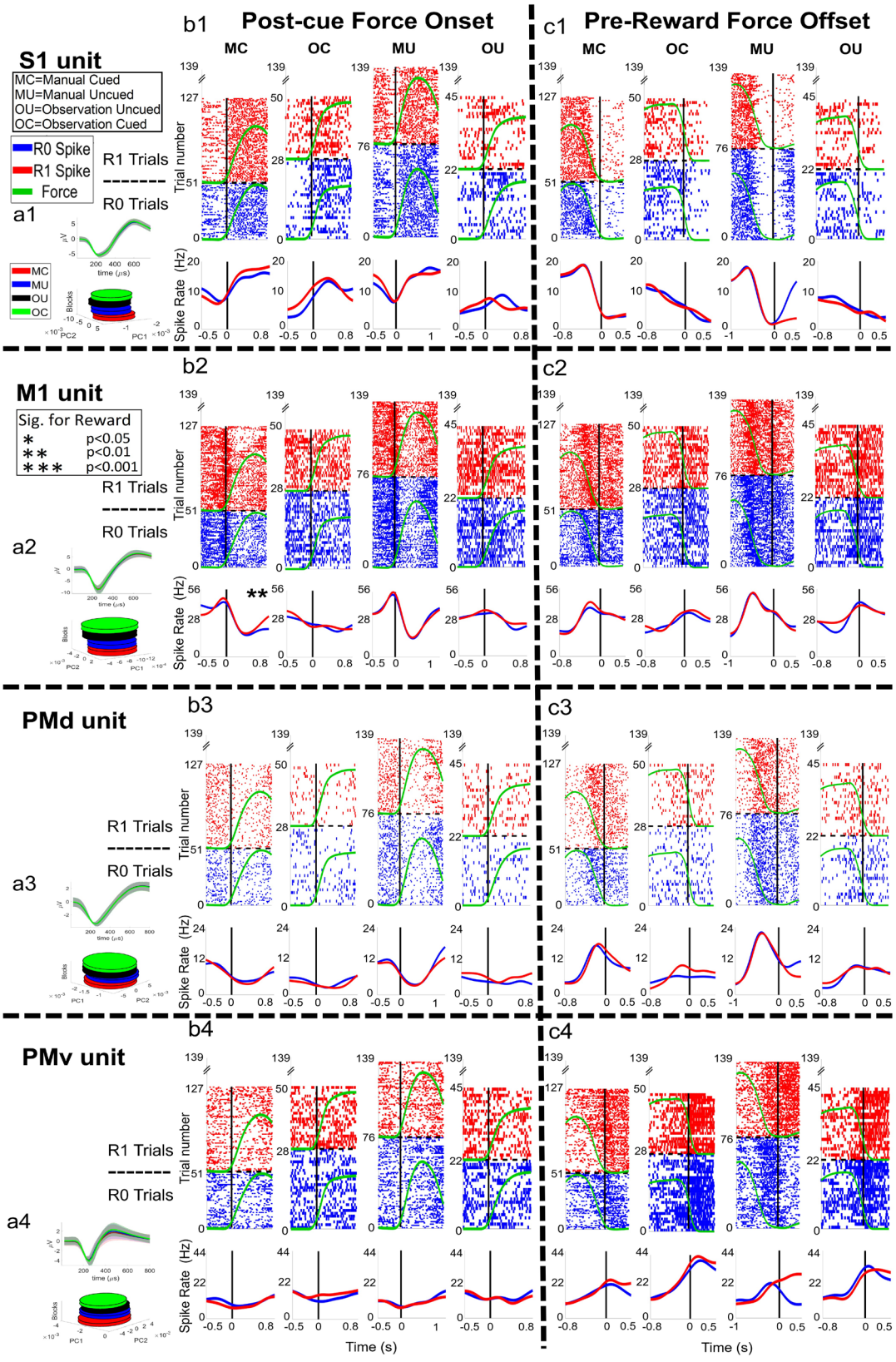

Figure 22: Mirror neuron activity in S1, M1, PMd and PMv (NHP P).

The raster plots of example units from NHP S (Figure 21) and NHP P (Figure 22) during the manual and observational blocks are given above. For both figures, the subplot numbers, 1-4, indicate the brain regions (1-4 for S1, M1, PMd and PMv respectively). The letters, a-c, after the numbers, 1-4, are associated with the (a) single unit waveform for an example unit, (b) force onset plots and (c) force offset plots. For (b) and (c) there are four plots for, manual cued task (MC), observational cued task (OC), manual uncued task (MU), and observational uncued task (OU) task sequentially. The post-force onset and pre-force offset time is set as 60% of the mean force length of all trials for that task. On each subplot (b, c), the x-axis represents time in seconds, for raster plots the y-axis represents trial number, for spike rate plots (bottom of subplots) y-axis is spike rate in 'Hz'. The dashed horizontal black line on each plot divides the R1 trials from R0 trials. Below the raster plots, solid red and blue lines indicate mean spike rate (Hz) for R1 and R0, respectively. An asterisk (*) indicates post force onset or pre-force offset spike activity is significantly (t-test, $p<0.05$, $p<0.01$ and $p<0.001$ denoted by *, ** and *** respectively) different between R0 and R1 trials.

The observational response to "force" was weaker compared to the actual force experienced during manual trials and did not always align with the force onset and offset times as precisely. To make it clear, by force onset and offset during observation means the time automatic system applied grip force and stopped applying grip force correspondingly. All units seen in Figure 21 and Figure 22, had significant fits to grip force (F-test, $p <0.05$). This F-test was performed on the regression model (equation 1) to test whether it was a better fit than a degenerate model, which consisted of only a constant

term. Figure 21 and Figure 22 show a total of 8 example units; 1 from each cortical region (M1, S1, PMd and PMv) for each NHP, P and S, from reward cued, and uncued blocks.

4.2 Reward Significance

The number of units significant for reward cue and reward feedback was recorded using a ranked significant t-test. The units were then post processed with FDR. The units that are significant after FDR correction from each cortices (S1, M1, PMd, and PMv) of both NHP (S and P) is given in Figure 23 and Figure 24.

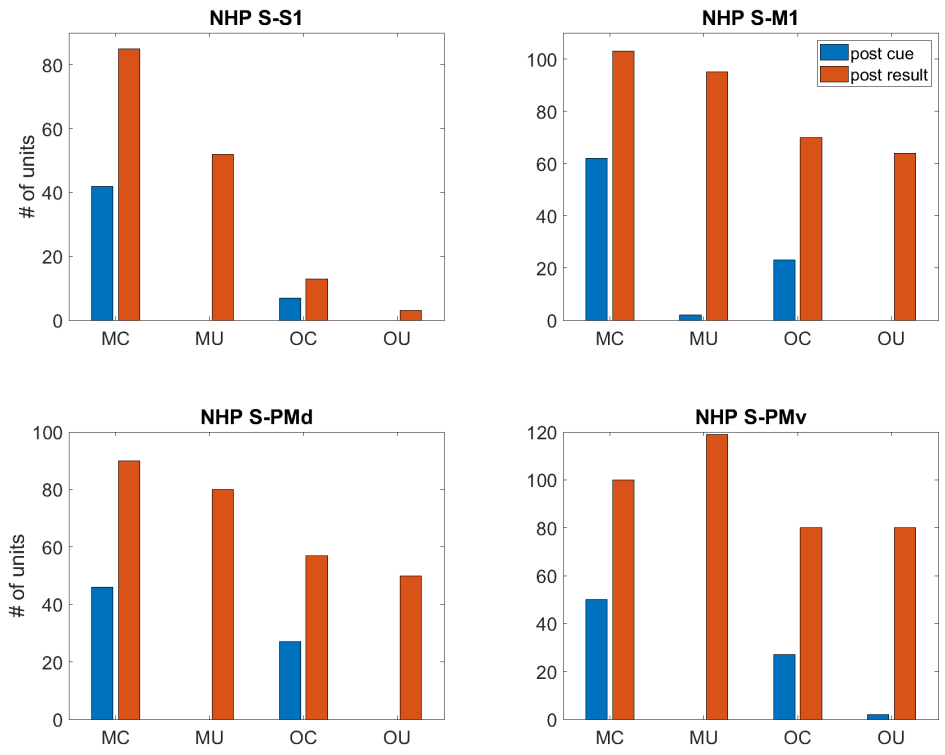

Figure 23: Units significant for reward cue and feedback (NHP S).

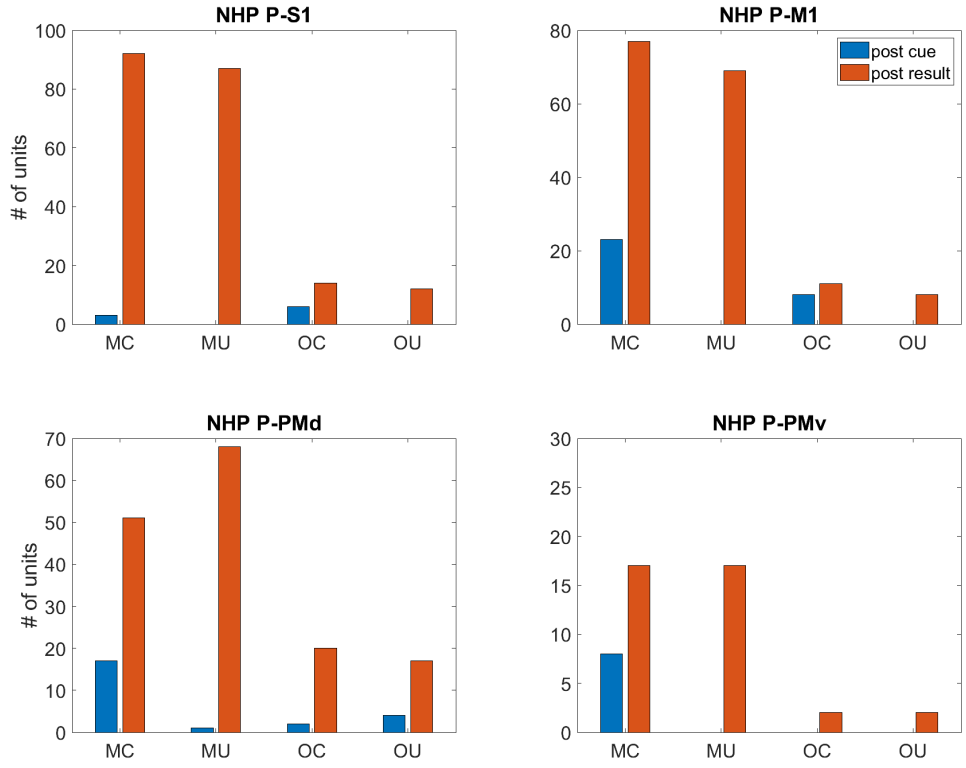

Figure 24: Units significant for reward cue and feedback (NHP P).

The x-axis shows the block type (MC, MU, OC and OU) and y-axis shows the number of units that are significant after FDR correction. The blue column shows the number of units significant for reward cue (post cue 0-500ms spike activity) and the red column shows the significance for post result period (post result 0-500ms spike activity was used). As expected, the post cue period for cued block types (MC and OC) showed significant units and uncued block type showed almost no significant units for cue. Post result period was more responsive to reward activity for both NHP S and P. In general from

overall result we can see that the reward activity is relatively high specially for reward cue in the case of NHP S (Figure 23) compared to NHP P (Figure 24).

The first aim of the thesis was to detect the influence of reward in sensorimotor cortices and show a comparison between the used cortices (S1, M1, PMd and PMv). Figure 23 and Figure 24 represent the total number of units that are significant for reward cue and given reward for NHP S and P. It is clear from the mentioned figures that the reward information is present during post reward cue and post reward delivery neural activity where the cue has a less effect compared to actual reward. Also, NHP P data overall was a little less responsive for reward cue compared to NHP S, considering the number units found significant.

The followings Figure 25-Figure 28 shows the raster plot of an example unit recorded from S1 (Figure 25), M1 (Figure 26), PMd (Figure 27), and PMv (Figure 28) cortex of NHP S. On each figure there was three sections of subplots where subplots in figure-section (a) showed the waveform (upper subplot) recorded from four data blocks for that units and the first two PCA space (bottom subplot) plotted for all the waveforms. This shows the units waveform had a consistent waveshape during all the data blocks used for analysis. The figure-section (b) shows four subplots of raster plot (upper part) and mean spike activity (bottom part) for four data blocks in the following order of MC, OC, MU, and OU from left side. The raster plots and mean spike plots on figure-section (b) show data around reward cue onset (black vertical line) from 0.5s pre spiking activity to 1 second post spiking activity. Figure-section (c) subplots show the plots for reward delivery onset. The Figure 29-Figure 32 show example units from NHP P in the similar order as described for NHP S above. For all the figures Red color is associated with data from Rewarding

trials (R1) and Blue is for non-rewarding (R0) trials. All the units chosen for Figure 25-Figure 32 are also the units considered as Mirror neuron (MN) units (Section "4.4 Force-Mirror Neuron Units:").

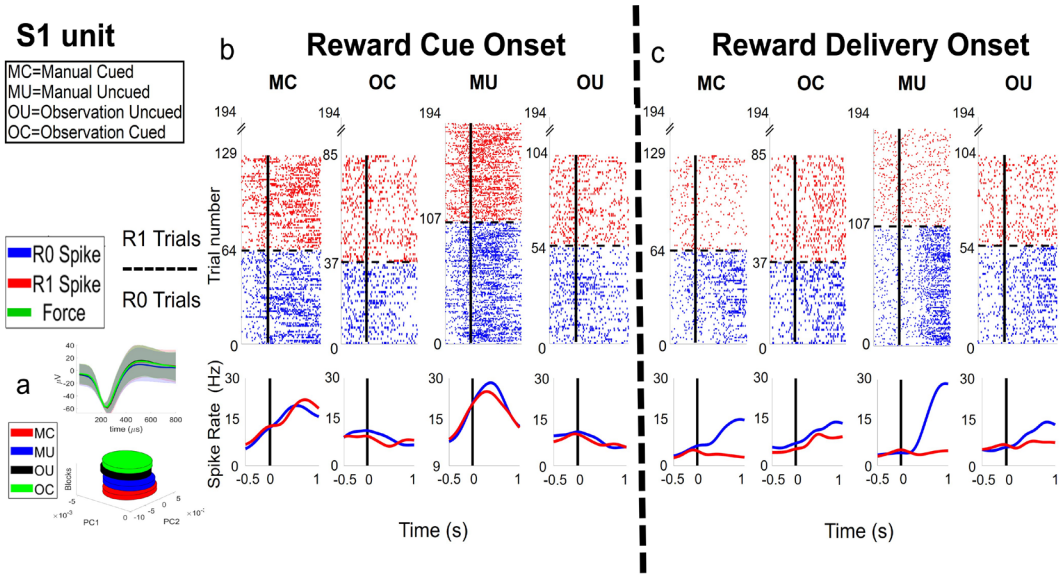

Figure 25: Reward cue (b) and delivery onset (c) for an example unit from S1 cortex of NHP S.

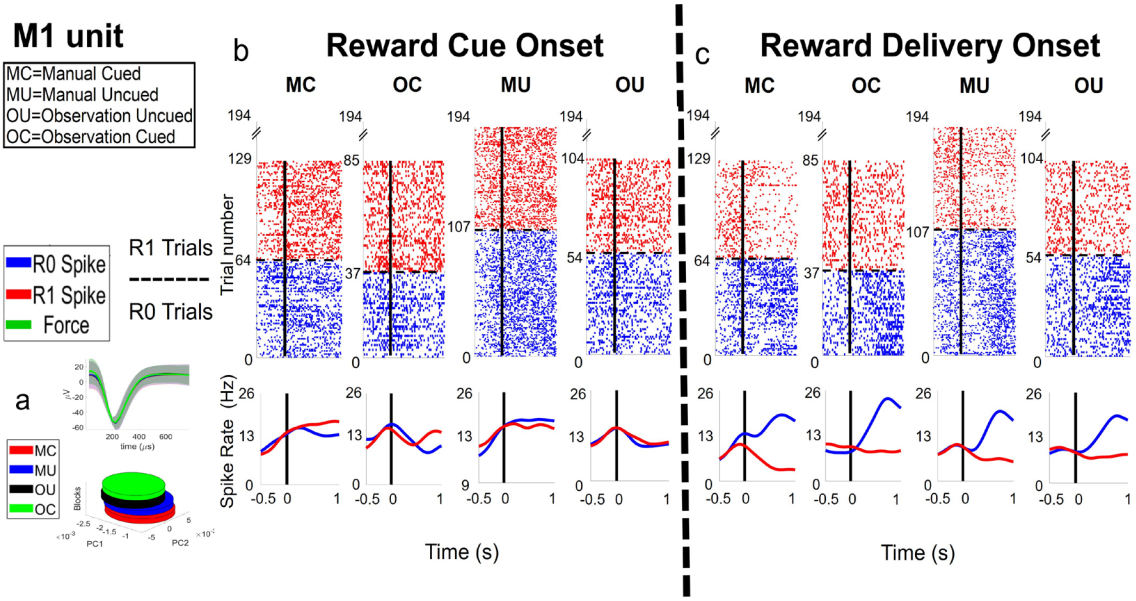

Figure 26: Reward cue (b) and delivery onset (c) for an example unit from M1 cortex of NHP S.

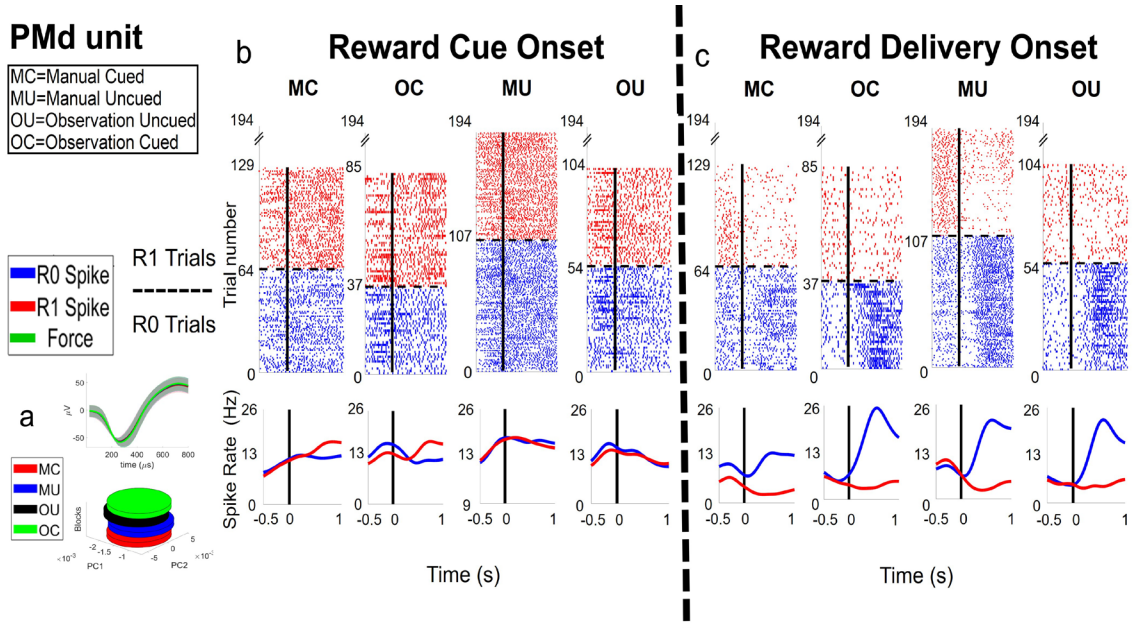

Figure 27: Reward cue (b) and delivery onset (c) for an example unit from PMd cortex of NHP S.

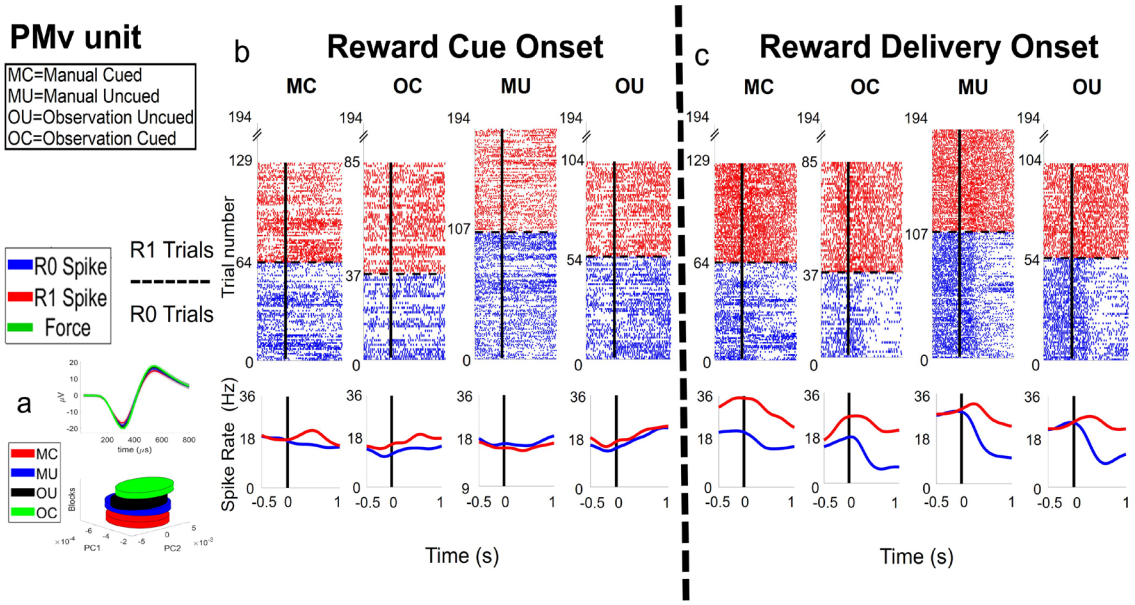

Figure 28: Reward cue (b) and delivery onset (c) for an example unit from PMv cortex of NHP S.

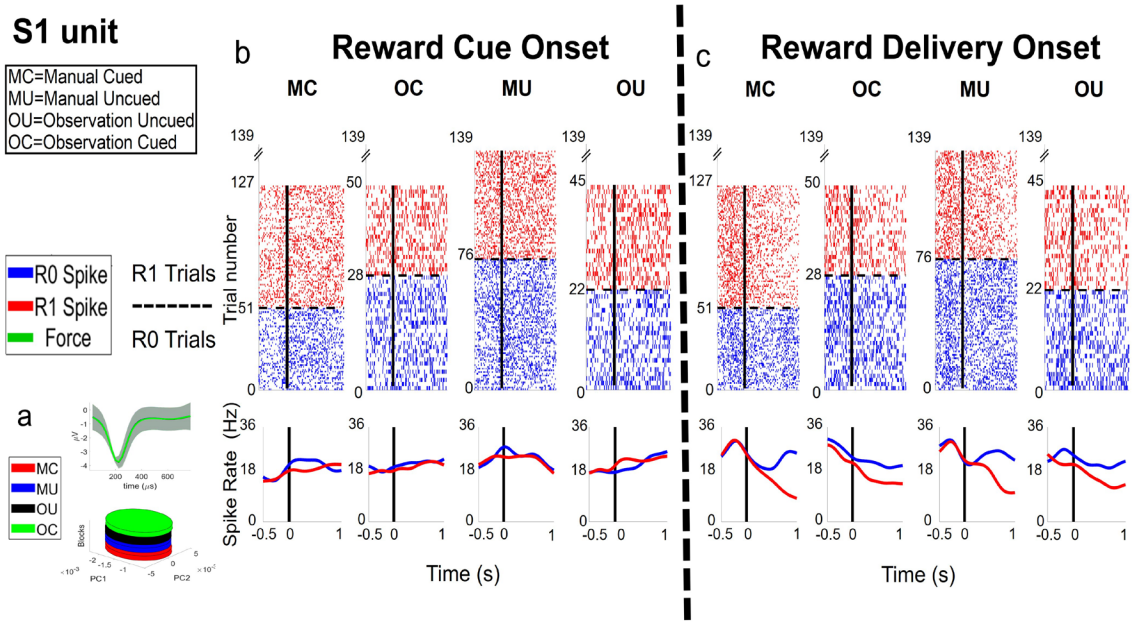

Figure 29: Reward cue (b) and delivery onset (c) for an example unit from S1 cortex of NHP P.

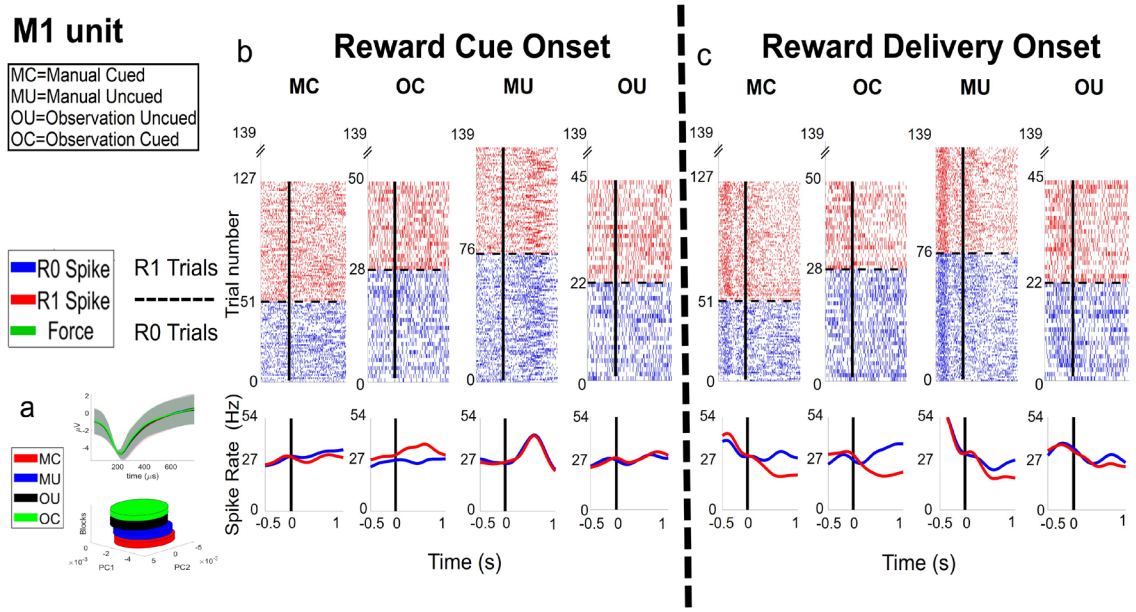

Figure 30: Reward cue (b) and delivery onset (c) for an example unit from M1 cortex of NHP P.

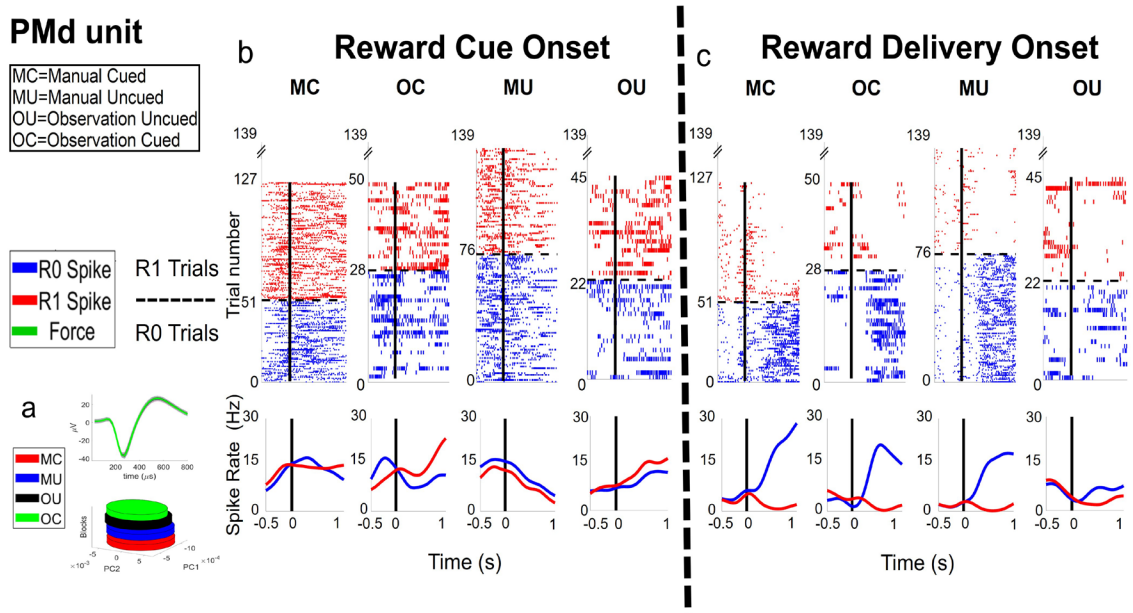

Figure 31: Reward cue (b) and delivery onset (c) for an example unit from PMd cortex of NHP P.

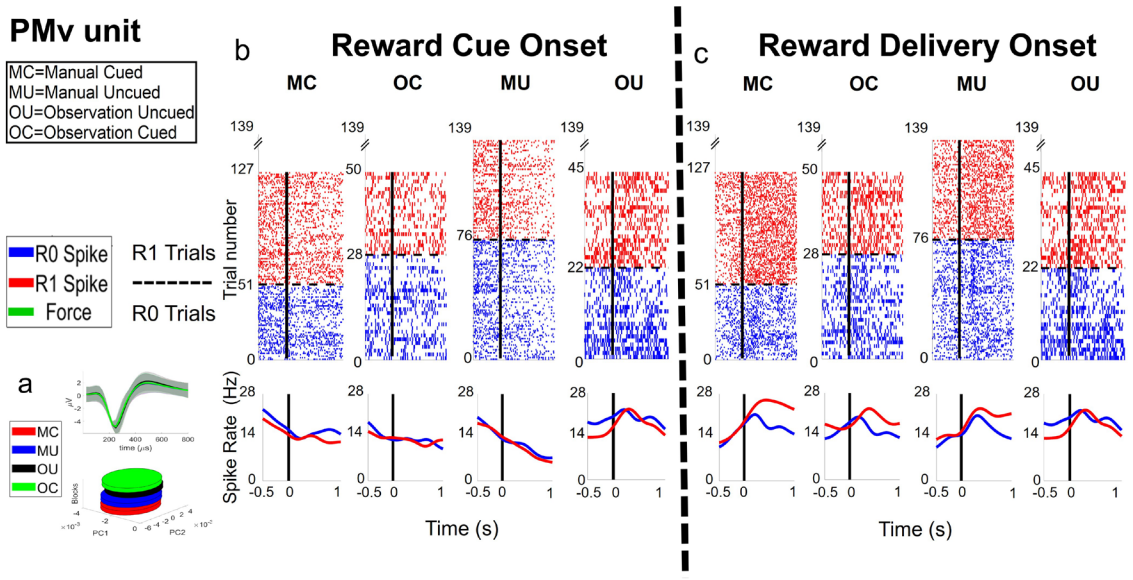

Figure 32: Reward cue (b) and delivery onset (c) for an example unit from S1 cortex of NHP P.

From Figure 25-Figure 32 it can be seen that the units show clear difference between the response (section (c) for all figures) for rewarding (R0, Red colored) and non-rewarding (R1, Blue colored) spiking activity for reward delivery. For reward cue (section

(b) for all figures). Most cases the cued manual and observational blocks (MC, OC) show separation between mean spike rate for R0 and R1 trials compared to uncued blocks (MU, OU). The response difference is much clearer for reward delivery compared to reward cue.

4.3 Grip Force Prediction

As described in the methods section and further in the supplementary section, data blocks were analyzed using a two-step process. We identified significant units related to force using the simple linear model eq.1, $\boldsymbol{y_f} = \boldsymbol{a}\mathbf{X}_{fr}^{n_i} + b$, where $\boldsymbol{y_f}$ is the vector of grip-force trajectory, $\boldsymbol{a}$ is the regression parameters that multiply unit $n_i's$ firing rate, and used the associated F-statistics with a ($p < 0.05$) for significance determination. Note, we utilized neural data around a given grip-force timepoint, from -0.5s to 0.5s in 100ms bins for this regression. We extracted single units with activity that improved force decoding. Model 1 variables $\boldsymbol{a}$ (10 per unit) and b were fit using least-squares estimates from 90% of the recorded data (see Figure 18 for data split cartoon). The remaining 10% of the data was used as a test set to verify the performance of force decoding. The R-squared values for decoding on the test set of force are shown below.

We found high prediction accuracies for both NHPs. The results shown in Figure 33 are force decoding prediction from S1, M1, PMd and PMv cortices for all manual blocks from Monkey S and Figure 34 for Monkey P. The grip force decoding prediction for all observational blocks are also given in Figure 35 (Monkey S) and Figure 36 (Monkey P). Note intertrial intervals have been clipped out for presentation purposes.

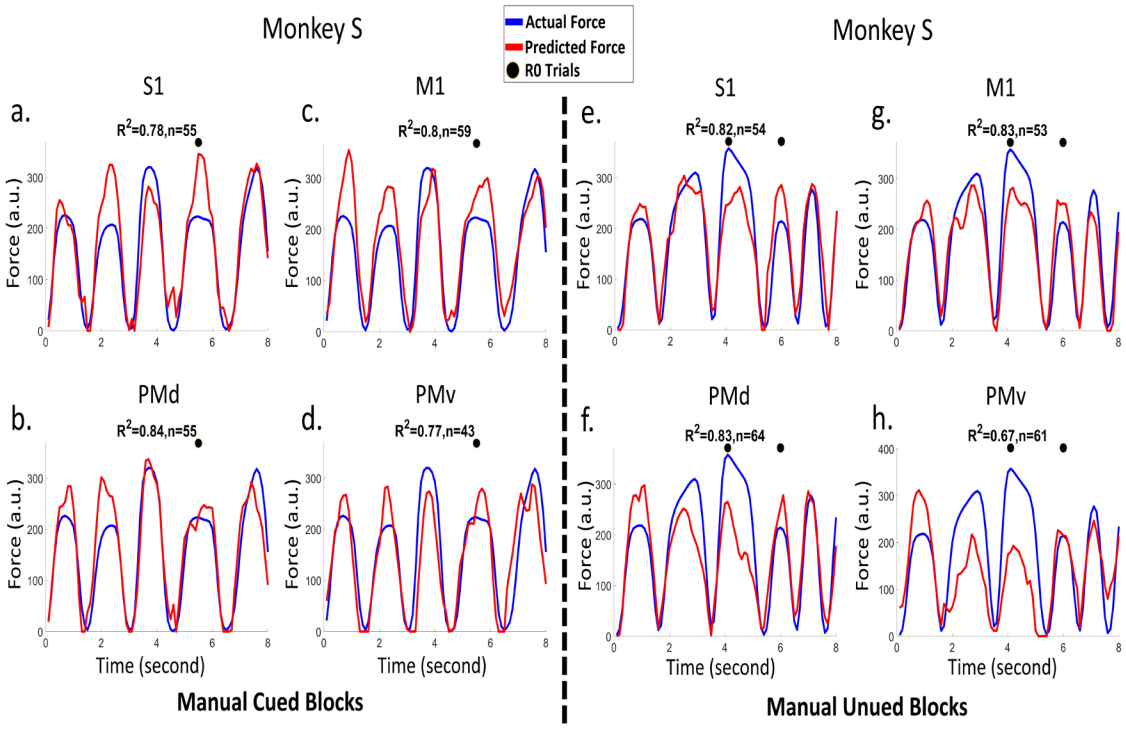

Figure 33: Grip force decoded from manual data blocks (Monkey S).

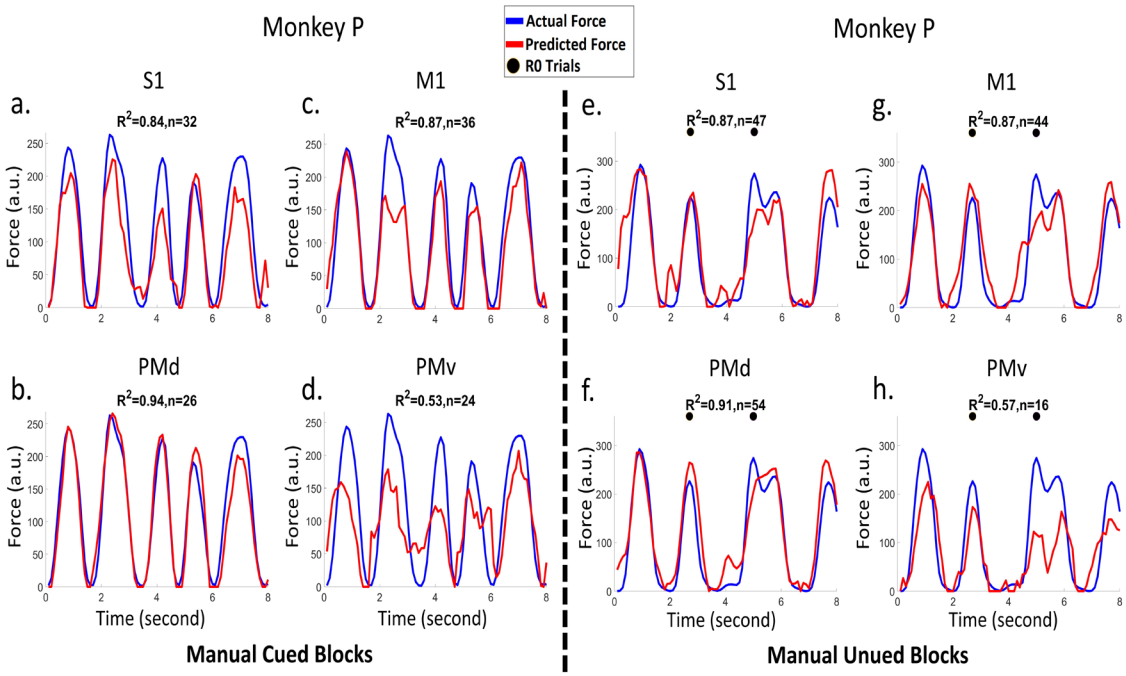

Figure 34: Grip force decoded from manual data blocks (Monkey P).

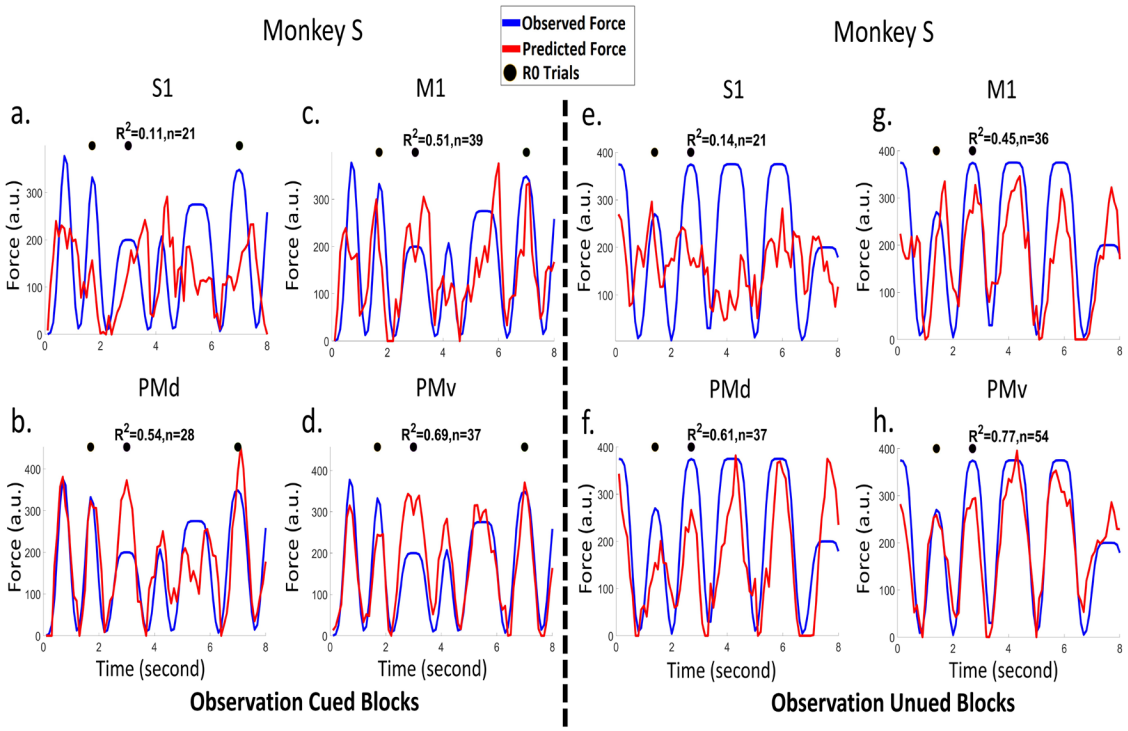

Figure 35: Grip force decoded from observational data blocks (Monkey S).

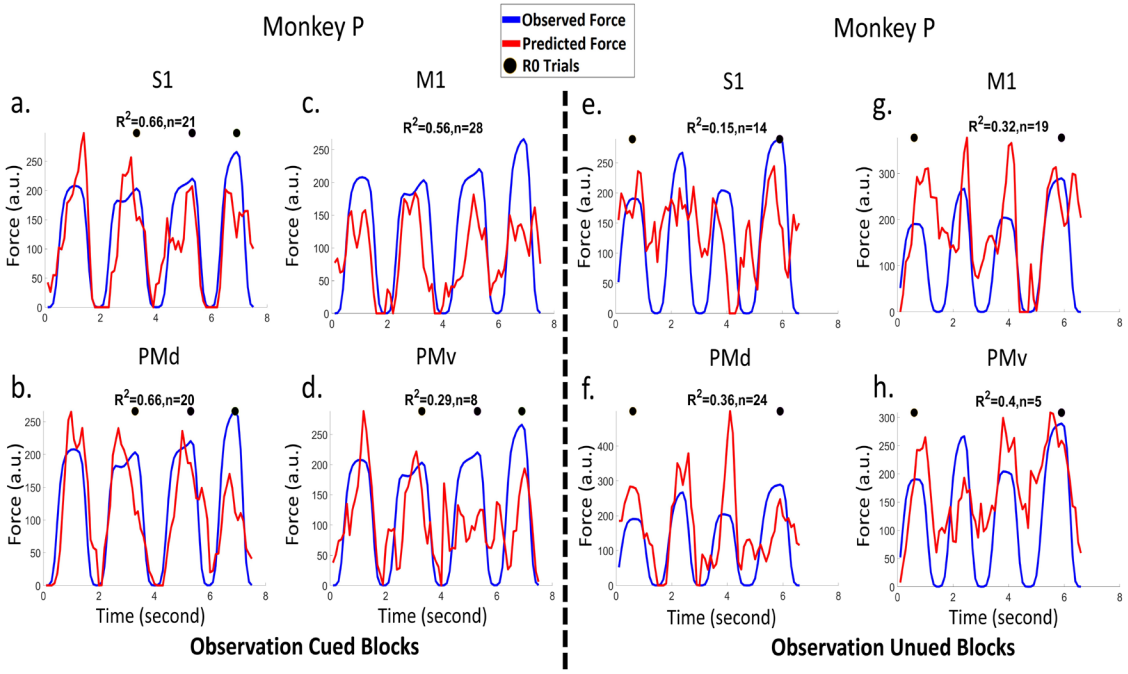

Figure 36: Grip force decoded from observational data blocks (Monkey P).

Force decoding (Red lines) from subpopulations of S1, M1, PMd, and PMv cortical recordings taken from manually performed blocks (Blue lines) top two rows, and observational blocks bottom two rows. Linear regression (eq. 2) was used to predict the force. The black dots on each plot indicate that force profile was taken from an R0 trial, while all others were R1 trials. Plots *a, b, c* and d show results for NHP S, for S1, M1, PMd and PMv cortices respectively. Plots e*, f, g,* and h show similar results for NHP P. The top of each figure shows R-squared values (R^2) using the 10% test set and the number (n) of significant units used for regression to predict force. See Table 1 (NHP S) and Table 3 (NHP P) for full stats on the regression models.

Table 1: Regression model output for NHP S.

NHP S - S1

Block	R^2-fit	p-value	F-stat	R^2-predict	p-value
Manual Cued	0.91	0	$F_{550,2173}$ =39.83	0.78	1.9e-101
Manual Uncued	0.89	0	$F_{540,3597}$ =51.68	0.82	3.5e-173
Obs Cued	0.34	7.4e-40	$F_{250,1330}$ =3.32	**0.11**	9.5e-6
Obs Uncued	0.29	9.4e-46	$F_{300,1679}$ =3.47	**0.14**	7.8e-9

NHP S – M1

Block	R^2-fit	p-value	F-stat	R^2-predict	p-value
Manual Cued	0.92	0	$F_{590,2133}$ =44.24	0.80	7.8e-109
Manual Uncued	0.93	0	$F_{530,3607}$ =85.7	0.83	1.2e-180
Obs Cued	0.69	1.7e-147	$F_{240,1340}$ =6.91	**0.51**	1.6e-28
Obs Uncued	0.65	1.2e-197	$F_{350,1629}$ =8.19	**0.45**	1.8e-30

Table 2: Regression model output for NHP S (continues).

NHP S –PMd					
Block	R^2-fit	p-value	F-stat	R^2-predict	p-value
Manual Cued	0.92	0	$F_{550,2173}$ =44.25	0.84	1.3e-122
Manual Uncued	0.92	0	$F_{640,3497}$ =58.86	0.83	9.1e-181
Obs Cued	0.66	6.3e-172	$F_{270,1310}$ =8.99	**0.54**	1.5e-31
Obs Uncued	0.73	2.5e-282	$F_{330,1649}$ =11.95	**0.61**	6.4e-47
NHP S –PMv					
Block	R^2-fit	p-value	F-stat	R^2-predict	p-value
Manual Cued	0.83	0	$F_{430,2293}$ =26.72	0.77	2.3e-97
Manual Uncued	0.87	0	$F_{610,3527}$ =40.29	0.67	4.4e-112
Obs Cued	0.81	4e-265	$F_{320,1260}$ =13.65	**0.69**	4.9e-46
Obs Uncued	0.86	0	$F_{430,1549}$ =16.25	**0.77**	7.1e-71

Table 3: Regression model output for NHP P.

NHP P – S1					
Block	R^2-fit	p-value	F-stat	R^2-predict	p-value
Manual Cued	0.78	0	$F_{320,2142}$ =24.19	0.84	2.26e-109
Manual Uncued	0.9	0	$F_{470,2528}$ =46.77	0.87	4.6e-148
Obs Cued	0.68	5e-88	$F_{220,707}$ =7.12	**0.66**	1.4e-25
Obs Uncued	0.47	2.3e-42	$F_{220,652}$ =4.6	**0.15**	9.5e-5

Table 4: Regression model output for NHP P (continues).

NHP P – M1					
Block	R^2-fit	p-value	F-stat	R^2-predict	p-value
Manual Cued	0.80	0	$F_{360,2102}$ =23.71	0.87	5.58e-123
Manual Uncued	0.89	0	$F_{440,2558}$ =46.22	0.87	1.6e-151
Obs Cued	0.76	6.3e-96	$F_{300,627}$ =7.29	**0.56**	7e-20
Obs Uncued	0.57	4.5e-52	$F_{180,692}$ =4.81	**0.32**	1.5e-09
NHP P – PMd					
Block	R^2-fit	p-value	F-stat	R^2-predict	p-value
Manual Cued	0.85	0	$F_{260,2202}$ =47.17	0.94	4.9e-164
Manual Uncued	0.93	0	$F_{540,2458}$ =63.09	0.91	6.4e-175
Obs Cued	0.73	1.3e-117	$F_{240,627}$ =9.79	**0.66**	1.4e-25
Obs Uncued	0.72	4.7e-82	$F_{200,672}$ =6.71	**0.36**	7.3e-11
NHP P – PMv					
Block	R^2-fit	p-value	F-stat	R^2-predict	p-value
Manual Cued	0.61	5.3e-308	$F_{24,2222}$ =14.26	0.53	9.3e-47
Manual Uncued	0.6	0	$F_{160,2838}$ =26.31	0.57	5.6e-63
Obs Cued	0.43	1.2e-60	$F_{80,847}$ =7.89	**0.29**	2.7e-09
Obs Uncued	0.33	7.9e-45	$F_{80,792}$ =8.15	**0.40**	2.9e-12

The above table Displays results from the regression analysis for NHPs S and P between neural activity and force trajectories. The table contains the R-square value for the model (eq. 2) fit and prediction including their corresponding p-values and F-statistics. We have used bold text for the prediction during observation tasks. Note all single units were followed through each of the 4 task types on a given day. From table 1 it appears that these

brain regions represent force during both the manual trails and the observational versions of these trials. In Figure 38 we show the number of single units that significantly predict force during both manual and observational (the grip force applied by the automatic system cued visually) trails indicating that these same units represent this information to some extent during both manual and observed movements, which may represent a new form of mirror neuron activity.

4.4 Force-Mirror Neuron Units:

It is clear the manual tasks generally had higher levels of prediction as compared to the observational versions. We detected the units that were consistently present in all four data blocks (two manual and two observational) and those significant for grip-force in all data blocks. For NHP S we found 31 units in S1, 42 in M1, 46 in PMd and 29 in PMv that were consistently present in all four data blocks. For NHP P the numbers were 107 in S1, 95 in M1, 79 in PMd and 49 in PMv. Below in Figure 38 we show the total percentage of these units from each region that showed significant linear regression model fit under both the manual and observational versions of the task that is the putative MNs. We used the peak value from the absolute correlation coefficients between grip force and each of the 10 bins of spike rate (100ms from -0.5ms pre grip force spike rate to 0.5s post, described "Grip force trajectory prediction" section inside method) to detect inhibitory or excitatory activity. Based on their inhibitory and excitatory activity we categorized the MNs into four different types that is shown in Figure 37 with diagram and spike rate collected from four example units from NHP P, S1 cortex. We considered a unit's representation excitatory if the actual value of that peak absolute correlation is positive otherwise it was considered inhibitory. We detected congruent units among the significant units that showed similar

activity in all four data blocks of either inhibitory (blue) or excitatory (red) spike rate in relation to grip-force. The units showed a decreased in spike rate during manual but increased spike rate during observational blocks are marked as noncongruent, decreased to increase (green) type and the opposite units are considered as noncongruent, increased to decreased (purple). Other (gray) units didn't follow any of the spike rate pattern given in Figure 37 during all four data blocks.

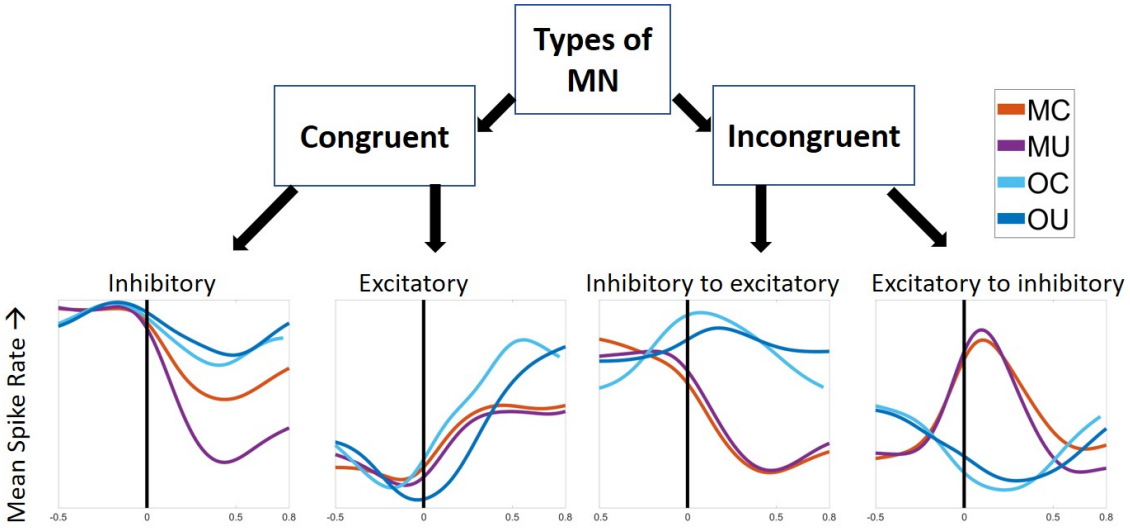

Figure 37: Diagram shows types of MN. Example units were taken from NHP P, S1 cortex and plotted around grip force onset (black vertical line).

Figure 38 shows the Percentage of well isolated MN single units from S1, M1, PMd and PMv that showed significant (F-test, FDR adjusted for number of units in the population) fit to grip-force during all four blocks of data (two manual and two observational) for each NHP. The different color bars represent inhibitory (blue), excitatory (red), noncongruent: decreased to increased (green), noncongruent: increased to decreased (purple) and other (gray) unit responses. The percentage shows how many units are significant for force from units present in all four data blocks. The y-axis shows the % of units with total number of units on top of each bar after the "#" sign.

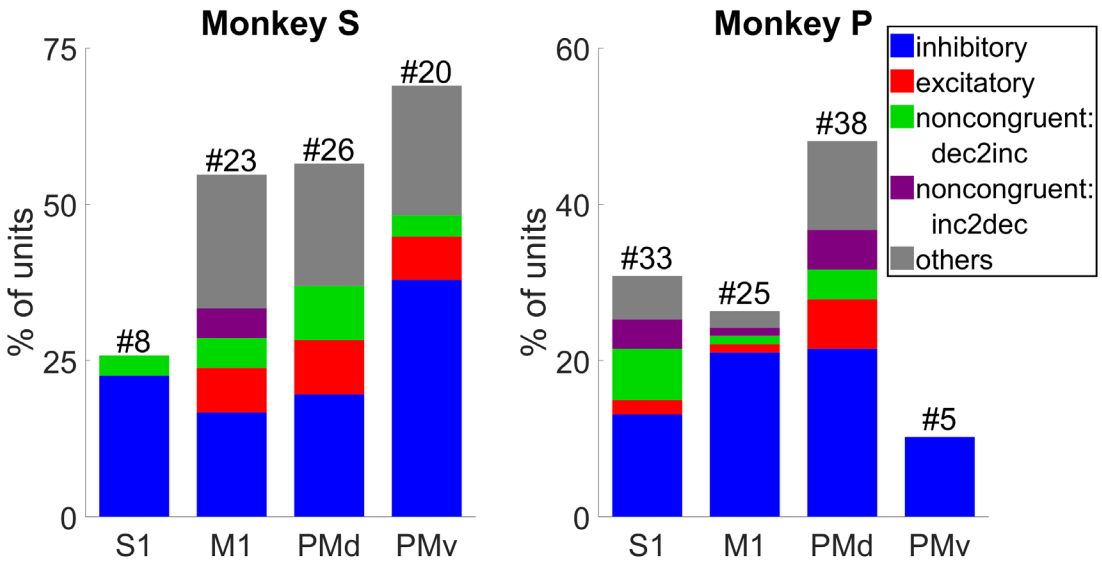

Figure 38: Units with grip force-mirror neuron properties.

The somatotopic location of the mirror neuron units (MN) (Figure 38) is shown in Figure 39, with respect to the electrode position which they were recorded. The position of four Utah arrays in relation to the central sulcus for NHP S (left) and P (right) is also marked. The four arrays were implanted in S1, M1, PMd and PMv cortices. The yellow line indicates the Central Sulcus. Note in NHP P we had to implant the M1 array more lateral then in NHP S due to a large blood vessel running through that region. Likewise, PMd was implanted more medial in NHP P for this same reason as compared to NHP S. The location of the mirror neuron with respect to the electrode from which it was recorded is shown on the top of the array. The color map for the number of units in each location is given on the right side of Figure 39.

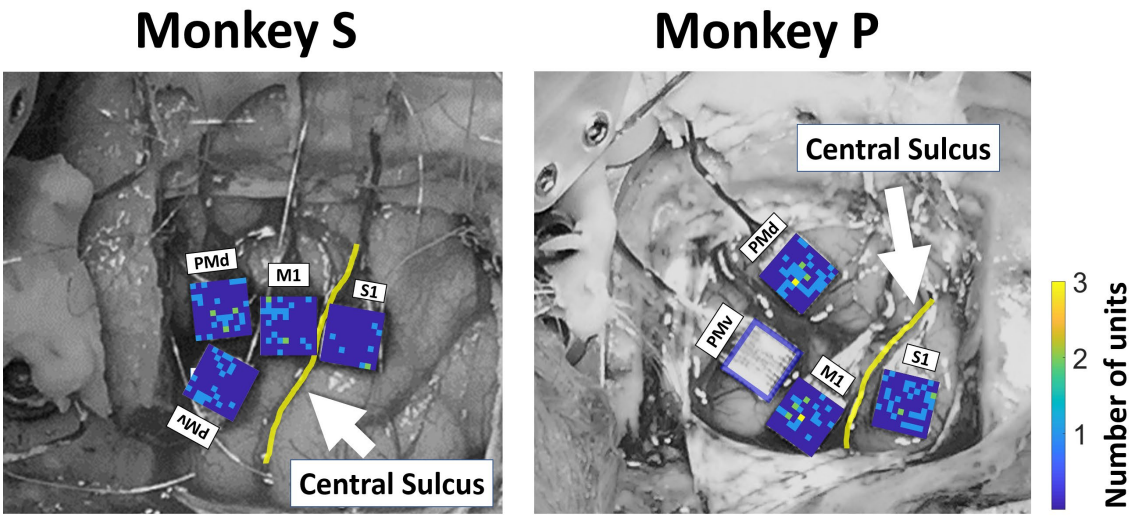

Figure 39: The somatotopic location of the mirror neuron units.

Types of responses of MN units' activity due to grip force for different data blocks was recorded and sorted in Figure 38. The following figures show the number of MN units in terms of their activity during different blocks. These units are already shown in Figure 38, but the other category was not elaborated there, which is given in details in Figure 40 and Figure 41 for NHP S and NHP P respectively. For analysis, all four data blocks were used.

In the following two figures (Figure 40 and Figure 41) show the gray units from Figure 38 in detail for each of the combination pattern. On the x-axis label shows four numbers for four data blocks in the order of (MC-MU-OU-OC) and a number '0' represents inhibitory activity for that block and '1' represents excitatory activity. For example, the bar with the first label '0000', shows the number of units that showed inhibitory spike rate during grip force activity during all four data blocks (MC, Mu, OU and OC). The bar colors are kept as in figure 6 and are given in the legend. The bars that contain the other unit category from figure 6 are kept gray colored here.

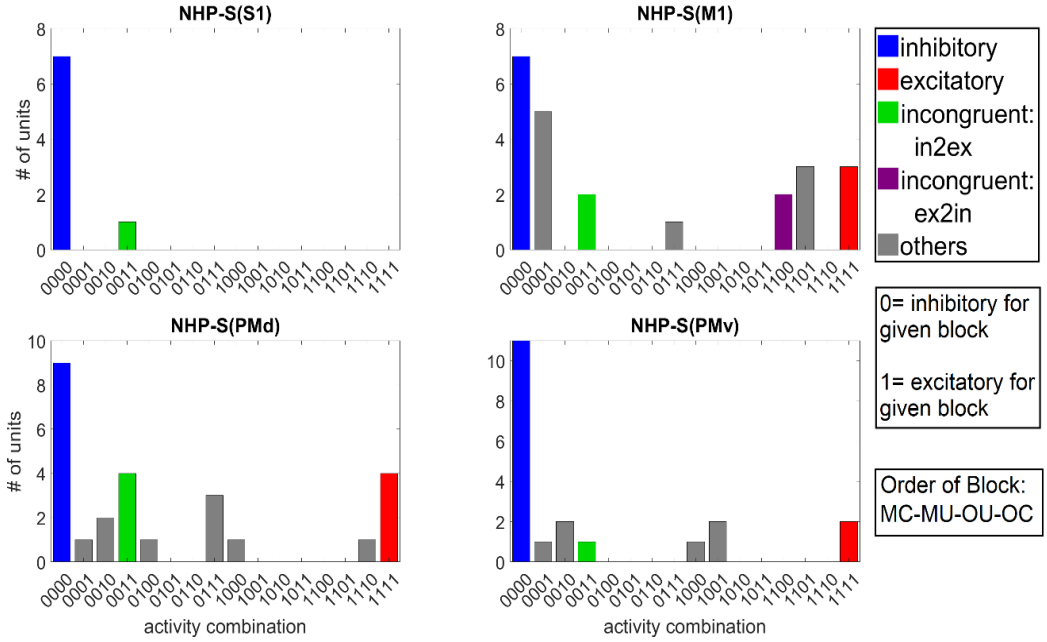

Figure 40: Mirror neuron units based on their activity during data blocks (NHP S).

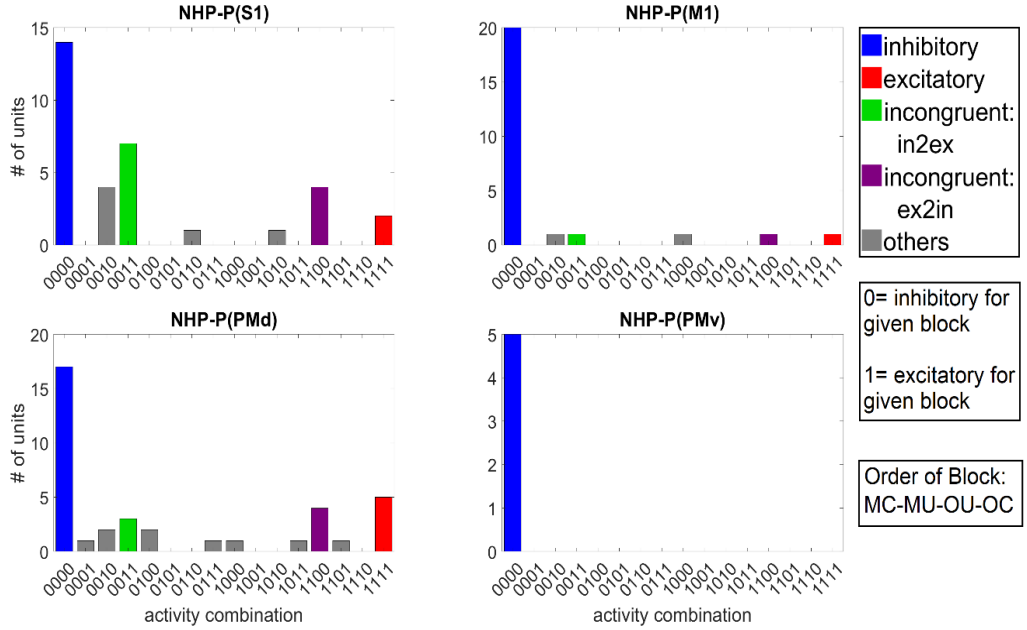

Figure 41: Mirror neuron units based on their activity during data blocks (NHP P).

The Number of MN units from NHP S (Figure 40) and P (Figure 41), for each possible activity combination during blocks in order of MC, MU, OU and OC is shown on the above figures. The y-axis represents the number of units and x-axis label shows the combination of inhibitory (0) or excitatory activity for the given four data blocks. The title on each subplot shows the corresponding cortex and NHP name.

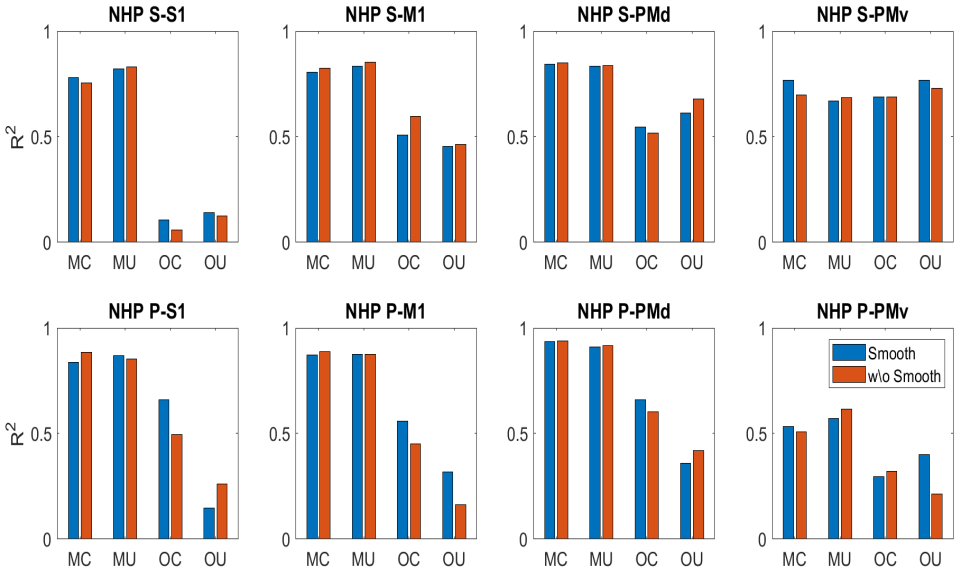

Figure 42: Grip force decoding with and without smoothening on the spike rate.

During pre-processing of the spike data, we applied smoothening with a gaussian kernel and square root transformed the binned spike rate to achieve a distribution close to gaussian. To make sure these two methods are not the main effector, we also tried our decoding method without smoothening and square root transformed and the following plot shows the comparison of decoding result with or without these two methods. We applied MLR (Multiple linear regression) to decoded grip force from smoothened spike rates (Figure 33Figure 36). To show that the smoothening was not playing a role in our decoding results we also tested the square root transformed spike rate without smoothing to decode

the force following the same procedure described in the method section. The above figure shows the R-square values of force decoding with (red) or without (blue) smoothening.

Figure 42 shows the R-square of the decoded grip force with (blue) or without (red) smoothening was applied on the spike rate data. The rows of subplots show data from S1, M1, PMd and PMv cortices of NHP S and bottom row is same for NHP P.

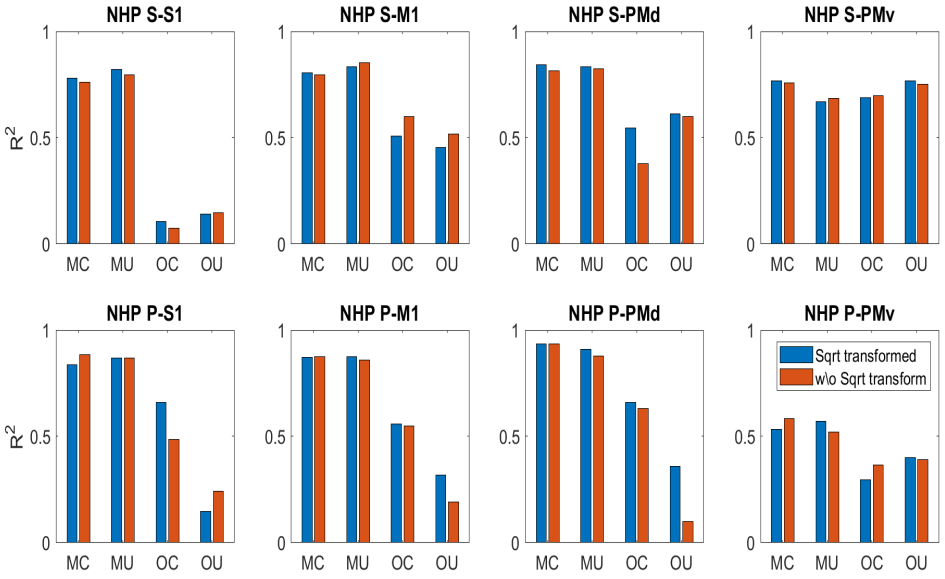

Figure 43: Grip force decoding with and without square root transformation on the spike rate.

In the Figure 43, we show a comparison between the grip decoding accuracy with R-square values between decoded grip force on the test set of data and the actual grip force applied (manual) or observed (observational). The bar plots showed that the R-squared doesn't deviate much when a square root transform is applied (blue) on the spike rate from the case when the transformation was not applied (Red). The figure 8 in the main text

shows that NHP S had a higher percentage of significant units, especially in M1, PMd and PMv cortex due to reward cue compared to NHP P.

Figure 43 shows the R-square of the decoded grip force with (blue) or without (red) square root transformation was applied on the spike rate data. The rows of subplot show data from S1, M1, PMd and PMv cortices of NHP S and bottom row is same for NHP P.

4.5 Peak Grip force significance:

As force profiles were stereotypical smooth Gaussian-like profiles, we wanted to make sure our regression model fits and predictions were meaningful, and not solely due to a unit having a phasic response that could be used to fit the stereotypical waveform. Therefore, we determined how neural activity correlated with the peak values of the Gaussian-shaped force profiles during each trial. We considered force values around the peak force applied on each trial (three values around the peak including the peak value) and we placed neural data, centered around each of them, into ten 100ms non-overlapping bins from 500ms pre peak force to 500ms post peak force neural activity. Each MN (Figure 38) was tested for peak force significance (F-test, FDR corrected for number of population that is the number of corresponding units) by fitting a linear regression model with peak force values and spike rate for each of the ten bins. The blue bars show the units with Force-Mirror-neuron properties (Figure 38). The red bars on Figure 44 show significant units for peak grip force activity among the force-mirror-neuron units.

Figure 44 shows the significant mirror neurons (MN) for grip force (blue) and peak grip force (red) for Cued and uncued Manual (left subplots) and Observational (right subplots) blocks from NHP P (bottom four subplots) and S (top four subplots). The blue bars represent units significant for grip force (F-test, FDR corrected for number of

population) and red bars represent units significant for peak grip force values (F-test, FDR corrected for number of population). This plot shows the mirror neuron units information from the Figure 38.

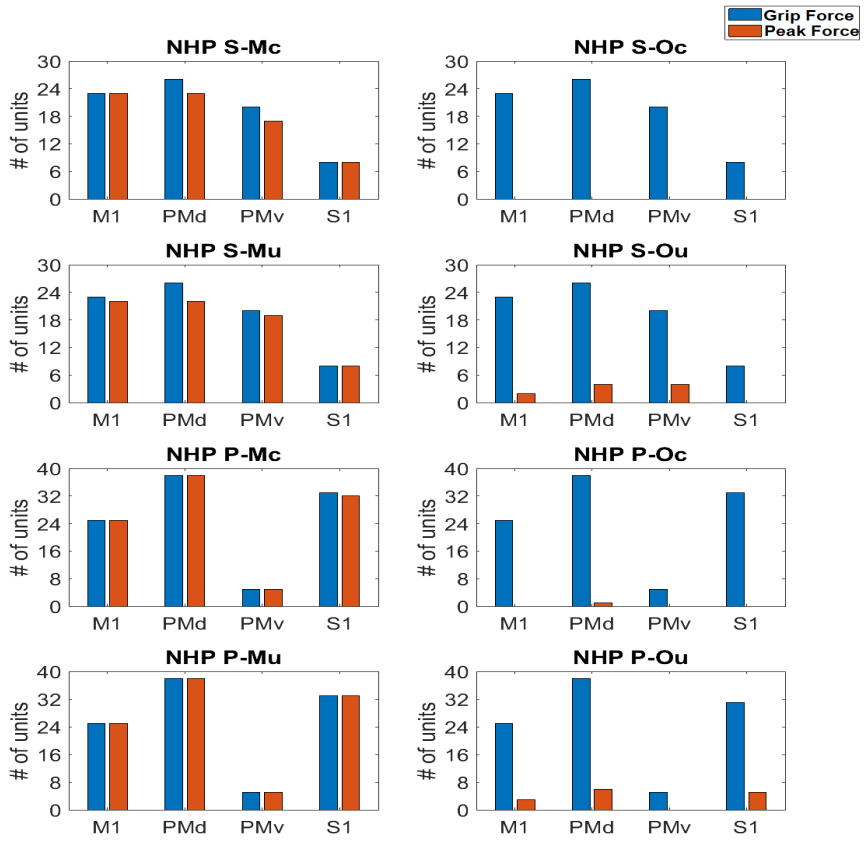

Figure 44: Significant mirror neuron units for grip force (blue) and peak grip force (red).

4.6 Force, Reward and Comodulation of Single Mirror Neurons:

Figure 45 shows the number and percentage of units that were significantly correlated with force or reward separately, as well as units that were significant for both simultaneously, and these same units were significant under both manual and observational trials. Single unit activities were tracked across manual and observational cued and uncued blocks to determine the significance of their correlation with force under these different

conditions. To clarify, a unit that was present during both cued manual and cued observational blocks was checked for significant correlation with reward and force and included in Figure 45 only if it was significant for both manual and observational trials towards possible discovery of mirror units. The same procedure was performed for uncued manual and observational blocks separately. The plots in Figure 45 show the total number of units (left y-axis) and percentage (top of each bar) for each category that was identified from S1, M1, PMd and PMv recordings. The red bars are for cued trials while the blue bars are for uncued trials. The analysis windows in Figure 45 for reward were, for post-cue from 0s to 0.5s, and for post-result from 0s to 0.5s while for force significance the window was 0.5s starting at pre-force-onset to 0.5s after post-force-offset. Note these time windows where not overlapping, thus Figure 45 is not describing results of force tuning modulation by reward, which is described in Figure 53.

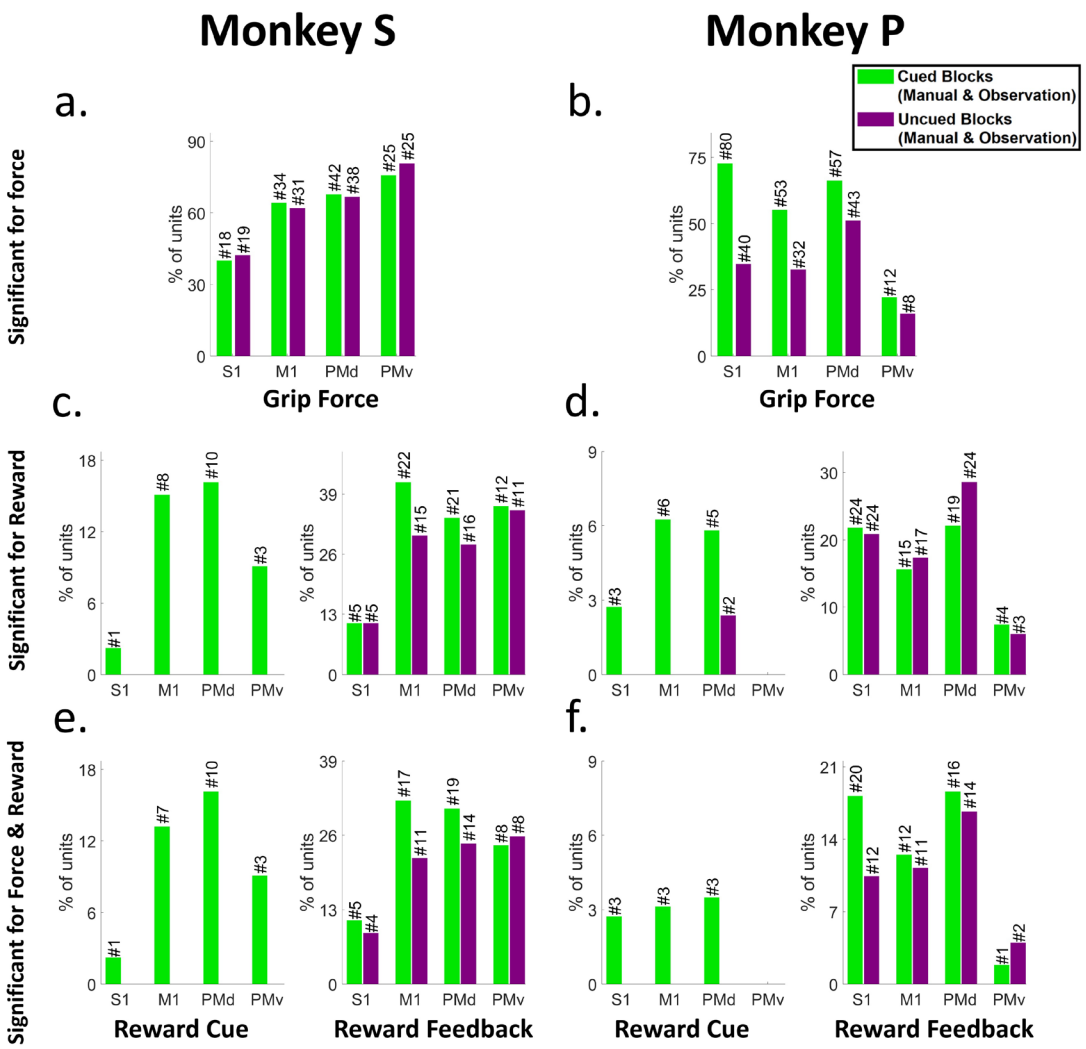

Figure 45: Number of force-mirror-neurons modulated by reward.

Figure 45 shows Mirror Neurons in S1, M1, PMd and PMv Encode Reward and Grip Force. The percentage of units with significant modulation via either grip force (F test, FDR adjusted for p=0.05), reward (post-cue or post-reward, t-test, FDR adjusted for p=0.05), or both, during manual and observational blocks of a similar type (e.g. cued or uncued). Green represents units for cued blocks and Purple for uncued blocks. Each subplot shows the percentage of significant units between cued/uncued for MN that is units showing such activity during both manual and observational blocks for Force (plot a and

b), Reward (plot c and d) and significant for both force and reward (plot e and f). For subplots c, d, e and f the left plot shows units for post reward cue and right plot shows unit for post reward feedback activity. The number of times the hypothesis was applied which is the number of neural populations for that corresponding block and cortex is used for FDR correction. The FDR method is described in the method section titled "grip force tuning curve analysis". The number of units is given on the top of each bar after the '#' sign.

4.7 Distribution of Peak Significant Correlation Time Lags Between Neural Activity and Force:

The analysis in this section was conducted in order to determine if there was an obvious shift in time lag between the neural correlates of force between manual trials and observational trials. One would expect the neural data responsible for force production, or imagining force production, to lead the force output, whereas classical MN activity would lag the viewed "force" output. However, this may not be the case for predictable movements, such as used in our task, as described by others (Maranesi et al., 2014), where MNs can still lead the observed task. In Figure 46 we have plotted the shift in time lags for the peak time bin significantly correlated with the force trajectories. We asked if these distributions significantly (signed Rank test, $p < 0.05$) deviated from zero between the manual and the observational versions of both the cued and uncued tasks. There were no significant shifts in the histograms for NHP P. NHP S showed three tasks with significant shifts for S1, PMd and PMv. For each plot the zero-time shift shows the probability of a unit not shifting in time between manual and observational. The positive differences are the classical MN response where observational neural activity lags the visual information,

whereas, the negative time shifts represent the probability of the observational neural response being earlier, or more "predictive" of moment, than during the manual trials.

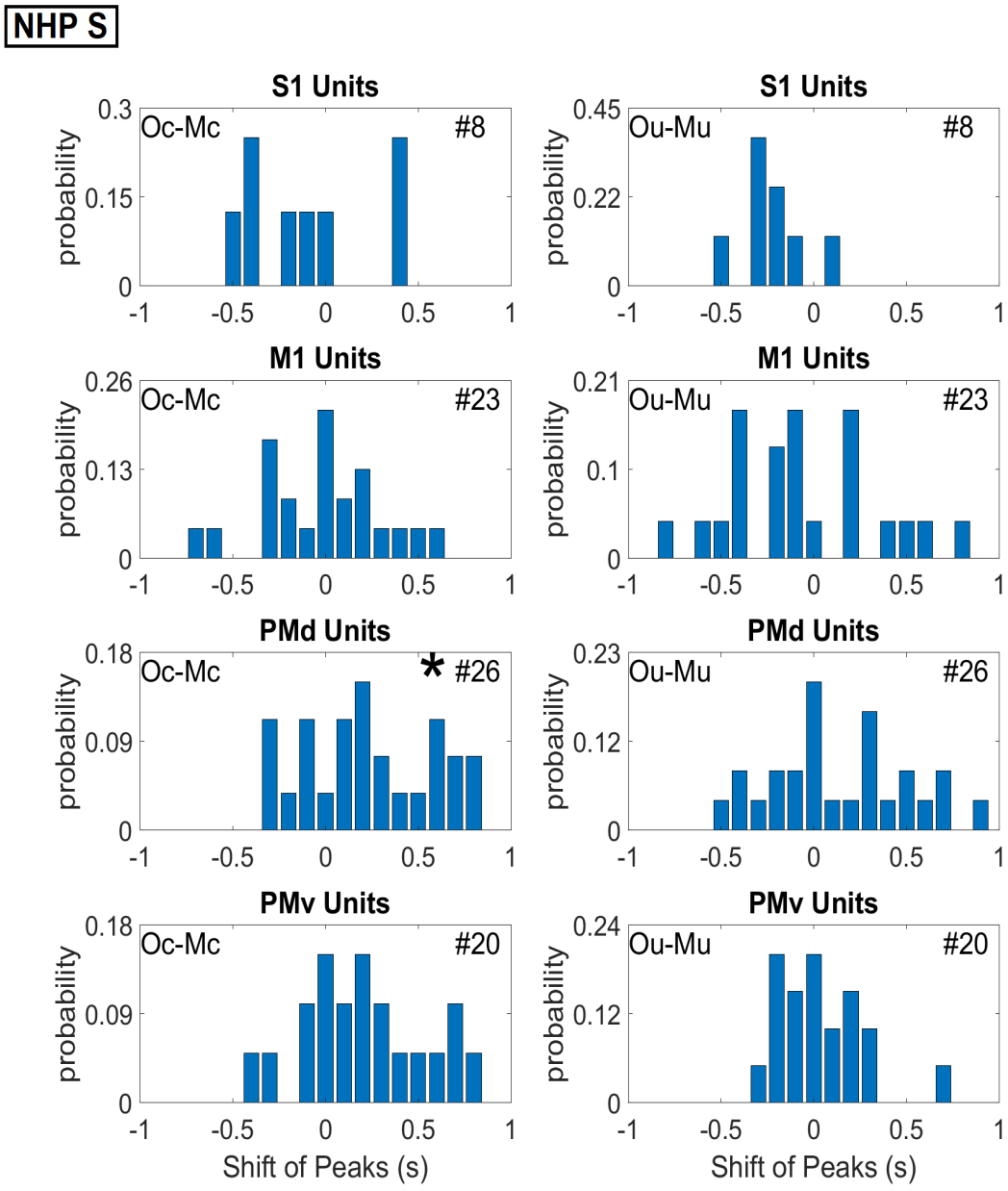

Figure 46: Changes in neural time lag (Obervational vs. Manual) for NHP S.

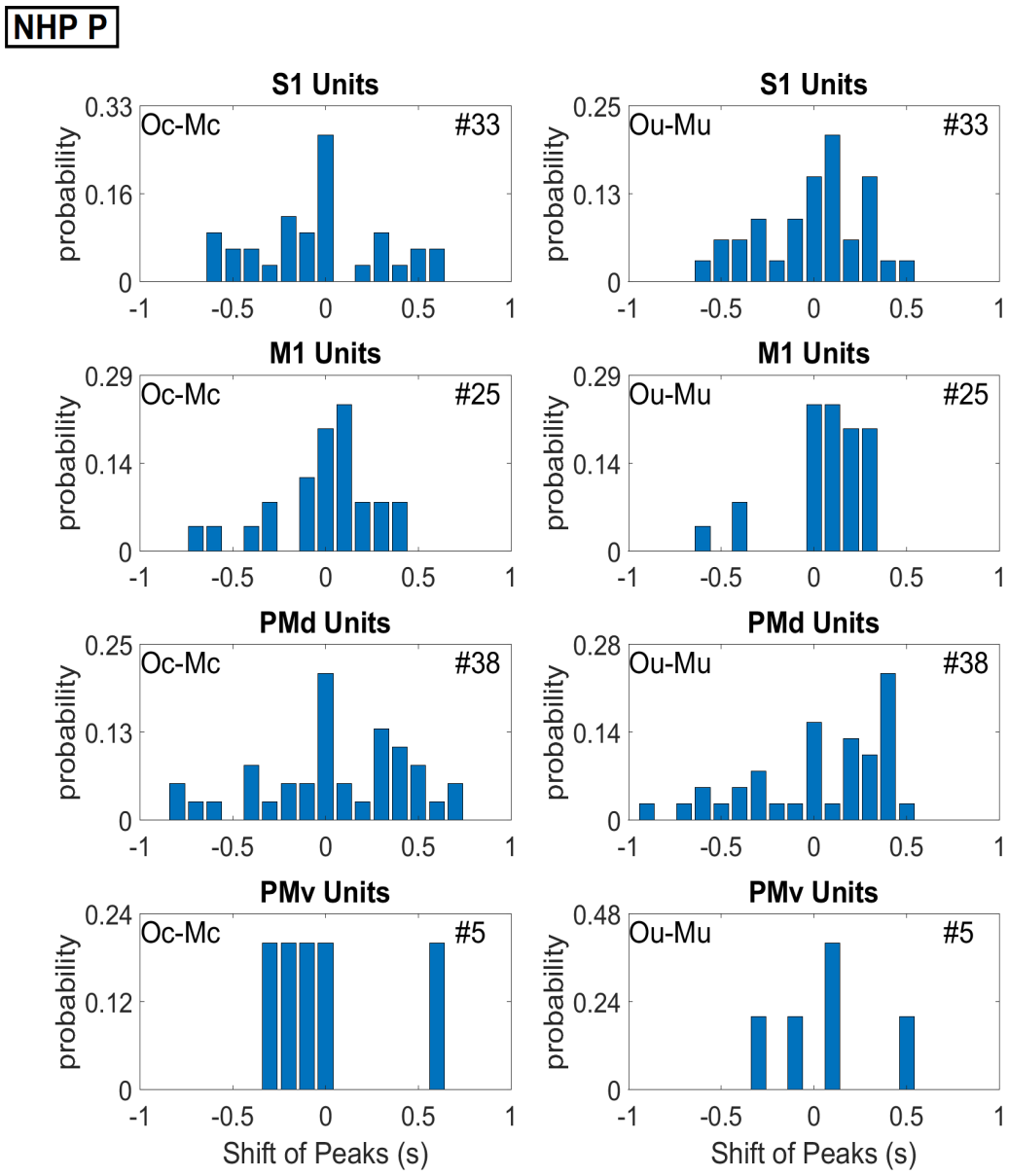

Figure 47: Changes in neural time lag (Obervational vs. Manual) for NHP P.

Figure 46 (NHP S) and Figure 47 (NHP P) shows the changes in neural time lags where neural data best correlate with peak grip force. Bar plots showing the shift of peak correlation between similar (cued/Uncued) Manual and Observational blocks for S1, M1, PMd and PMv cortices (cortex is labelled on the title of each subplot). The shift from a

block type to another block type (manual-to-observational) is at the top right of each subplot for each NHP. The number of units used is indicated in the upper right corner of each subplot. The left column for each NHP shows the shift between cued blocks and the right column shows the shift between uncued block. An asterisk (*) symbol before the number of units represents a significant shift in histogram from manual to observational tasks. Probability of unit shifts was calculated by subtracting the position of the peak correlation time bin for observational blocks as compared to the manual tasks for the same unit.

The following Figure 47 (NHP S) and Figure 49 (NHP P) shows the time shift of significant peak correlation from manual cued blocks to manual uncued blocks and from observation cued blocks to observation uncued blocks.

The shift of peak force correlation from manual to manual and observational to observational block is given in Figure 48 and Figure 49. Bar plots showing the shift of peak correlation between Manual blocks and Observational blocks for S1, M1, PMd and PMv cortex for individual MNs. The shift from a block type to another block type is given on the left to of each figure. The number of units used is included on the upper left corner of each subplot. An asterisk (*) symbol before the number of units represents a significant shift in histogram between the blocks used for that subplot. Shift was calculated by subtracting the manual histogram for cued trials from the Manual histogram for uncued trials and similarly for the observational cases.

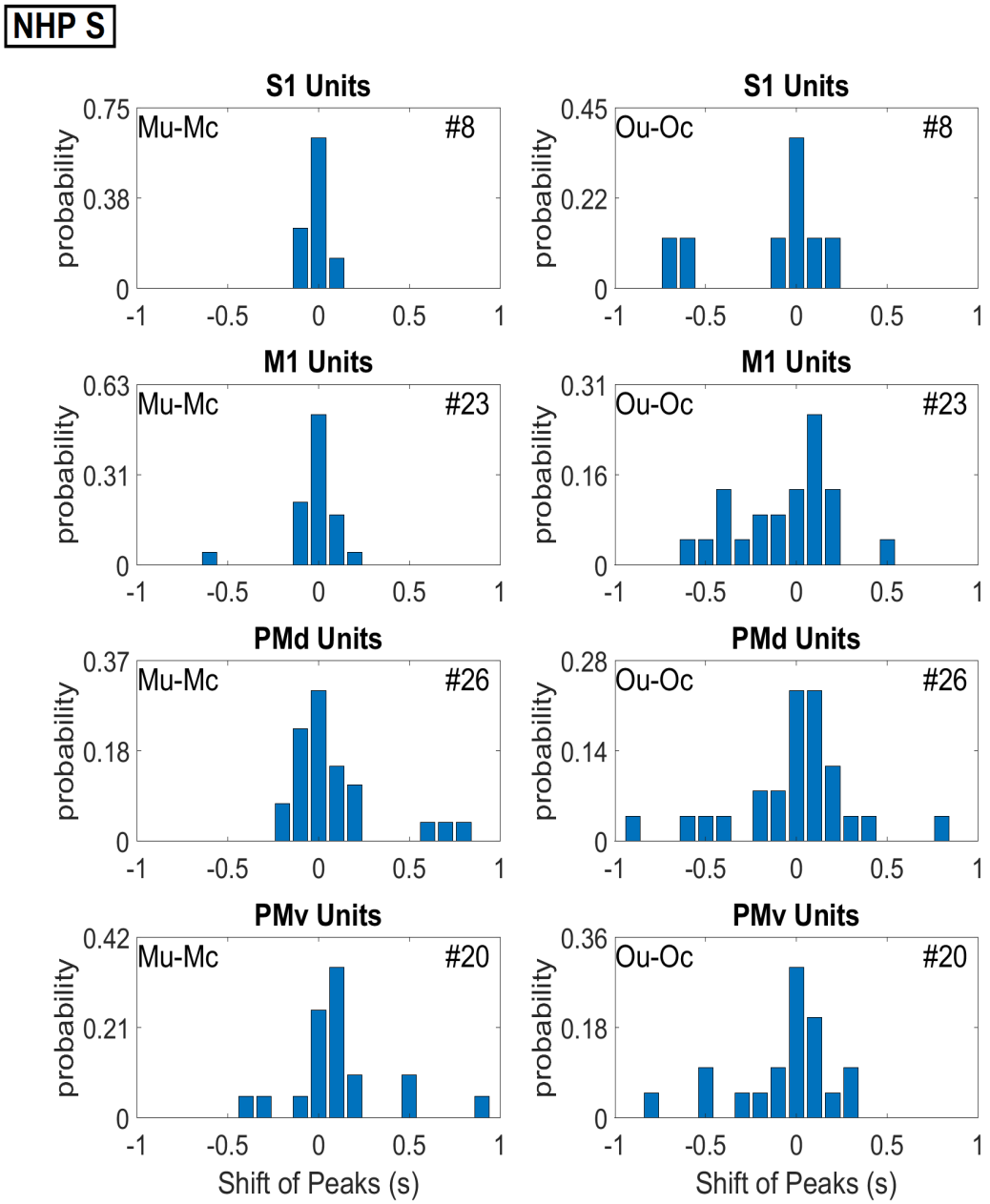

Figure 48: Changes in neural time lag (Obervational vs. Observatinal and Manual vs. Manual) for NHP S.

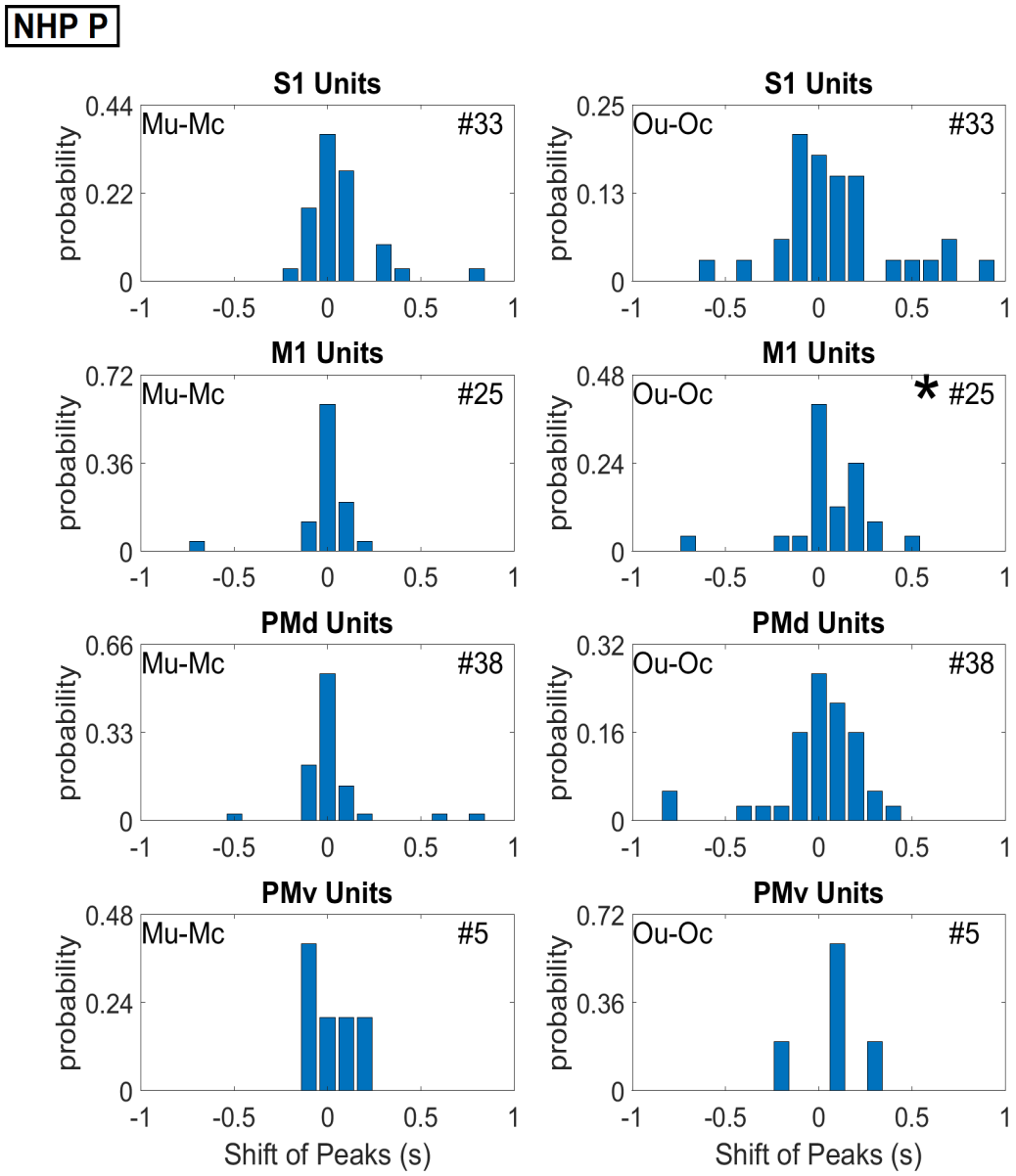

Figure 49: Changes in neural time lag (Obervational vs. Observatinal and Manual vs. Manual) for NHP P.

The time dependent peak correlation plots for all the blocks are given here on the following Figure 50. Only the units tracked through all manual and observational blocks and were significant for force are shown here. For each NHP the trend of the distribution of units is similar between blocks but different for each NHP specially for the manual blocks. See Figure 46 and Figure 48 for differences between block types.

Figure 50 shows the number of units that had their highest correlation between force and spike rate for each time bin are shown leading (0.5s before) or lagging (0.5s after) each force value (100ms non-overlapping time bins). Units significant (F-test, $p < 0.05$) on all block types were plotted in the time bin where their correlation coefficient with force was most negative or positive. The y-axis represents the number of units (positively correlated units on the upper side and negatively correlated units on the lower). The x-axis represents the time lag/lead for which the maximum correlation was found. Units from S1 (a, b), M1 (c, d), PMd (e, f) and PMv (g, h) cortex are given on each plot and the legend shows the color diagram for each cortex.

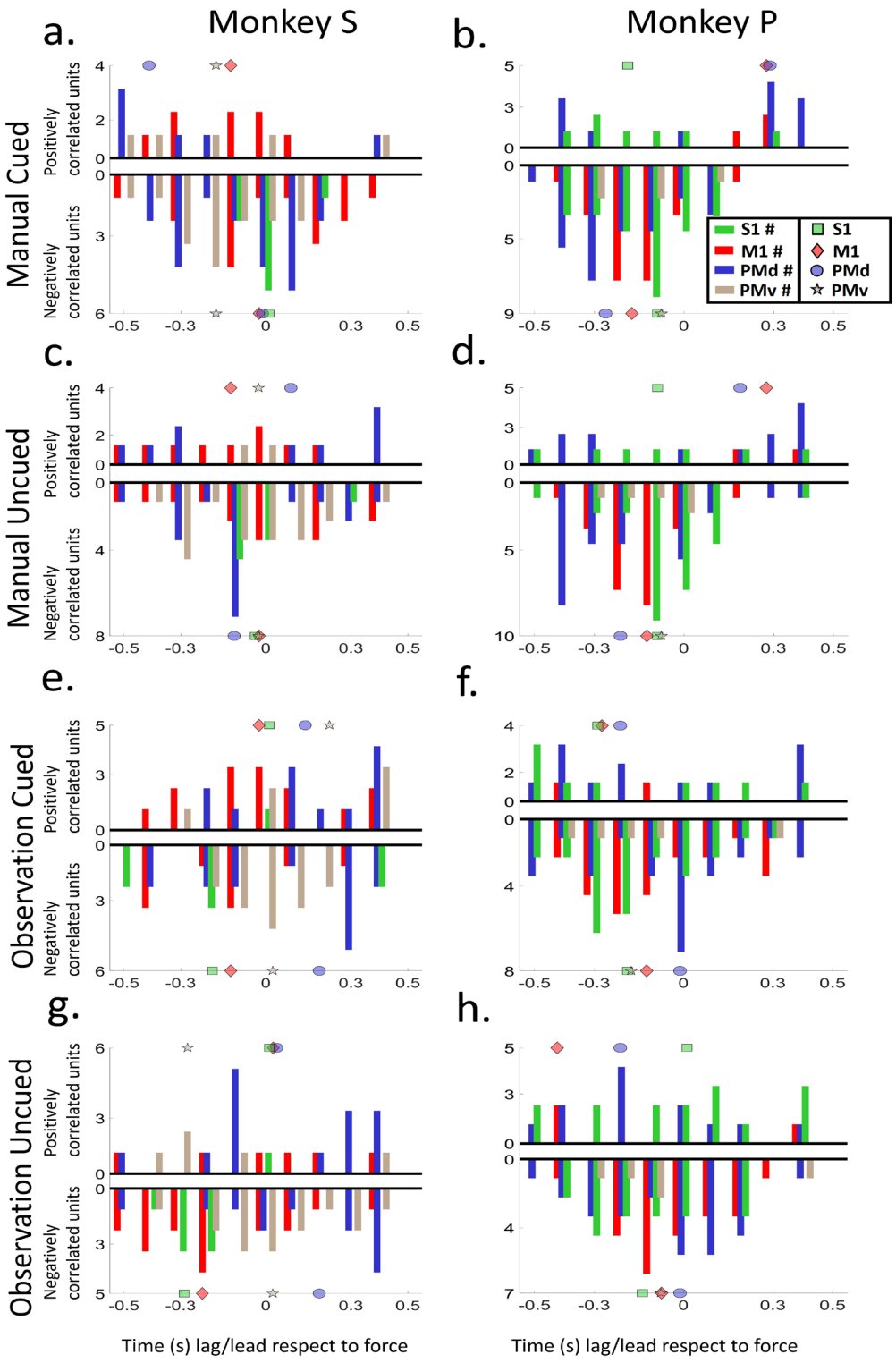

Figure 50: Time dependent correlation analysis.

4.8 Modulation of Force Tuning Curves by Cued Reward Level:

In Figure 51-Figure 53, we are asking questions about the modulation of the force tuning curves and if MNs have such properties of force tuning being modulated by reward level. Force tuning curves for R1 and R0 trials and significant differences between their slopes were calculated as described in the methods using MATLAB's ANCOVA function where the grip force value is used as covariates. F-statistics were conducted on the reward group*force interaction which expresses the difference in slopes and the p-value for that interaction was collected. Figure 51 shows the force tuning curves for example units recorded from cued observational blocks for each brain region and Figure 52 shows the results for manual blocks. It shows the relationship between R1 and R0 trials as spike rate varied with force. Note this is in comparison to the previous sections when force decoding meant the neural activity could be used to determine the force level, whereas here we are looking at the change in firing rate as a change in force level and its modulation by reward (encoding). Subplots (Figure 51 and Figure 52) to the left side of each sub-figure show smoothed spike rate against force, while the line graphs to the right show force tuning curves obtained from R0 and R1 data. The two example units from each NHP, S and P, had a significant difference between R0 and R1, in agreement with our previous M1 results (Zhao et al., 2018).

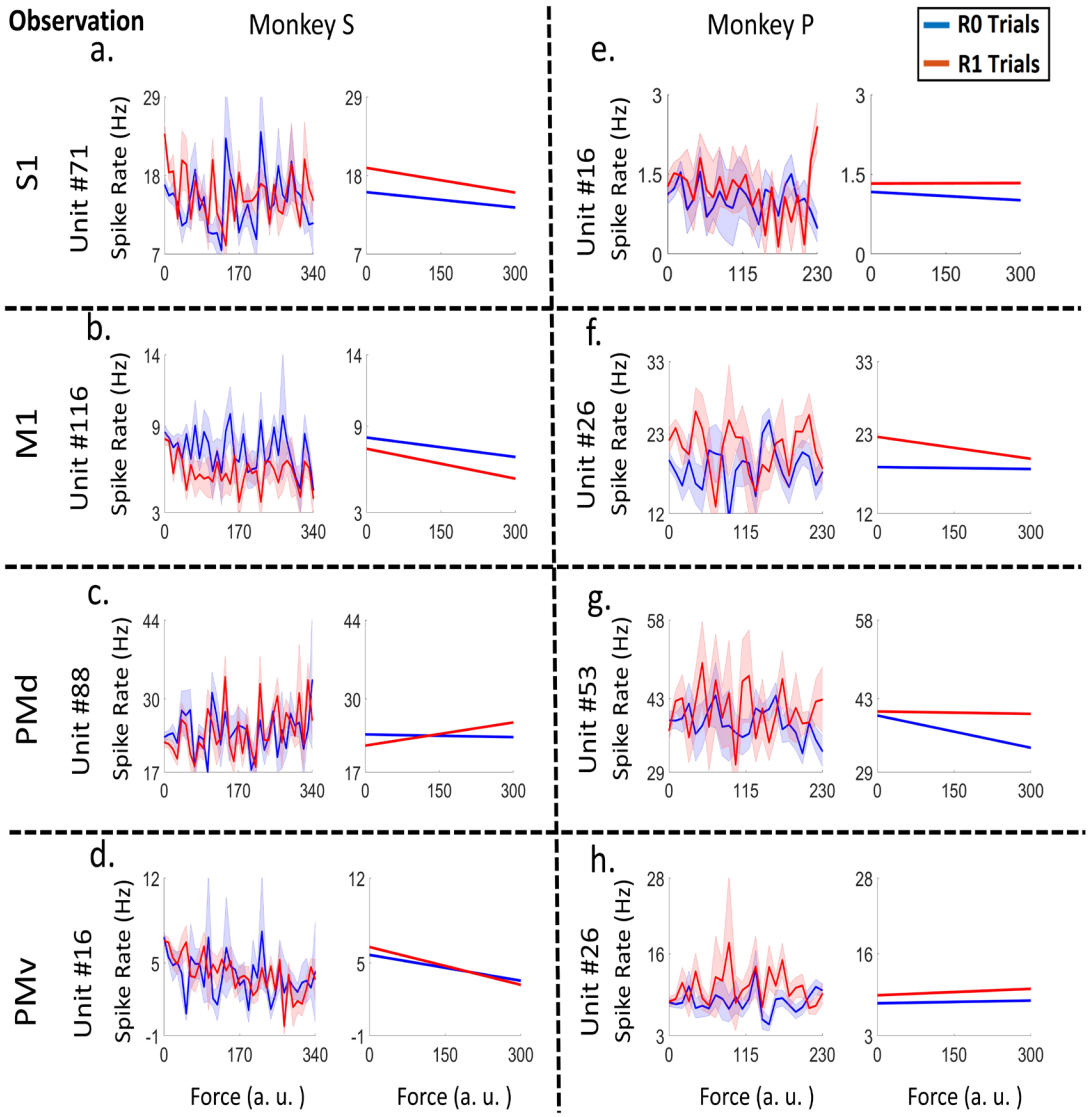

Figure 51: Spike rate vs. force plot for observational blocks.

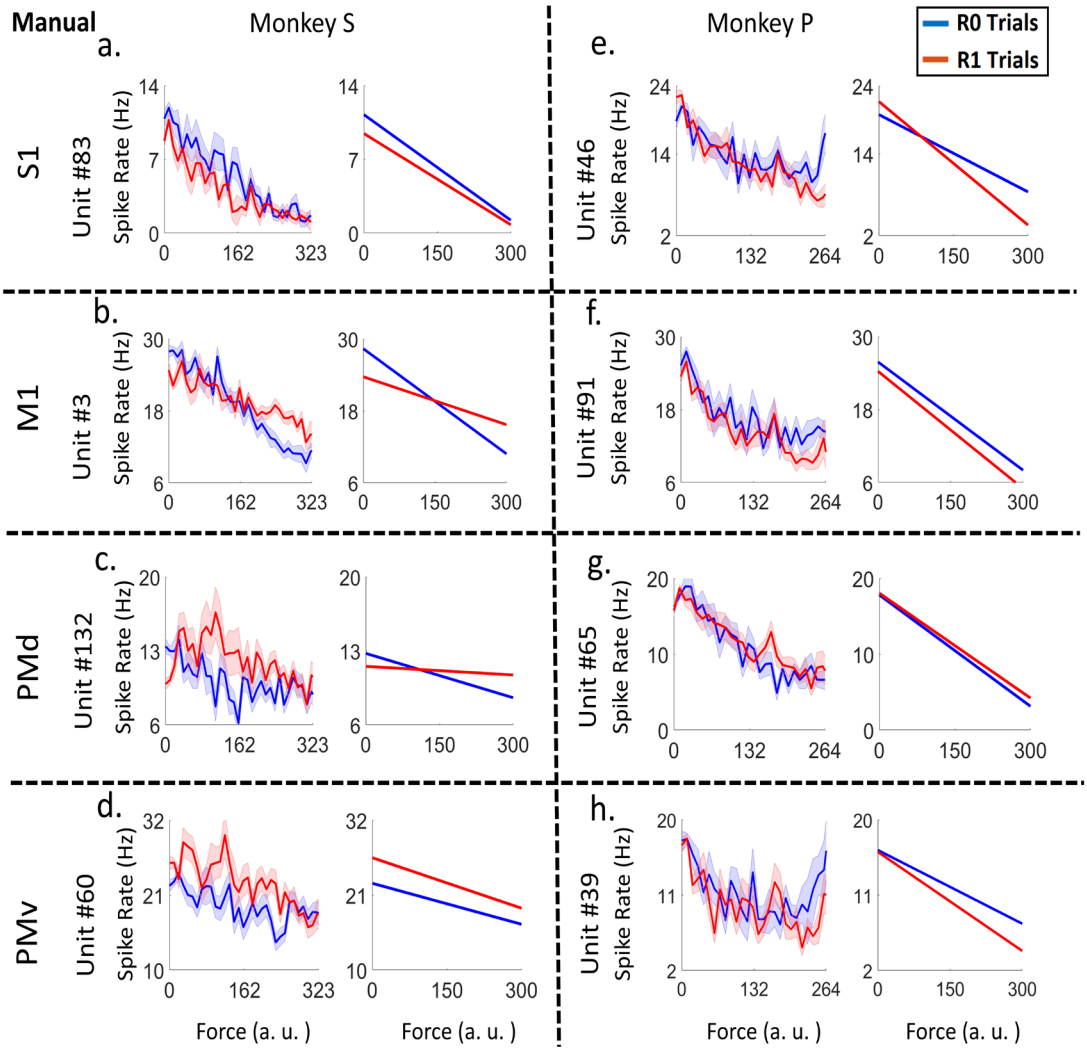

Figure 52: Spike rate vs. force plot for manual blocks.

Figure 51 and Figure 52 shows the plots of spike rate vs force (left subplots) and their linear tuning curves (right subplots) for example units from S1 (plot *a, e*), M1 (plot *b, f*), PMd (plot *c, g*) and PMv (plot *d, h*) cortices of both NHPs (for NHP S plots *a, b, c* and *d* and for NHP P plots *e, f, g* and *h*). The units presented here had significant differences between R0 and R1 groups (ANCOVA, F-test, $p<0.05$) force tuning curves during observed (Figure 51) and manually performed (Figure 52) blocks. Red lines indicate

rewarding trials (R1) and blue indicate non-rewarding trials (R0). See Figure 53 for population results.

Figure 53 shows the percentage of single units that have grip force tuning curves significantly modulated by cued-reward level during cued blocks for each NHP (S and P) and each cortex (S1, M1, PMd and PMv). The Green bar shows the percentage of significant units ($p<0.05$, ANCOVA) and the red bar inside shows the percentage of force-mirror neurons (Figure 38). Here the heights of the bars are the percentage information and the widths of the bars are just for the purpose of representation. The purple and yellow bars represent the data after FDR correction was applied. The purple bar is the percentage of significant units and yellow bars represent the percentage of such units that are also force-mirror neurons (Figure 38) after FDR correction was applied. For NHP P observation case none of the units remained significant for grip force tuning curve after false discovery rate correction.

The percentage of single units with force tuning curves that are modulated by reward level. Units with significantly different force tuning curves between R0 and R1 trials. The titles represent which NHP and block type are plotted, p-values were adjusted using the Benjamini-Hochberg method (FDR method) correcting for false discovery rate where the correction was applied using $p=0.05$. For FDR correction the number of times hypothesis test was applied (number of population) is used. The y-axis is the percentage of units and x-axis represents the cortex. The green bar shows the number of significant units ($p<0.05$, ANCOVA) and red shows the MN population among them. The purple bar shows the significant units after FDR correction was applied. The yellow bar inside the purple shows the percentage of putative MNs after FDR correction. The number after the '#' sign

on top of each bar shows the number of significant units for that given case and the number presented with 'n' is the total units recorded for that case.

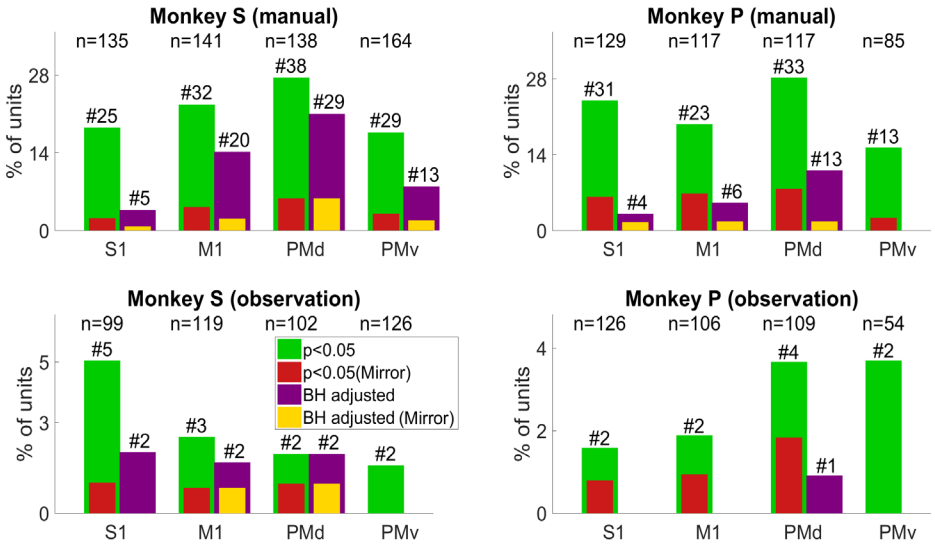

Figure 53: Percentage of single units with force tuning curves that are modulated by reward.

The units with significantly different slopes for the force tuning curves between R0 and R1 are given in Table 5. The values in parentheses show the adjusted significant units after Benjamini and Hochberg's method accounting for the false discovery rate was applied. The FDR correction applied for number of populations is described in the method section titled "grip force tuning curve analysis".

Table 5: Number and percentage of units with significantly different slope

	S1 #	S1 %	M1 #	M1 %	PMd #	PMd %	PMv #	PMv %
NHP S Manual	25 (5)	19% (4%)	32 (20)	23% (14%)	38 (29)	28% (21%)	29 (13)	18% (8%)
NHP P Manual	31 (4)	24% (3%)	23 (6)	20% (5%)	33 (13)	28% (10%)	13 (0)	15% (0%)
NHP S Obs.	5 (2)	5% (2%)	3 (2)	3% (2%)	2 (2)	2% (2%)	2 (0)	2% (0%)
NHP P Obs.	2 (0)	2% (0%)	2 (0)	2% (0%)	4 (1)	4% (1%)	2 (1)	3% (1%)

The units with significantly different y-intercept for the force tuning curves for R0 and R1 are given in Table 6. The values in parentheses show the adjusted significant units after Benjamini and Hochberg's method accounting for the false discovery rate was applied. The FDR correction applied for number of populations is described in the method section titled "grip force tuning curve analysis".

Table 6: Number and percentage of units with significantly different estimate.

	S1 #	S1 %	M1 #	M1 %	PMd #	PMd %	PMv #	PMv %
NHP S Manual	29 (8)	21% (6%)	45 (31)	32% (22%)	50 (39)	36% (28%)	36 (28)	22% (17%)
NHP P Manual	18 (2)	14% (2%)	24 (2)	21% (2%)	33 (14)	28% (12%)	9 (0)	11% (0%)
NHP S Obs.	4 (3)	4% (3%)	5 (5)	4% (4%)	3 (1)	3% (1%)	6 (4)	5% (3%)
NHP P Obs.	1 (0)	1% (0%)	2 (0)	2% (2%)	4 (0)	4% (0%)	2 (2)	3% (3%)

CHAPTER 5

DISCUSSION

At the starting of this thesis we described three aims in chapter 2 to support the three hypotheses and in the result section represents figures to support those claims. The first aim was to detect the influence of reward cue and actual reward in the spike activity of sensorimotor cortices (S1, M1, PMd and PMv). On section 4.2 Reward Significance, Figure 23 and Figure 24 for NHP S and P shows the results to present the influence of reward. The second aim was to decode the grip force from the neural data during observation and manual blocks to represents the presence of grip force related modulation. Figure 33-Figure 36 and Table 1-Table 3 from section "4.3 Grip Force Prediction" shows the decoded grip force with the coefficient of determinant as decoding accuracy. To present grip force related mirror neuron activity on specific unit that was significant for grip force during manual and observational block, we presented raw neural spike data for example units in Figure 21-Figure 22 and population data in Figure 38-Figure 41. Our third and last aim was to find any modulation of grip force representation due to reward expectation and the Figure 51-Figure 53 in section "4.8 Modulation of Force Tuning Curves by Cued Reward Level:" was included to present the results for that aim.

In this report we have presented the following points: first, we showed results indicate that S1, M1, PMd, and PMv all have MNs that have activity related to visually cued grip force; second, we have shown that the firing rate in each of these regions is also modulated by reward expectation during the post-cue period for cued reward level trials, and during the post-feedback time period for both cued and uncued reward level trials; third, that the MNs activity of visually cued grip force can coexist within single units that

also code for reward level; fourth, that the MN activity during observational trials, as compared to manual trials, could shift their temporal relationship predicting/responding to visually cued force about equally in either the predictive or responsive time lag directions; fifth, that the neural grip force tuning functions can be modulated by reward expectation in all 4 brain regions under study (S1, M1, PMd and PMv, see Figure 53) during both manual and observational trials.

To the best of our knowledge, we are reporting the first evidence of mirror neural responses to expected, or visually cued effort (grip force), within these sensorimotor regions. As the NHPs had a great deal of experience with the grip force task we expect the mirror responses were due to the visual cueing of force output that the NHPs had come to understand based on their manual trials. In Figure 46 and Figure 48. we showed that the shift in peak correlation between cued force and neural time lag could be in either the direction expected for motor production, or that expected from sensory stimulation, which would be more in line with the initial MN work (Gallese et al., 1996), and the former more in line with movement rehearsal (Cisek & Kalaska, 2004). We predict that such force MN activity could be seen in more natural settings if the context was understood by the NHPs, such as lifting heavy vs. light objects that they were familiar with, or perhaps when the NHP squeezes a deformable object, or observes such a grasp, again with knowledge of the object's physical properties. However, further work is needed to show such activity exists under more natural conditions within each of these regions. It should be noted that this type of prior knowledge being necessary for MN activity patterns is not new. Mirror neurons that encode subjective value in addition to grasping information clearly need the NHP to

have familiarity with the object in some way to have formed a subjective value (Caggiano et al., 2012).

We have shown that reward modulation can occur post-cue, when the cue indicates the reward value of the current trial, as well as post-feedback when the reward level that was cued is delivered. When there is no reward cue given in uncued blocks there is no "post-cue" reward modulation as expected, but there is still post-feedback modulation in each of the 4 brain regions, and again during both manual and observational trial types. Based on the evidence we have presented, we see that S1, M1, PMd and PMv contain units that encode reward expectation and reward itself, as has been shown previously for the task used in this work as well as other tasks for M1 (An et al., 2019; Brandi T. Marsh et al., 2015; Ramakrishnan et al., 2017; Zhao et al., 2018), indicating this reward modulation may be a generalized broadcast signal to regions involved in the ongoing sensorimotor planning and production of movement, as well as during observation of such movements, in a manner that can be predictive, as expected during mental simulation, and responsive to the visual stimuli, as expected for MNs as first described (Gallese et al., 1996). These results demonstrate that reward is encoded in the primary somatosensory cortex (S1) similarly to that shown for M1 in previous work (Brandi T. Marsh et al., 2015; Ramakrishnan et al., 2017) and premotor regions (Ramkumar et al., 2016; M. R. Roesch & Olson, 2007). In addition, we have now shown such reward modulation simultaneously for M1, S1, PMd and PMv during both manual and observational trial types for the same single units tracked between tasks.

There are several limitations to the work presented here that should be addressed in future work. EMGs were not available for these particular datasets that allowed us to track

single units between manual and observational trials, and therefore we can't state with certainty that the NHPs were not activating their arm muscles covertly, however, they were not making obvious movements, and did not have access to the force transducing handle, in addition, our previous studies found no correlation between EMGs and curser motion in observational trials of a reaching task (Brandi T. Marsh et al., 2015). In addition, we show in Fig.S.6 for both NHPs there was no significant EMG activity during observational trials on different days when the EMG signals were usable. The grip force output in the current task was generally phasic in nature with a bell-shaped profile, even if the cued amplitudes were different, the force profiles were still fairly stereotyped, and so it is possible that some other phasic neural response was allowing the regression models to predict force output, which was bell-shaped, by some non-force related phasic response, such as that related to the cued reward information. However, the regression models did not fall apart in the uncued reward level task, which indicates at least cued reward does not explain our force decoding results. In addition, when we conducted analysis on the time series of just the peak force amplitude of each trial, we still obtained positive results showing MNs for force, although clearly not as strong as when using the fuller dataset including the force trajectories (see Figure 44).

The work presented here has a practical application past basic neuroscience. We believe it is important to continue gaining a better understanding of encoded information, such as reward, within the sensorimotor cortices toward the development of a close-loop brain machine interface (BMI) for the restoration of motor control and beyond, such as towards a better understanding and tracking of psychological state of the individual. BMI neural signals are often recorded and decoded from a subset of S1, M1, PMd, and PMv

while sensory feedback is obtained either by natural vision, or stimuli routed to S1, such as via the thalamus (Choi et al., 2016) for somatosensory feedback. It has recently been shown that reward expectation can change directional and force based tuning curves in M1 and S1 (Ramakrishnan et al., 2017; Zhao et al., 2018), and here we have shown that all of these brain regions are influenced by reward expectation, effort, or sensory feedback on expected effort, and therefore research into these relationship is warranted. Differentiating between mirror activity in these regions and intentional activity for movement is key towards making BMIs more stable with respect to the users intended movements compared to observed movements, and our future work will address these issues.

REFERENCES

Alaerts, K., de Beukelaar, T. T., Swinnen, S. P., & Wenderoth, N. (2012). Observing how others lift light or heavy objects: Time-dependent encoding of grip force in the primary motor cortex. *Psychological Research*, *76*(4), 503–513. https://doi.org/10.1007/s00426-011-0380-1

An, J., Yadav, T., Ahmadi, M. B., Tarigoppula, V. S. A., & Francis, J. T. (2018). Near Perfect Neural Critic from Motor Cortical Activity Toward an Autonomously Updating Brain Machine Interface. *2018 40th Annual International Conference of the IEEE Engineering in Medicine and Biology Society (EMBC)*, 73–76. https://doi.org/10.1109/EMBC.2018.8512274

An, J., Yadav, T., Hessburg, J. P., & Francis, J. T. (2019). Reward Expectation Modulates Local Field Potentials, Spiking Activity and Spike-Field Coherence in the Primary Motor Cortex. *ENeuro*, *6*(3). https://doi.org/10.1523/ENEURO.0178-19.2019

Atique, M. M., & Francis, J. T. (2019). *Reward and force modulation of neurons in the primate primary somatosensory cortex (S1)*. https://www.abstractsonline.com/pp8/#!/7883/presentation/59642

Benjamini, Y., & Hochberg, Y. (1995). Controlling the False Discovery Rate: A Practical and Powerful Approach to Multiple Testing. *Journal of the Royal Statistical Society: Series B (Methodological)*, *57*(1), 289–300. https://doi.org/10.1111/j.2517-6161.1995.tb02031.x

Caggiano, V., Fogassi, L., Rizzolatti, G., Casile, A., Giese, M. A., & Thier, P. (2012). Mirror neurons encode the subjective value of an observed action. *Proc Natl Acad Sci U S A*, *109*(29), 11848–11853. https://doi.org/10.1073/pnas.1205553109

Chhatbar, P. Y., von Kraus, L. M., Semework, M., & Francis, J. T. (2010). A bio-friendly and economical technique for chronic implantation of multiple microelectrode arrays. *Journal of Neuroscience Methods*, *188*(2), 187–194. https://doi.org/10.1016/j.jneumeth.2010.02.006

Choi, J. S., Brockmeier, A. J., McNiel, D. B., Kraus, L. M. von, Príncipe, J. C., & Francis, J. T. (2016). Eliciting naturalistic cortical responses with a sensory prosthesis via optimized microstimulation. *Journal of Neural Engineering*, *13*(5), 056007. https://doi.org/10.1088/1741-2560/13/5/056007

Cisek, P., & Kalaska, J. F. (2004). Neural correlates of mental rehearsal in dorsal premotor cortex. *Nature*, *431*(7011), 993–996. https://doi.org/10.1038/nature03005

Cohen, J. Y., Haesler, S., Vong, L., Lowell, B. B., & Uchida, N. (2012). Neuron-type-specific signals for reward and punishment in the ventral tegmental area. *Nature*, *482*(7383), 85–88. https://doi.org/10.1038/nature10754

Dushanova, J., & Donoghue, J. (2010). Neurons in primary motor cortex engaged during action observation. *European Journal of Neuroscience*, *31*(2), 386–398. https://doi.org/10.1111/j.1460-9568.2009.07067.x

Gallese, V., Fadiga, L., Fogassi, L., & Rizzolatti, G. (1996). Action recognition in the premotor cortex. *Brain: A Journal of Neurology*, *119 (Pt 2)*, 593–609. https://doi.org/10.1093/brain/119.2.593

Gazzola, V., & Keysers, C. (2009). The Observation and Execution of Actions Share Motor and Somatosensory Voxels in all Tested Subjects: Single-Subject Analyses of Unsmoothed fMRI Data. *Cerebral Cortex (New York, NY)*, *19*(6), 1239–1255. https://doi.org/10.1093/cercor/bhn181

Glimcher, P. W., Fehr, E., Camerer, C., & Poldrack, R. A. (Eds.). (2008). *Neuroeconomics: Decision Making and the Brain* (1 edition). Academic Press.

Keisker, B., Hepp-Reymond, M.-C., Blickenstorfer, A., Meyer, M., & Kollias, S. S. (2009). Differential force scaling of fine-graded power grip force in the sensorimotor network. *Human Brain Mapping*, *30*(8), 2453–2465. https://doi.org/10.1002/hbm.20676

Keysers, C., Kaas, J. H., & Gazzola, V. (2010). Somatosensation in social perception. *Nature Reviews Neuroscience*, *11*(6), 417–428. https://doi.org/10.1038/nrn2833

Kipke, D. R., Vetter, R. J., Williams, J. C., & Hetke, J. F. (2003). Silicon-substrate intracortical microelectrode arrays for long-term recording of neuronal spike activity in cerebral cortex. *IEEE Transactions on Neural Systems and Rehabilitation Engineering*, *11*(2), 151–155. https://doi.org/10.1109/TNSRE.2003.814443

Klein, P.-A., Olivier, E., & Duque, J. (2012). Influence of Reward on Corticospinal Excitability during Movement Preparation. *Journal of Neuroscience*, *32*(50), 18124–18136. https://doi.org/10.1523/JNEUROSCI.1701-12.2012

Kretzberg, J., Coors, T., & Furche, J. (2009). Comparison of valley seeking and T-distributed EM algorithm for spike sorting. *BMC Neuroscience*, *10*(1), P47. https://doi.org/10.1186/1471-2202-10-S1-P47

Maranesi, M., Livi, A., Fogassi, L., Rizzolatti, G., & Bonini, L. (2014). Mirror neuron activation prior to action observation in a predictable context. *J Neurosci*, *34*(45), 14827–14832. https://doi.org/10.1523/JNEUROSCI.2705-14.2014

Marsh, B. T., Tarigoppula, V. S., Chen, C., & Francis, J. T. (2015). Toward an autonomous brain machine interface: Integrating sensorimotor reward modulation and reinforcement learning. *J Neurosci*, *35*(19), 7374–7387. https://doi.org/10.1523/JNEUROSCI.1802-14.2015

Marsh, Brandi T., Tarigoppula, V. S. A., Chen, C., & Francis, J. T. (2015). Toward an Autonomous Brain Machine Interface: Integrating Sensorimotor Reward Modulation and Reinforcement Learning. *Journal of Neuroscience*, *35*(19), 7374–7387. https://doi.org/10.1523/JNEUROSCI.1802-14.2015

Mazurek, K. A., Rouse, A. G., & Schieber, M. H. (2018). Mirror Neuron Populations Represent Sequences of Behavioral Epochs During Both Execution and Observation. *Journal of Neuroscience*, *38*(18), 4441–4455. https://doi.org/10.1523/JNEUROSCI.3481-17.2018

McNiel, D. B., Choi, J. S., Hessburg, J. P., & Francis, J. T. (2016). *Reward value is encoded in primary somatosensory cortex and can be decoded from neural activity during performance of a psychophysical task*. 3064–3067.

McNiel, D., Bataineh, M., Choi, J., Hessburg, J., & Francis, J. (2016). Classifier Performance in Primary Somatosensory Cortex Towards Implementation of a Reinforcement Learning Based Brain Machine Interface. *2016 32nd Southern Biomedical Engineering Conference (SBEC)*, 17–18. https://doi.org/10.1109/SBEC.2016.19

Murray, G. K., Corlett, P. R., Clark, L., Pessiglione, M., Blackwell, A. D., Honey, G., Jones, P. B., Bullmore, E. T., Robbins, T. W., & Fletcher, P. C. (2008). Substantia nigra/ventral tegmental reward prediction error disruption in psychosis. *Molecular Psychiatry*, *13*(3), 267–276. https://doi.org/10.1038/sj.mp.4002058

Pleger, B., Blankenburg, F., Ruff, C. C., Driver, J., & Dolan, R. J. (2008). Reward Facilitates Tactile Judgments and Modulates Hemodynamic Responses in Human Primary Somatosensory Cortex. *Journal of Neuroscience*, *28*(33), 8161–8168. https://doi.org/10.1523/JNEUROSCI.1093-08.2008

Pohlmeyer, E. A., Mahmoudi, B., Geng, S., Prins, N., & Sanchez, J. C. (2012). Brain-machine interface control of a robot arm using actor-critic rainforcement learning. *2012 Annual International Conference of the IEEE Engineering in Medicine and Biology Society*, 4108–4111. https://doi.org/10.1109/EMBC.2012.6346870

Pohlmeyer, E. A., Mahmoudi, B., Geng, S., Prins, N. W., & Sanchez, J. C. (2014). Using Reinforcement Learning to Provide Stable Brain-Machine Interface Control Despite Neural Input Reorganization. *PLoS ONE*, *9*(1). https://doi.org/10.1371/journal.pone.0087253

Quigley, M., Conley, K., Gerkey, B., Faust, J., Foote, T., Leibs, J., Wheeler, R., & Ng, A. Y. (2009). ROS: An open-source Robot Operating System. *ICRA Workshop on Open Source Software*, *3*, 5.

Ramakrishnan, A., Byun, Y. W., Rand, K., Pedersen, C. E., Lebedev, M. A., & Nicolelis, M. A. L. (2017). Cortical neurons multiplex reward-related signals along with sensory and motor information. *Proceedings of the National Academy of Sciences*, *114*(24), E4841–E4850. https://doi.org/10.1073/pnas.1703668114

Ramkumar, P., Dekleva, B., Cooler, S., Miller, L., & Kording, K. (2016). Premotor and Motor Cortices Encode Reward. *PLOS ONE*, *11*(8), e0160851. https://doi.org/10.1371/journal.pone.0160851

Rizzolatti, G., Camarda, R., Fogassi, L., Gentilucci, M., Luppino, G., & Matelli, M. (1988). Functional organization of inferior area 6 in the macaque monkey. II. Area F5 and the control of distal movements. *Experimental Brain Research*, *71*(3), 491–507. https://doi.org/10.1007/BF00248742

Rizzolatti, Giacomo. (2005). The mirror neuron system and its function in humans. *Anatomy and Embryology*, *210*(5–6), 419–421. https://doi.org/10.1007/s00429-005-0039-z

Rizzolatti, Giacomo, & Craighero, L. (2004). The Mirror-Neuron System. *Annual Review of Neuroscience*, *27*(1), 169–192. https://doi.org/10.1146/annurev.neuro.27.070203.144230

Rizzolatti, Giacomo, Fogassi, L., & Gallese, V. (2001). Neurophysiological mechanisms underlying the understanding and imitation of action. *Nature Reviews Neuroscience*, *2*(9), 661–670. https://doi.org/10.1038/35090060

Roesch, M. R., & Olson, C. R. (2007). Neuronal activity related to anticipated reward in frontal cortex: Does it represent value or reflect motivation? *Ann N Y Acad Sci*, *1121*, 431–446. https://doi.org/10.1196/annals.1401.004

Roesch, Matthew R., & Olson, C. R. (2003). Impact of Expected Reward on Neuronal Activity in Prefrontal Cortex, Frontal and Supplementary Eye Fields and Premotor Cortex. *Journal of Neurophysiology*, *90*(3), 1766–1789. https://doi.org/10.1152/jn.00019.2003

Rolls, E. T. (2014). *Emotion and decision-making explained* (First edition.). Oxford University Press.

Rossi, S., Tecchio, F., Pasqualetti, P., Ulivelli, M., Pizzella, V., Romani, G. L., Passero, S., Battistini, N., & Rossini, P. M. (2002). Somatosensory processing during movement observation in humans. *Clinical Neurophysiology*, *113*(1), 16–24. https://doi.org/10.1016/S1388-2457(01)00725-8

Sanchez, J. C., Tarigoppula, A., Choi, J. S., Marsh, B. T., Chhatbar, P. Y., Mahmoudi, B., & Francis, J. T. (2011). Control of a center-out reaching task using a reinforcement learning Brain-Machine Interface. *2011 5th International IEEE/EMBS Conference on Neural Engineering*, 525–528. https://doi.org/10.1109/NER.2011.5910601

Sato, M., & Hikosaka, O. (2002). Role of Primate Substantia Nigra Pars Reticulata in Reward-Oriented Saccadic Eye Movement. *Journal of Neuroscience*, *22*(6), 2363–2373. https://doi.org/10.1523/JNEUROSCI.22-06-02363.2002

Schultz, W., Dayan, P., & Montague, P. R. (1997). A Neural Substrate of Prediction and Reward. *Science*, *275*(5306), 1593–1599. https://doi.org/10.1126/science.275.5306.1593

Tkach, D., Reimer, J., & Hatsopoulos, N. G. (2007). *Journal of Neuroscience*, *27*(48), 13241–13250. https://doi.org/10.1523/JNEUROSCI.2895-07.2007

Tremblay, L., & Schultz, W. (1999). Relative reward preference in primate orbitofrontal cortex. *Nature*, *398*(6729), 704–708. https://doi.org/10.1038/19525

Vigneswaran, G., Philipp, R., Lemon, R. N., & Kraskov, A. (2013). M1 corticospinal mirror neurons and their role in movement suppression during action observation. *Curr Biol*, *23*(3), 236–243. https://doi.org/10.1016/j.cub.2012.12.006

Vigneswaran, Ganesh, Philipp, R., Lemon, R. N., & Kraskov, A. (2013). M1 Corticospinal Mirror Neurons and Their Role in Movement Suppression during Action Observation. *Current Biology*, *23*(3), 236–243. https://doi.org/10.1016/j.cub.2012.12.006

Yuan, Y., Yang, C., & Si, J. (2012). The M-Sorter: An automatic and robust spike detection and classification system. *Journal of Neuroscience Methods*, *210*(2), 281–290. https://doi.org/10.1016/j.jneumeth.2012.07.012

Zaghloul, K. A., Blanco, J. A., Weidemann, C. T., McGill, K., Jaggi, J. L., Baltuch, G. H., & Kahana, M. J. (2009). Human Substantia Nigra Neurons Encode Unexpected Financial Rewards. *Science*, *323*(5920), 1496–1499. https://doi.org/10.1126/science.1167342

Zhao, Y., Hessburg, J. P., Asok Kumar, J. N., & Francis, J. T. (2018). Paradigm Shift in Sensorimotor Control Research and Brain Machine Interface Control: The Influence of Context on Sensorimotor Representations. *Frontiers in Neuroscience*, *12*. https://doi.org/10.3389/fnins.2018.00579

APPENDIX

EMG Analysis:

The data used in the main text had corrupted EMG and we were unable to confirm whether the NHPs were still using their arm muscles during the observation task, however, from observation notes of the experiments, and the clear decrease in activity seen in Figure 21 and Figure 22 of the main text, and the fact that the NHPs could not reach for, or touch the force transducing handle, we do not believe the NHPs were physically rehearsing grip movements during observation. In addition, as seen below in Figure 54, EMG on other days from these same NHPs was available during observation trials and did show any obvious activation patterns in the mean activity, however, it appears there was some small and insignificant increase in biceps for NHP P. The neural results of these below data sets held to that shown in the main text and figs. This does not rule out the NHPs covertly imagining movement, which was addressed in the main text.

Figure 54 shows the EMG collected from the Biceps (section a and b) and Forearm (section c and d) of NHP S (section a and c) and P (section b and d) recorded on different day. The blue color represents manual blocks (execution) and red is for observation. On each of four sections a, b, c and d, left plots show the mean EMG (0.5s pre-force onset to 1s post force onset activity) for all the trials with standard deviation as shaded error bar. The right plots show the mean power spectral density (PSD) with standard deviation for same data. A band pass filter was applied on the EMG for the power line noise and its harmonics (30Hz, 60Hz, 90Hz… etc) and the effect of that can be seen in the PSD plots

(b). The p-value for the significance test between the mean manual and observational is given on the title of each subplot.

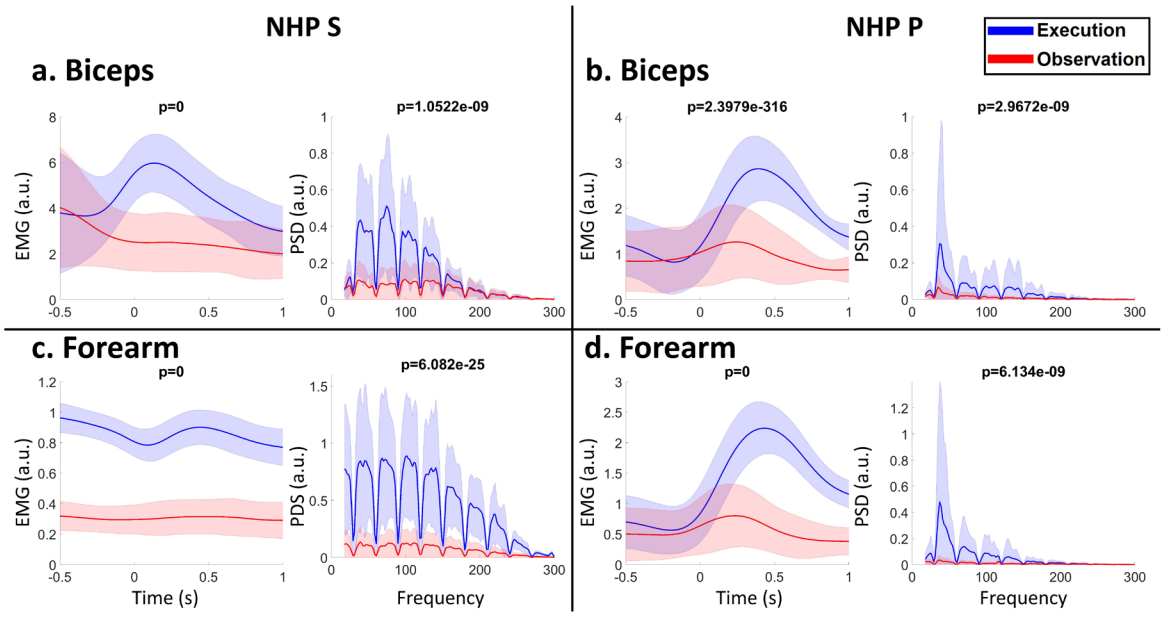

Figure 54: EMG from during observational and manual blocks recorded on a different day.

Observation Results on force:

This Figure 55 shows raster plots of some more example units from each of the 4 cortices during grip force onset and offset taken from observation blocks showing the full average force time period with both increases and decreases to force onset.

Figure 55 shows raster plots for units from S1 (plots a, b, c and d), M1 region (plots e, f, g and h), PMd (plots i, j, k and l) and PMv (plots m, n, o and p) are shown for NHPs S and P. These plots show the grip force values expected given the cued force targets shown to the NHPs during observational blocks. The black bold line on each raster and spike rate plot shows the onset of "force" and the dotted horizontal line divides R1 (top, red) and R0 (bottom, blue) trials. On each neural data subplots, the x-axis represents time in seconds and for raster plots y-axis represents trial number (upper part of the subplots) and for the

spike rate plot y-axis is spike rate in 'Hz' (bottom part of the subplots). The Asterisk (*) symbol on the right top corner of the mean spike rate plots represents, that unit was significant (F-test, $p<0.05$) for force fit using linear regression model in eq 1.

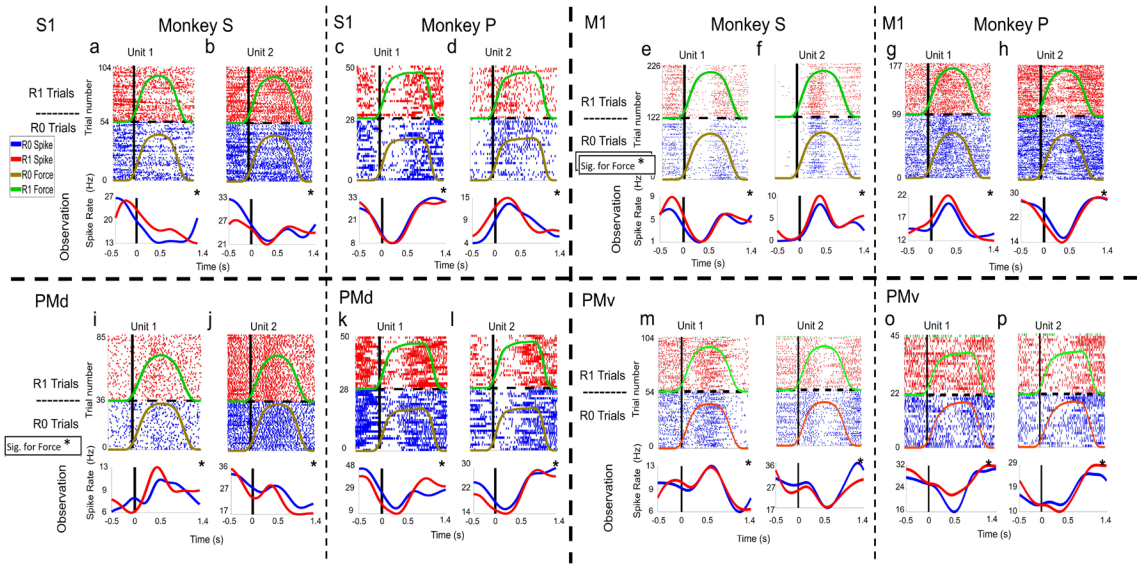

Figure 55: Example raster plots for spike activity during grip force observation.

Regression on additional observational blocks:

Table 7 (NHP S) and Table 8 (NHP P) shows the regression data analysis for NHP S and P. The table contains the R-square value for model fit given in equation 1 and the corresponding p-value and F-statistic. The R-squared value for prediction and its p-value is also shown on the table. This table contains two additional observational blocks that were recorded on a different day from the data shown in the main text.

Table 7: Regression model output for NHP S for the two additional observational blocks recorded on a different day.

NHP S - S1					
Block	R-fit	p-value	F-stat	R-predict	p-value
Observation Cued	0.28	3e-91	3.81	0.19	8.3e-21
Observation Uncued	0.34	4.3e-154	4.79	0.04	9.3e-6
NHP S – M1					
Block	R-fit	p-value	F-stat	R-predict	p-value
Observation Cued	0.65	0	11.59	0.6	2.6e-87
Observation Uncued	0.76	0	21.19	0.66	4.3e-113
NHP S – PMd					
Block	R-fit	p-value	F-stat	R-predict	p-value
Observation Cued	0.53	1.9e-273	6.63	0.36	2.7e-43
Observation Uncued	0.67	0	11.57	0.39	0.55
NHP S – PMv					
Block	R-fit	p-value	F-stat	R-predict	p-value
Observation Cued	0.6	0	11.84	0.72	5.7e-121
Observation Uncued	0.8	0	34.11	0.72	6.1e-134

Table 8: Regression model output for NHP P for the two additional observational blocks recorded on a different day.

NHP P – S1

Block	R-fit	p-value	F-stat	R-predict	p-value
Observation Cued	0.46	1.3e-229	8.34	0.27	1.9e-26
Observation Uncued	0.53	0	10.09	0.13	1.8e-14

NHP P – M1

Block	R-fit	p-value	F-stat	R-predict	p-value
Observation Cued	0.61	0	13.19	0.55	2.7e-64
Observation Uncued	0.69	0	18.07	0.55	3.1e-75

NHP P – PMd

Block	R-fit	p-value	F-stat	R-predict	p-value
Observation Cued	0.5	6.4e-274	10	0.52	6.3e-59
Observation Uncued	0.55	0	13.14	0.37	2e-44

NHP P – PMv

Block	R-fit	p-value	F-stat	R-predict	p-value
Observation Cued	0.35	3.5e-197	11.24	0.28	4.9e-27
Observation Uncued	0.46	0	13.18	0.36	1.4e-42